

University of Minnesota
St. Anthony Falls Hydraulic Laboratory

Project Report No. 213

MODEL STUDY OF THE MINNESOTA RIVER
NEAR TRUNK HIGHWAY NO. 169 BRIDGE,
MINNESOTA

by

Gary Parker, Ismael Martinez,
and Randy Hills

Prepared for

STATE OF MINNESOTA
MINNESOTA DEPARTMENT OF TRANSPORTATION

September, 1982

The University of Minnesota is committed to the policy that all persons shall have equal access to its programs, facilities, and employment without regard to race, creed, color, sex, national origin, or handicap.

ABSTRACT

The Minnesota Trunk Highway No. 169 crosses the Minnesota River just north of the town of Le Sueur. The bridge is immediately downstream of the confluence of the Minnesota River and a small tributary, Le Sueur Creek, entering from the east.

The bridge was completed in 1960. The approaches were designed so as to preclude overtopping. In fact, they were not overtopped during the largest flood on record, which occurred in 1965. During severe floods, the entire floodplain carries a considerable discharge. The severe constriction at the bridge was partially alleviated by excavating the western bank and immediately adjacent floodplain to provide a floodway. The bridge spans the original channel (east side), where the piers are deep, and the original floodway (west side), where the piers are shallow.

During the episodic flood of 1965, the severe constriction of overbank flow at the bridge caused scour that endangered the western approach. The recession of the flood waters revealed a large bar at the mouth of the tributary. This bar had occupied the old channel and forced the river to the west, against the shallow floodway piers. At one point several of these piers were subjected to scour below their seals.

Although various corrective measures were taken, the problem became progressively worse. In 1981, contingency measures were implemented, including filling of a portion of the west side with riprap and excavating a portion of the east side to provide a pilot channel. In addition, the model study described herein was commenced, in order to obtain guidance as regards more permanent corrective measures.

The model study was conducted using Froude similarity with a horizontal scale of 1:200 and a vertical scale of 1:40. Crushed walnut shells were used to model the bed sediment.

The model study indicated that scour resulting from the severe constriction at the bridge becomes an increasingly difficult problem as the fraction of discharge that is overbank increases. During severe floods, sediment from Le Sueur Creek cannot enter the channel due to slack water at the mouth of the tributary. Sediment collects in Le Sueur Creek, and enters the channel as a slug as flood flows recede. Additional deposition can occur when the Minnesota River is low, but the tributary is high.

It was found necessary to distinguish between corrective measures operable at below- and above-bankfull stages. At above-bankfull stages, a T-spur dike on the western floodplain adjacent to the channel can pull floodplain flow away from the western approach and deflect it to the east,

near the mouth of the tributary. At lower flows, two in-channel permeable dikes can encourage deposition on the west side, and deflect the flow to the east side. The height of the permeable dike must be well below bankfull stage in order that appropriate conveyance be provided for higher flows. These, and certain other maintenance-oriented corrective measures, are proposed in order to return the channel to its original position and control the growth of the bar at the mouth of the tributary.

At flows above about 60,000 cfs, severe scour is induced at the bridge due to the intense constriction of floodplain and channel flow. Increased conveyance would reduce the potential for severe scour. If this cannot be provided, extensive riprapping of pier footings is recommended.

TABLE OF CONTENTS

	<u>Page No.</u>
Abstract	i
List of Figures	iv
Introduction	1
The Setting	1
History of the Problem	4
Options for Rectification	8
Design of the Model Study	11
Overview of the Experiments	13
Experimental Results	17
Implications for the Bridge	29
Conclusions and Recommendations	29
Acknowledgements	31
Figures	32-81
References	82
Appendix: A Guide to the Videotapes	83

LIST OF FIGURES

- Fig. 1. Topographical map of vicinity of the trunk highway No. 169 bridge; taken from the U. S. Geological Survey topographical map of the Le Sueur quadrangle.
- Fig. 2. Preconstruction bridge site on September 28, 1957.
- Fig. 3. Bridge site during flood of 1965 (April 9, 1965).
- Fig. 4. Bridge site on April 30, 1968.
- Fig. 5. Bridge site on January 3, 1981.
- Fig. 6. Bridge site on November 11, 1981.
- Fig. 7. Three typical size distributions of bed material in the Minnesota River near the Trunk Highway No. 169 bridge.
- Fig. 8. View of denuded slope of gravel mining operation from Le Sueur Creek. Aquatic grasses at bottom denote margin of creek. The rubble embankment in the foreground does not appear to be more than a decade old.
- Fig. 9. The 1873, 1940, 1957, 1968, and 1980 channels of the Minnesota River near the State Highway No. 93 bridge.
- Fig. 10. Sketch of the bridge footings and seals, and several cross sections at the bridge. Elevation is in feet above sea level. The water surface elevation of the peak of the 1965 flood at the bridge was 744 ft above sea level.
- Fig. 11. Sketch of the contingency measures (riprap and excavation of pilot channel) implemented in the summer of 1981. The left side is the west side. Elevation is in feet above sea level.
- Fig. 12. The head of the bar is covered in many places with pea and coarser gravel. The pilot channel is paved with even coarser material.
- Fig. 13. Various countermeasures: 1) cut down vegetation on bars; 2) riprap to pier 4; 3) pilot channel; 4) riprap to pier 6; 5) deeper footings, piers 1-5; 6) lengthen spur dike; 7) remove channel debris; 8) permeable dike; 9) separate bridge deck, Le Sueur Creek; 10) culvert.

- Fig. 14. Schematic of model basin.
- Fig. 15. Size distributions of various model sediments.
- Fig. 16. One of the model sediment feed devices.
- Fig. 17. A view of the model basin looking downstream.
- Fig. 18. Results of model calibration. Water surface elevations measured in the model just upstream of the bridge have been scaled up to prototype dimensions; they are compared with water surface elevations from the field. Also shown is the sediment feed rate necessary in the model to obtain equilibrium as a function of prototype water discharge.
- Fig. 19. Bed profiles and water surface elevations at the bridge for the experiments of Series 5.
- Fig. 20. Bed profiles and water surface elevations at the bridge for the experiments of Series 6.
- Fig. 21. Streamlines for a main stem flow of 22,000 cfs and the tributary flow on.
- Fig. 22. Streamlines for a main stem flow of 22,000 cfs and the tributary flow off.
- Fig. 23. Bed topography created by a main stem flow of 22,000 cfs with the tributary flow on. Most of the riprap from piers 1 to 6 is visible.
- Fig. 24. Streamlines for a main stem flow of 60,000 cfs and the tributary flow on.
- Fig. 25. Streamlines for a main stem flow of 60,000 cfs and the tributary flow off.
- Fig. 26. Bed topography created by a main stem flow of 60,000 cfs with the tributary flow on.
- Fig. 27. Streamlines for a main stem flow of 100,000 cfs and the tributary flow off.
- Fig. 28. Bed topography created by a main stem flow of 100,000 cfs with the tributary flow on.
- Fig. 29. Bed topography created by a main stem flow of 100,000 cfs, with all but a remnant of the riprap removed.

- Fig. 30. Flow patterns associated with the best configuration of the sheet-metal T-spur dike at 60,000 cfs.
- Fig. 31. Bed topography created by a main stem flow of 60,000 cfs with the sheet metal T-spur dike in place.
- Fig. 32. Bed topography created by a main stem flow of 60,000 cfs with one version of the concreted T-spur dike in place.
- Fig. 33. Flow streamlines at 60,000 cfs associated with the concreted T-spur dike of Fig. 32.
- Fig. 34. Flow streamlines at 100,000 cfs with the concreted T-spur dike of Fig. 32 in place.
- Fig. 35. Bed topography produced by a flow of 100,000 cfs with the concreted T-spur dike of Fig. 32 in place.
- Fig. 36. Flow streamlines at 80,000 cfs, with a shortened version of the T-spur dike. Dike angle has also been modified.
- Fig. 37. Flow streamlines at 80,000 cfs, with an excavation, and then an elevated portion, upstream of the T-spur dike. The formed excavation suppresses separation, and allows the tip of the T-spur dike to be angled more strongly downstream.
- Fig. 38. A view of the bar at the mouth of the tributary created by feeding sediment to the tributary at the rate of 80 grams/minute, or about half the main stem rate of 165 grams/minutes.
- Fig. 39. Flow streamlines at 22,000 cfs with the two permeable dikes in place and sediment feed to the tributary turned off.
- Fig. 40. Top view of the bed topography produced by the flow of Fig. 39.
- Fig. 41. Side view of the bed topography produced by the flow of Fig. 39.
- Fig. 42. Bed topography at the end of run 10-3.
- Fig. 43. Water surface elevations and bed profiles for the runs of Series 10. The main stem and tributary sediment feed rates, in grams/minute, are listed for each run.
- Fig. 44. Flow streamlines for run 10-3.
- Fig. 45. Water surface elevation and bed profiles for the runs of Series 11. The main stem and tributary sediment feed rates are listed in grams/minute for each run.
- Fig. 46. Flow streamlines for run 11-4.
- Fig. 47. Bed topography at the end of run 11-4.

- Fig. 48. Water surface elevation, water surface slope, discharge, and minimum bed elevation at the bridge as a function of time for the hydrograph run of Series 12. Time is listed in terms of hours in the model; all other parameters have been scale up to prototype values.
- Fig. 49. Water surface elevations and bed profiles for the rising limb of the hydrograph run.
- Fig. 50. Water surface elevation and bed profiles at the peak of the hydrograph, before, at the time of, and after placement of riprap.
- Fig. 51. Water surface elevations and bed profiles for the falling limb of the hydrograph run.
- Fig. 52. Flow patterns at 40,000 cfs (rising limb) for the hydrograph run.
- Fig. 53. Flow patterns at 60,000 cfs (rising limb) for the hydrograph run.
- Fig. 54. Flow patterns at 80,000 cfs (rising limb) for the hydrograph run.
- Fig. 55. Flow patterns at 100,000 cfs for the hydrograph run.
- Fig. 56. Bed profiles for the rising limb of the hydrograph run near the downstream permeable dike. Next to each discharge (in cfs) in parentheses is the time in hours at which that discharge was terminated.
- Fig. 57. Bed profiles for the falling limb of the hydrograph run near the downstream permeable dike. Next to each discharge (in cfs) in parentheses is the time in hours at which that discharge was terminated.
- Fig. 58. Plan view of the bridge crossing, with the recommended positions for the T-spur dike and the two permeable dikes.
- Fig. 59. Possible design for clump-pile permeable dikes.
- Fig. 60. The diagram illustrates the recommended setting for the top elevation of permeable dike No. 1 (downstream permeable dike), based on the results of the model study. The vertical west and east channel walls are artifacts of the model. The bottom elevation of the piles is shown only as an illustration. Appropriate pile depths must be selected in conjunction with Figs. 56 and 57.
- Fig. 61. The diagram illustrates the recommended setting of the top elevation of permeable Dike No. 2 (upstream permeable dike). See Fig. 60 for further explanation.

MODEL STUDY OF THE MINNESOTA RIVER
NEAR TRUNK HIGHWAY NO. 169 BRIDGE, MINNESOTA

INTRODUCTION

Trunk Highway No. 169 crosses the Minnesota River just downstream of the town of Le Sueur, Minnesota (Fig. 1). A small tributary, Le Sueur Creek, enters the river on the east side immediately upstream of the bridge. The bridge was completed in 1960. In 1965, the largest recorded flood occurred. After the flood receded, a large bar was seen to have formed in the channel of the Minnesota River at the mouth of the tributary. The bar pushed the channel to the west from its original position (Fig. 4). The five westernmost bridge piers, not being originally located in the channel proper, are considerably shallower than those on the east side. The movement of the main thread of flow against them produced scour that endangered their footings.

In time, the bar grew and the problem worsened (Fig. 5). In late 1980, the Minnesota Department of Transportation contacted the St. Anthony Falls Hydraulic Laboratory in regard to the problem, and in June of 1981 a model study was commenced. This report is intended to summarize the problem and report on the results of the model study as well as to present proposed corrective measures.

THE SETTING

The Minnesota River originates at Big Stone Lake near the border of Minnesota and South Dakota. For most of its length, it flows in a fairly wide alluvial valley incised below the surrounding plains. From its source to Mankato it flows in a southeasterly direction. From Mankato the river abruptly changes direction and flows northeasterly toward its confluence with the Mississippi River at St. Paul, Minnesota.

The Trunk Highway No. 93 bridge crossing near Le Sueur is located about halfway between Mankato and Jordan. The river is gaged at these latter two sites.

The river valley. Near the town of Le Sueur, the valley of the Minnesota River has roughly straight, parallel walls directed along a southwest-northeast axis (Fig. 1). The valley has a bottom width of about 4250 ft (1300 m) and is incised approximately 165 ft (50 m) below the surrounding plains. The valley shows no obvious terraces, and is entirely inundated during large floods (Fig. 3).

Borehole logs obtained from the Minnesota Geological Survey suggest that the valley is filled with deep alluvium and unconsolidated glacial till. The shale and sandstone bedrock is reached at an elevation of about 572 ft (174 m) above mean sea level, or about 168 ft (51 m) below a typical floodplain elevation of 740 ft (226 m). The downvalley slope is approximately 0.000156 over a reach 11,650 ft (3550 m) in length, chosen to include the Trunk Highway No. 169 bridge. The floodplain in the vicinity of the bridge is mostly in cultivation, with some forest (Fig. 4).

Channel planform. In the vicinity of the reach in question, and indeed throughout most of the length from Mankato to the confluence with the Mississippi River, the Minnesota River is a classical meandering stream. The point bars show well-developed scroll bars, evidencing an orderly downstream progression of bends due to differential accretion and erosion. Oxbow lakes are common in the flood plain.

The bridge is located at a site which was originally the apex of a gentle bend (Fig. 2). Before construction of the bridge, Le Sueur Creek entered the Minnesota River at the outside of this bend.

The reach in the immediate vicinity of the bridge is of rather low sinuosity. A region of considerable sinuosity exists just upstream of the State Highway No. 93 bridge about 1.5 miles (2.4 km) upvalley of the Trunk Highway No. 169 bridge (Fig. 1), and the channel also becomes somewhat more sinuous about 1.5 miles (2.4 km) downvalley of the Trunk Highway No. 169 bridge.

The channel gives no evidence of recent aggradation or degradation relative to its flood plain, which is essentially the entire valley. The reach near the bridge thus appears to be in grade.

Channel bed and bank material. The channel of the Minnesota River bed is dominated by medium sand, although coarser and finer material are present locally. The channel banks and floodplain contain large amounts of silty fine sand. Although lenses of cohesive material could be observed in cutbanks recently exposed by erosion, cohesiveness does not appear to play a significant role in the channel mechanics of the reach in question.

In February, 1981, the Minnesota Department of Transportation took extensive samples of bed material in the Minnesota River near the bridge. Three typical grain size distributions are shown in Fig. 7. A typical grain size is about 0.4 mm.

Hydrology. The reach of the Minnesota River near Le Sueur is not gaged. Inferences can nevertheless be made concerning hydrologic conditions from the gaging stations at Mankato and Jordan. The difference between Mankato and Jordan is not large due to the lack of intervening tributaries of substantial size. Flows at the Trunk Highway No. 169 bridge were estimated by the arithmetic mean of the flows at Mankato and Jordan. Hydrologic information is provided in Table 1. Bankfull flows are realized about once in three years.

TABLE 1
MODEL AND PROTOTYPE PARAMETERS

Parameter	Prototype	Model
Water surface slope	0.000097	0.000485
Bankfull top-bank width	304 ft	1.52 ft
Mean bankfull depth	13.3 ft	0.332 ft
Mean bankfull velocity	5.44 ft/s	0.86 ft/s
Bankfull Froude No.	0.26	0.26
Mean discharge (M.R.)	3100	0.061
(L.S.C.)	?	?
1.2 yr. flood (M.R.)	7000	0.138
(L.S.C.)	300	0.0059
3.0 yr. flood (M.R.)(bankfull)	22,000	0.435
(L.S.C.)	1000	0.0198
7.5 yr. flood (M.R.)	40,000	0.791
(L.S.C.)	1,900	0.0376
18 yr. flood (M.R.)	60,000	1.19
(L.S.C.)	2,900	0.0573
38 yr. flood (M.R.)	80,000	1.58
(L.S.C.)	4,000	0.0791
74 yr. flood (M.R.)	100,000	1.98
(1965) (L.S.C.)	5,000	0.0988
100 yr. flood (M.R.)	110,000	2.17
(L.S.C.)	5,400	0.107

NOTE: M.R. = Minnesota River
L.S.C. = Le Sueur Creek
Discharges are in cfs.

Channel geometry. The channel of the Minnesota River was surveyed and sounded on February 27, 1981, at a low discharge near 1200 cfs (34 cumecs). Cross-sectional data were used in conjunction with a one-foot contour topographical map of the area to estimate average bankfull geometry in that portion of the reach not immediately affected by the bridge. Estimated values are shown in Table 1.

Le Sueur Creek. Le Sueur Creek enters the Minnesota River just upstream of the bridge. Approximately 2000 ft (610 m) upstream of the confluence, Le Sueur Creek is joined by a major tributary, Forest Prairie Creek. The two streams drain a basin the majority of which is cultivated. As both streams approach the valley of the Minnesota River, they become incised into the surrounding plains, occupying narrow, v-shaped valleys with a modest amount of floodplain. The major source of sediment appears to be sand and gravel from the valley walls obtained via bank erosion. Sand predominates, but material as coarse as 50 mm is clearly being carried by the streams. The problem of sediment supply is complicated by the existence of several gravel mining operations along the walls of the valley of Le Sueur Creek (Fig. 1). A valley wall denuded by such operations is shown in Fig. 8. The material on the slope is loose and easily erodible.

Tributary stream gradients are low on the plains and on the floodplain of the Minnesota River, but are quite steep where incised, i.e. of the order of 0.002. The steep slope aids the movement of coarse material supplied to the tributaries.

In the vicinity of the gravel operations, Le Sueur Creek has a bed surface of coarse gravel and cobbles. As the flood plain of the Minnesota River is approached, sand becomes progressively more common on the bed of the stream. Immediately upstream of the delta, the depositional sequence consists of thick layers of sand alternating with thinner layers of gravel.

Le Sueur Creek is not gaged. Estimates of flood flows near the delta were obtained by means of regional hydrology techniques (Guetzkow, 1977). These estimates are shown in Table 1.

HISTORY OF THE PROBLEM

Immediately prior to the construction of the bridge, Le Sueur Creek entered the Minnesota River at the outside of a gentle bend, a little upstream of the apex (Fig. 2). A small bar was present at the mouth of the tributary, producing a local, slight deflection of the flow toward the opposite bank.

Such a configuration tends to stabilize the growth of the bar. The westward depositional tendency on the east bank created as the tributary debouches into the main stem can be balanced by the eastward erosional tendency in the main stem as the main thread of flow shifts toward the outside of the bend. In time, the channel can adjust so that the capacity to

transport extra sediment supplied to the outside of the bend can approximately balance the supply.

This adjustment seems to be a historical fact maintained at least since 1873. The history of the channel planform since that time is delineated in Fig. 9, which is based on aerial photographs and maps. Although considerable channel migration has occurred upstream and downstream of the bridge, the reach in the immediate vicinity of the bridge was fairly stable from 1873 until construction. The gentle bend at the confluence migrated downstream somewhat during this period, but the tributary always entered on the outside of the bend.

Examination of other tributaries on the Minnesota River and other streams indicated that most do enter on the outside of bends, usually upstream of the bend apex.

Construction of the bridge and approaches was commenced in 1958. It was recommended that the bridge be designed for a flood of 66,000 cfs, at a water surface stage of 739.5 ft. The approaches were designed to be sufficiently high as to preclude overtopping. The channel itself was only about 300 ft (90 m) wide at the bridge. During severe floods, however, the floodplain, which is about 4250 ft (1300 m) wide, carries a substantial flow (Fig. 3). In recognition of the consequences of the severe constriction that would have resulted if the bridge spanned the channel only, extra floodway was provided. The channel being located near the eastern side of the valley at the proposed point of crossing, excavation was proposed along the west bank. The area of excavation can be seen by comparing Figs. 2 and 4.

The excavation was intended to provide extra conveyance during floods. Thus, it was not excavated to the level of the bottom of the channel proper, but rather to 720 ft (219.5) above mean sea level, a value that is typically about 5 ft (1.5 m) higher than the deepest portion of the channel at typical low flow. The excavation is shown in Fig. 10.

The bridge was provided with nine piers, shown in Fig. 10. The three easternmost piers (piers 7, 8, and 9) are large and deep, with seals at 701 ft (213.7 m). They were originally located within the channel proper. Piers 1, 2, 3, 4, and 5 were originally located in the floodway; they are shallow, with seals at 709 ft (216.1 m). Pier 6 is an intermediate pier, with a seal at 705 ft (214.9 m). The total length of the bridge span is 1100 ft (335.3 m).

Before the construction of the bridge, Le Sueur Creek entered the channel of the Minnesota River just downstream of the proposed bridge. In 1957, consideration was given to providing a separate span (or lengthened main span) for Le Sueur Creek, but the idea was abandoned later, primarily because of the cost. Instead, during construction the tributary was shifted so as to enter the main stem just upstream of the bridge.

In retrospect, it can be said that construction of a bridge downstream of a tributary large enough to significantly affect the morphology of the

main stem is inadvisable. Today, other case histories documenting similar problems are available (Brice, et al., 1978). The body of documented experience with similar cases was probably much less, however, at the time of construction.

The problem was compounded by the severe constriction of overbank flow, and the fact that the extra conveyance which was necessary to compensate for it had to be located on the inside of the bend (on the western side), because most of the floodplain lies to the west of the bridge. The floodway excavation was to a level 11 ft (3.4 m) below a bankfull stage of about 731 ft, or 222.8 m, and thus the floodway at the inside of the bend was occupied by flow even at stages well below bankfull.

Events between 1960 and 1965 are not documented well. It can, however, be surmised that the dispersal of flows over a much wider cross section at discharges from bankfull to as low as about twice the mean annual discharge tended to break up the strong main thread of flow that scoured the tributary mouth. Where before erosion and deposition were in balance, the mouth of the tributary likely became a depositional zone, so that a bar grew westward, forcing the main thread toward the floodway.

The largest flood on record at Mankato and Jordan (about 100,000 cfs, or 2830 cumecs at Le Sueur) occurred in the spring of 1965 (Fig. 3). As the flood receded, it became apparent that the bar had completely filled the original channel, and the channel thalweg had moved against piers 1, 2, and 3 in the original floodway. The severe constriction of overbank flows at the bridge caused scour well below the seals of these piers (Fig. 10). The constriction also gave rise to very swift velocities along the western approach adjacent to the bridge, causing scour.

The model study suggests that the following reconstruction of events during the flood may be accurate. During the flood peak the piers were probably subjected to severe general scour wherever dense vegetation had not become established. The deep backwater at the mouth of the tributary prevented its sediment load from entering the channel proper. This material was stored in the adjacent channel and floodplain of Le Sueur Creek. As the flood receded below bankfull, a thread of flow re-emerged in the backwater zone of Le Sueur Creek, moving the temporarily stored sediment as a slug onto the bar on the east side, and forcing the channel to the west. This reconstruction is supported by the field observation of similar phenomena on other streams (Patton, Baker, and Kochel, 1979).

Matters appear to have been complicated by the formation of a large log jam centered at pier 6, which likely aided the accretion of sediment onto the bar.

The above reconstruction indicates the very different ways in which the above-bankfull and below-bankfull flows respond to the bridge. At above-bankfull stages, the bridge acts as a constriction and the tendency is scouring at all points where dense vegetation has not taken root. At below-bankfull stage the excavation caused the region under the bridge to

behave as an expansion, encouraging deposition in general, and especially near a source of sediment such as the mouth of the tributary.

The bar emerged during the subsequent low flow, and eventually became densely vegetated, and finally forested. The dense vegetation caused the bar to become essentially impervious to overland erosion, even though similarly vegetated floodplain deposits are readily eroded by side-cutting at the outside of bends not far from the site in question (Fig. 9).

The reason that the bar was not subsequently removed by side-cutting is readily apparent in Fig. 4. The bar is seen to be so large that it has changed the sense of the bend. Le Sueur Creek is seen to enter on the inside of the bend. Any tendencies for bank erosion are subsequently directed at the western side of the channel, rather than against the bar on the east side. The depositional tendency of the tributary thus combined with the depositional environment created by the main stem on the downstream, inside portion of the bend (the downstream western edge of the bar) to create a very unstable state of affairs. Nothing exists to counter deposition on most of the bar. It can only grow westward and downstream, leading to progressively less favorable conditions.

After the flood of 1965, a spur dike was constructed on the western floodplain adjacent to the channel in an attempt to alleviate scour at the western approach, and to provide a more natural approach to the bridge. This spur dike is visible in Fig. 4. In 1969, another major flood (about 80,000 cfs, or 2260 cumecs) occurred, which eroded the tip of the spur dike, and excavated a deep scour hole (as much as 22 ft or 6.7 m deep) along it (Fig. 5). The approach just beyond the western abutment was severely eroded, and subsequently was protected with riprap.

Between, 1969 and 1980, the problem became progressively worse. The new bend of reversed sense began to behave like a typical bend and started to migrate downstream. Thus on the outside (west side) of the bend, deposition occurred upstream of the apex (the bridge itself), and erosion occurred downstream of the apex. By 1980 the upstream deposition had filled much of the floodway excavation up to near the original level of the floodplain (Fig. 5). The downstream erosion has been mercifully modest in light of the proximity of a sewage lagoon, visible in Fig. 5. Scour continued to occur to unacceptably deep levels at the western piers during high flow. Meanwhile, as the bar grew, piers 8 and 9 became buried in deposits 20 ft (6.1 m) above the top of the footings (Fig. 11).

The problem became of enough concern by 1980 that a search for remedial action was commenced. As contingency measures, the bar was stripped of vegetation to stump level, the channel between piers 1 to 4 was filled with riprap to an elevation of about 720 ft (219.5 m), and a pilot channel was dug between piers 7 and 8, along a course roughly approximating the original channel (Fig. 11). Serious consideration was also given to deepening the footings of several of the western piers, a technique that had worked successfully elsewhere (Anderson, 1965). Finally, the services of St. Anthony Falls Hydraulic Laboratory were obtained for the performance of a model study to test a variety of remedial measures.

The contingency measures proved to be modestly successful. The pilot channel widened considerably, and the spring flood of 1982, which peaked at 16,700 cfs (473 cumecs), did not result in any worsening of conditions. On the other hand, the flow worked its way around the tip of the riprap and excavated a major low-flow channel between piers 4 and 5. By the summer of 1982, most of the low flow was carried by this channel, rather than the pilot channel between piers 7 and 8. In addition, a new bar began to build outward from the mouth of the tributary, deflecting the pilot channel westward (Fig. 6).

The new bar is as yet small. The deposits on it contain, however, a large percentage of gravel. Much of the surface of the bar is covered by a gravel armor, and the pilot channel itself is even more heavily armored (Fig. 12). It is estimated that flow velocities in excess of 6 ft/s (1.8 m/s) are necessary to mobilize this armor.

OPTIONS FOR RECTIFICATION

The existing problems with the bridge can be categorized as follows:

1. Floodplain flow is severely constricted. During floods capable of inundating the floodplain, flows distributed over a valley width of about 4250 ft (1300 m) must be forced underneath a bridge span of 1100 ft (335 m). The constriction can be expected to induce considerable general scour underneath the span during severe floods.

The constriction is, furthermore, more severe than the above numbers indicate. The bridge crosses the Minnesota River perpendicular to the pre-construction channel, but at an angle to a line drawn perpendicular to the downvalley direction. This causes floodplain flows to approach the bridge obliquely.

2. The western approach and piers are particularly susceptible to scour. Because the bridge is located on the east side of the valley, the effect of the constriction is felt most prominently on the west side. The spur dike constructed after the 1965 flood provided partial, but not complete, relief to the western abutment, as is evidenced by the scour there in 1969. The spur dike is apparently not adequate to throw the floodplain flow to the east against the deeper piers as it enters the channel.

3. The growth of the delta at the mouth of Le Sueur Creek has forced the low-flow channel to the west, has buried the deepest piers in sediment, and has reversed the sense of the bend. The reversing of the sense of the bend has made the bar at the mouth of Le Sueur Creek a predominately depositional zone at below-bankfull stages. The westward forcing of the river was reinforced by growth of the bar followed colonization by vegetation, preventing a balancing scour during floods. As the bar grew, the main thread of flow at below-bankfull flows moved westward against the shallowest piers at a progressively less favorable angle of attack.

In the course of discussion concerning the problem, several possible countermeasures were considered by the Minnesota Department of Transportation and St. Anthony Falls Hydraulic Laboratory. These are shown in Fig. 13. As enumerated previously, the contingency countermeasures implemented in 1981 included the following:

1. Trees and brush were cut down to as low a level as possible on the bar at the mouth of the delta. This improves conveyance and makes the bar more susceptible to erosion.

2. Piers 1 to 4 were protected with riprap.

3. A pilot channel was excavated between piers 7 and 8 in an attempt to encourage the river to return to its previous course.

Additional countermeasures were contemplated at various stages of the planning (Fig. 13). They included the following:

4. Extension of the riprap to pier 6 to protect the western piers from scour.

5. Construction of larger, lower seals for piers 1 to 5. The bottom of the new seals would be 700.5 ft (213.5 m). The piers would also be provided with longer piles. This would allow for additional protection against scour.

6. Extension of the spur dike to make it 400 ft (121.9 m) long rather than the present 250 ft (76.2 m). This would provide more protection for the western approach.

7. Implementation of various maintenance measures to control channel debris and bar and floodplain vegetation. This would improve overall conveyance and flow patterns.

Option 4 was investigated in the present study. Option 5 was initially rejected due to cost and the low clearance for pile driving. There are, however, other reasons for rejecting it. This option assumes that the channel thalweg would remain where it is, with a very poor angle of attack. In fact the sense of the bend dictates that the bar will continue to force the channel westward, worsening the angle of attack and rendering deeper seals only a temporary solution. In addition, piers 7, 8, and 9 already have seals at the depths proposed for the western piers; a low-flow channel passing underneath them would have the right sense to keep the mouth of the tributary scoured out.

In short, then, countermeasures should be tailored toward restoring the channel to its original position before construction.

Option 4 would contribute to this end by leaving only the region between piers 7, 8, and 9 available for scour. It represents, however, a sudden obstruction 524 ft (160 m) long perpendicular to the local flow (Fig.

13). A similar easterly deflection could be accomplished more gently and gradually by means of the option listed below.

8. The construction of one or more permeable dikes extending from the west bank diagonally into the flow upstream of the bridge (Fig. 13).

The main purpose of the permeable dikes would be to deflect much of the flow eastward into the pilot channel and against the mouth of the tributary. The flow passing through the permeable dike would be slowed, and would tend to drop its sediment out as a bar on the west side of the channel. A low, vegetated bar on the west side would help restore the correct sense of the bend, and maintain a scouring action against the mouth of Le Sueur Creek. Considerable experience with permeable dikes suggests that they work well in environments where an abundance of suspended sediment is available for deposition (e.g. Brown, McQuivey, and Miller, 1981).

There are several technical matters that need consideration in conjunction with option 8. If the permeable dike is set too high, the dike and the resulting bar on the west side would seriously reduce conveyance through the bridge during floods. In order to minimize this problem, the top of the permeable dike must be set well below bankfull stage, so that the in-channel deflecting and obstructing action is strong at low flows, moderate at bankfull flows, and weak at high flows. Some guidelines are available concerning such submerged dikes (Anderson and Davenport, 1968; Dhamotharan, Wetzell, and Dahlin, 1977).

A second consideration relates to debris. Permeable dikes, by their very nature, tend to collect debris, a certain amount of which improves their performance. Large debris, however, must be removed periodically. If the downstream end of the permeable dike is too close to the bridge, snagged large debris could induce scour and poor flow alignment.

A third consideration relates to the connection between the in-channel permeable dike and the floodplain spur dike. If a gap is left between the two, floodplain flows would be forced between the tip of the spur dike and the upstream end of the permeable dike, eroding the desired western bar and possibly endangering the western piers. The two, then, must be tied appropriately. This can be accomplished by means of a T-spur dike (Fig. 13).

An additional benefit to a combination of options 6 and 8 is the ability to use the T-spur dike to deflect floodplain flows eastward, maintaining a bias toward scour at the mouth of the tributary even at high flows. The bias must not be too great, or it would interfere with efficient conveyance and lead to poor angles of attack.

It was decided that a model study be used to evaluate options 4, 6, and 8, and to find the combination and setting most likely to alleviate the problem at the bridge. Option 5 was not considered, and option 7, although necessary, cannot be evaluated in the laboratory.

It should be mentioned that two seemingly obvious and effective options were not considered at all (Fig. 13).

9. Construction of a second bridge span on Le Sueur Creek, so as to allow it to enter the Minnesota River downstream of the present bridge.

10. Construction of a series of culverts under the western approach, alleviating the severe flow constriction of the bridge during floods.

Option 9 is considered to constitute only a last resort because of the high cost involved. It is difficult to implement option 10 because of the sewage lagoons just downvalley of the western approach (Fig. 13).

DESIGN OF THE MODEL

The area selected for modelling is shown in Fig. 1. The length of the reach modeled is 10,000 ft (3050 m) and the width is 4,600 ft (1400 m), i.e. the entire valley. A model basin with dimensions 60 ft (18.3 m) by 27.5 (8.4 m) was chosen for the study. Due to the necessity for inlet boxes, sediment traps, and other items, the useful area was reduced to a rectangular area 50 ft (15.2 m) by 23.5 ft (7.2 m) in size for the Minnesota River and its flood plain, and a smaller adjacent area (14 ft by 4 ft, or 4.3 m by 1.2 m) for Le Sueur Creek (Fig. 14). The area to be modeled fits into the basin at a scale of 1:200.

The scale of 1:200 applies only to horizontal distances. The vertical scale was distorted by a factor of five, so that the vertical scale ratio is 1:40. The necessity for this is related to bed mobility, which can be measured in terms of the Shields stress τ^* , where

$$\tau^* = \frac{HS}{RD_{50}}$$

and H is cross-sectionally averaged depth, S is downstream energy slope, R is the submerged specific gravity of the bed material (about 1.65 for sand) and D_{50} is a median bed material size (about 0.4 mm). At prototype bankfull flows, τ^* takes a value of about 0.60, or about 15 times the value required for the initiation of motion. At an undistorted scale of 1:200, model valley slope would be unaltered at 0.000156, model bankfull depth would be 0.8" (2 cm), and model grain size would be two microns. The small slope implies an elevation drop of 0.075" (1.9 mm) over a valley length of 40 ft (12.2 m). It is very difficult to accurately set an elevation difference in water surface of less than two millimeters. At a depth of 0.8" (2 cm), small-scale ripples are likely to interfere with the bed pattern. Finally, two-micron material is clay, and thus cohesive; it would not move at all in the model.

At a 1:5 distortion, model valley slope becomes 0.00078, implying an elevation of difference of 0.375" (9.5 mm) over a 40 ft (12.2 m) reach: bankfull depth becomes 4" (10.1 cm). These values are manageable in the laboratory. Even if sediment size is scaled with the vertical scale alone, however, the resulting diameter is 10 microns, which is still unacceptably small.

One solution to this dilemma is to employ the same size sand in the model as in the field, relying on the five-fold increase in slope in the distorted model to render the sand mobile. In the present case, this would lead to a model bankfull Shields stress of about 0.077, or less than twice the value required for motion. At such low Shields stresses, transport rates would be so low that several weeks would be required to attain equilibrium for each different discharge. In addition, scour and fill at bends, constrictions, and expansions may be inaccurately predicted by the model if τ^* is not of the same order of magnitude in the model and prototype.

A way out of this dilemma is provided by the use of lightweight model bed material. In fact, crushed walnut shells, with a submerged specific gravity R of about 0.35, were employed. Two grades were tested, one with a D_{50} of about 0.31 mm, and one with a D_{50} of about 0.66 mm (Fig. 15). In the model, τ^* is about 12 times the value required for the initiation of motion in the former case, and 5 times that value in the latter case. These values are of the same order of magnitude as the prototype; they assure a mobile bed and also some suspension. As is outlined subsequently, the coarser grade proved to be the more appropriate of the two. The size distributions are shown in Fig. 15.

Froude modelling was employed to scale the flows; that is, for each flow, model Froude number and estimated prototype Froude number were made to match. The general form of the distorted Froude scaling law for discharge is

$$(Q)_m = (Q)_p \lambda_v^{3/2} \lambda_h$$

where Q denotes discharge, the subscripts m and p denote model and prototype, respectively, λ_v is the vertical scale ratio (1:40), and λ_h is the horizontal scale ratio (1:200). For the present study, then,

$$(Q)_m = 1.98 \times 10^{-5} (Q)_p$$

Model and prototype values of various parameters for the Minnesota River and Le Sueur Creek are shown in Table 1.

Water is introduced to the model basin from a headbox at the upstream end of the Minnesota River, a headbox to the side for Le Sueur Creek, and

a manifold across the upstream end of the basin to ensure even initiation of overbank flow when required (Fig. 14). Discharge is monitored with standard orifice meters calibrated with the weighing tanks available at St. Anthony Falls Hydraulic Laboratory.

Model sediment is introduced to the Minnesota River and Le Sueur Creek via two Accu-Rate Co. screw feeders, each placed adjacent to the appropriate headbox. The feeders proved to be quite reliable. A view of one is shown in Fig. 16.

The model itself was constructed based on a 1-ft contour topographic map of the region from Mark Hurd Co., and channel cross sections taken by the Minnesota Department of Transportation. Templates were constructed from sheet metal to the shape of the topography, and these were secured to the floor of the basin. Fill of bricks, sand, and finally concrete was used to form the complete topography. It should be noted that the auxiliary basin for Le Sueur Creek does not accurately model prototype conditions. Le Sueur Creek has been bent to the south so as to fit within the available space, and provided with a steep initial slope so that sediment can be introduced upstream of the zone of slack water at high flows. A view of the model basin is shown in Fig. 17.

Model tailwater is controlled with an adjustable tailgate. Walnut shells can be collected from the sediment trap (Fig. 14), dried, and reused. Elevation measurements can be taken with a point gauge from a carriage riding on rails that can be accurately leveled.

An appropriately distorted model of the bridge, including deck, piers, footing, seal, and several piles each, was constructed from plastic.

Model construction commenced in the middle of July, 1981; except for minor details, the model was complete by the end of October, 1981.

OVERVIEW OF THE EXPERIMENTS

In a sediment-feed movable-bed model, water discharge, sediment feed rate, and tailgate weir elevation can be set independently. Once these parameters are set, the flow and bed topography in the model will eventually reach an equilibrium state, with a certain pattern of bed topography, flow depth, and water surface slope. In a Froude model, discharge can be set a priori to the correct value. Sediment feed rate and tailgate elevation must be determined by trial and error so that the desired water surface slopes and depths are obtained. In short, the model must be calibrated to reproduce the field situation.

The detail of calibration is partly determined by the availability of field data. In the case of the present study, typical parameters at bankfull stage for unconstricted cross sections (i.e. cross sections not adjacent to the bridge) could be estimated from hydrologic records, cross-

sectional data, and topographic maps. These estimates are shown in Table 1. Since the reach in question appears to be in grade, the values of Table 1 presumably also apply to the preconstruction channel.

The vicinity of the bridge was provided with several detachable concrete pieces, the insertion of which allowed for the replication of the preconstruction channel. Several months of time were expended in an attempt to find the correct feed rates for the reproduction of bankfull flow.

Information for the verification of flows other than bankfull is sketchy. The high-water mark on the upstream side of the bridge in the flood of 1965 was at 743.9 ft (226.7 m); peak discharge was about 100,000 cfs (2830 cumecs). In the flood of 1969 the flow crested at about 742.9 ft (226.4 m) and 80,000 cfs (2260 cumecs). In the absence of better information, overbank flows were calibrated by adjusting the tailgate and feed rate until the following criteria were satisfied.

1. The overall down-channel water surface slope over a reach much longer than that affected by the bridge should approximate the bankfull value. This provides for fairly even inundation of the floodplain, except near the constriction at the bridge.

2. Typical in-channel flow depths should be about the same upstream and downstream of the bridge, with an overall bed slope roughly parallel to the water surface slope. Scour at narrower sections, and fill at wider sections, proved to be very prominent at the higher flows, rendering the evaluation of this criterion less than straightforward.

3. Where a peak water surface elevation was known, the model was adjusted to reproduce it.

In order to cover a wide range of flow, the following discharges were chosen for testing; 7000 cfs (200 cumecs), 22,000 cfs (620 cumecs), 40,000 cfs (1130 cumecs), 60,000 cfs (1700 cumecs), 80,000 cfs (2260 cumecs), and 100,000 cfs (2830 cumecs). Corresponding flood frequencies and estimated flows for Le Sueur Creek are shown in Table 1. All runs except those of the last series were performed at constant discharge, assuming that the main stem and tributary are perfectly in phase. Constant discharge and feed rate were continued for a long time, until water surface slope, water surface elevation at the bridge, and bed topography approached a steady state.

At the highest discharges, the observed scour and fill resulting from a long, steady continuation of the discharge in question is likely more than would be observed during the passage of a typical hydrograph. In particular, general scour at the bridge constriction at the three highest flows is probably somewhat excessive. An attempt was made to correct for this by running a step hydrograph in the last series.

At least one effect of phase could be seen at the higher flows. Experiments were often terminated or temporarily halted by first shutting

the flow to the main stem, and then shutting the flow to the tributary. The often dramatic growth of the bar at the mouth of the tributary is described in some detail subsequently.

Entrance and exit effects proved to be severe at the highest discharges, and were typically manifested in terms of an excess of floodplain (compared to channel) flow. Minor adjustments were made with the use of submerged angle irons on the floodplain.

After trial runs with two other types of model bed material, 20-30 grade crushed walnut shells were chosen for the main body of experiments. The size distribution is shown in Fig. 15. The main stem feed rates and water surface elevations (just upstream of the bridge) obtained via calibration are shown in Fig. 18.

The total set of runs can be divided into twelve series. A brief description of each series is provided below. Several of the series are described in more detail in the next chapter.

Series 1. Based on a consideration of similarity of sediment motion and the Engelund-Hansen (1967) load equation, crushed walnut shells with a typical size between 0.3 and 0.4 mm were chosen for the model. An appropriate material is sold commercially as 30-100 grade crushed walnut shells; it proved to have a median size D_{50} of 0.31 mm (Fig. 15). An attempt was made to calibrate the model with this material at discharges of 22,000 cfs (620 cumecs) and 80,000 cfs (2260 cumecs).

Calibration could be successfully accomplished at the lower (bankfull) discharge. The sediment moved actively in both the modes of bedload and suspended load. Required feed rates proved, however, to be about three times higher than estimated. The relative ease of suspension caused much of the material to escape the sediment trap and wash down the drain, so that supplies were depleted quickly.

At the higher discharge, the predilection of the material to be suspended was very high, and in many places the channel bottom was swept clean. Large deposits developed on the floodplain. The amount of scour was considered to be unrealistic, and it was decided that a coarser grade of walnut shells was necessary. To this end, 20-30 grade walnut shells were ordered.

Series 2. The coarser walnut shells required three weeks for delivery due to bad weather. In the interim, exploratory experiments were made with an available grade of sand with a D_{50} of 0.46 mm (Fig. 15). As expected, bed motion was negligible at bankfull flow.

Series 3. The coarser walnut shells proved to have a D_{50} of 0.72 mm. Later, when supplies ran low, an additional batch of the same material was ordered; it proved to be somewhat finer, with a D_{50} of 0.60 mm (Fig. 15). Calibration was successfully attempted at discharges of 22,000, 80,000, and 100,000 cfs (620, 2260, and 2830 cumecs). The sediment moved both as

bedload and suspended load, but the amount of suspension was much less than was the case for the 30-100 grade material.

At the time of these experiments, it was surmised that the bar at the mouth of the Le Sueur Creek had been deposited during flood flows. An attempt was thus made to reproduce the large bar at the mouth of Le Sueur Creek (Figs. 4, 5) by gradually increasing the feed rate to Le Sueur Creek at main stem flows of 80,000 cfs (2260 cumecs) and 100,000 cfs (2830 cumecs). It proved impossible to form a bar at any feed rate.

The reason for this was the slack floodwater at the mouth of the creek. As the sediment-laden flow of the creek entered this slack water region, the sediment dropped out in the channel and adjacent floodplain, and eventually accumulated in copious amounts without entering the main stem. An attempt was made to force sediment into the main stem by providing the tributary with low concrete dikes on either side to concentrate the flow. These dikes, visible in Fig. 21, proved to be useless. They were later removed.

Shutdown was often accomplished by turning off the main stem first and the tributary later. It was noticed during one such shutdown that as stage declined to near- and below-bankfull levels in the main stem, a strong tributary current re-emerged from the slackwater zone, moving large amounts of floodplain sediment into the channel. This led to the formation of the desired bar. It was later found that the bar could be reproduced at constant discharges and feed rates, as long as the main stem was at or below bankfull stage.

Series 4. The experiments of Series 4, 5, and 6 coincided with the approach of the 1982 spring flood season. Near-record quantities of snow being on the ground, there was worry that a severe flood could occur on the Minnesota River. Series 4 was devoted to testing the efficiency of the riprap from the western abutment to pier 4, installed as a contingency measure in 1981. A possible extension of riprap to pier 6 was tested as well. The bar at the mouth of the tributary was purposely constructed in the channel from 9 mm gravel, leaving the bed movable (except for the riprap) between the western abutment and pier 6. The channel was run to equilibrium at 22,000 cfs (620 cumecs), i.e. bankfull flow, and riprap was set from the western abutment to between pier 3 and pier 4. A run was conducted at 80,000 cfs (2260 cumecs). Then riprap was extended to pier 6 and another test was done at 80,000 cfs (2830 cumecs). The results from this series warranted the more detailed testing of the next two series. All the subsequent series are outlined below and discussed in more detail in the next chapter.

Series 5. In these runs, the large bar at the mouth of the tributary was again simulated in gravel, and riprap was placed from the western abutment to between piers 3 and 4. Runs were conducted at 40,000, 60,000, 80,000, and 100,000 cfs (1130, 1700, 2260, and 2830 cumecs).

Series 6. The large riprap bar at the mouth of the tributary was tested in conjunction with riprap from the western abutment to pier 6.

Runs were conducted at 22,000, 60,000 and 100,000 cfs (620, 1700, and 2830 cumecs). A final run was conducted at 100,000 cfs (2830 cumecs) with no riprap or gravel bar.

Series 7. This long series of runs was conducted in order to find an appropriate position, size and angle for the T-spur dike. All runs were conducted at 60,000 cfs (1700 cumecs) using a mock-up of the spur dike constructed from sheet metal. After completion of these runs the T-spur dike was formed in concrete.

Series 8. The formal testing of the concreted T-spur dike was conducted at 60,000 cfs (1700 cumecs), then 100,000 cfs (2830 cumecs), and then 80,000 cfs (2260 cumecs), all the while making adjustments. During the last run a first version of the submerged permeable dike was installed in order to test its effect on conveyance during a severe flood.

Series 9. The submerged permeable dike was tested at bankfull flow (22,000 cfs or 620 cumecs) with a high feed rate from Le Sueur Creek. The bar at the mouth of Le Sueur Creek formed readily, but the permeable dike clipped its western growth, and induced a low bar on the opposite bank. A second submerged permeable dike was placed upstream. Later, the feed from Le Sueur Creek was halted, and erosion of the bar at the mouth of the tributary was observed.

Series 10. The permeable dikes were tested at 7000 cfs (200 cumecs) in three successive runs, with no feed, a low feed rate, and a high feed rate from Le Sueur Creek.

Series 11. The permeable dikes were again tested at 22,000 cfs (620 cumecs), with no feed, and then with increasingly higher feed rates from Le Sueur Creek.

Series 12. Final adjustments were made to the T-spur dike, and the permeable dikes and the T-spur dike were tested using a simulated hydrograph beginning at 22,000 cfs (620 cumecs), increasing to 100,000 cfs (2830 cumecs), and again declining to 22,000 cfs (620 cumecs). Series 12 was the last series of the study.

EXPERIMENTAL RESULTS

The most detailed runs are those of series 5 to series 12. Documentation included water surface and bed profiles, and photographic and videotape records for runs 6 to 12. Experimental results for these runs are described below. A guide to the videotapes is provided in the appendix.

Series 5. The experiments in this series were conducted at above bankfull discharges. Their purpose was to detect the stability of the riprap placed as an emergency measure from the west bank to pier 4 when

subjected to floods of various severities. The riprap used in the field was limestone quarry rubble. During a site visit, twelve fairly typical grains were selected, and their b-axes were measured. The average length of the b-axis was found to be 90 mm. It was decided to model the riprap in sand rather than a lightweight material, so that the submerged specific gravity R is approximately the same in the laboratory as it is in the field. The appropriate modeling criterion is that the Shields mobility parameter based on riprap size D_r be the same in both the model and the prototype; where

$$\tau_r^* = \frac{HS}{RD_r} ,$$

it is required that

$$(\tau_r^*)_m = (\tau_r^*)_p$$

In the distorted Froude model, cross-sectionally averaged depth transforms as

$$(H)_m = \lambda_v (H)_p$$

and slope S transforms as

$$(S)_m = \frac{\lambda_v}{\lambda_h} (S)_p$$

It follows from the above four equations that if $(R)_p = (R)_m$, then

$$(D_r)_m = \frac{\lambda_v^2}{\lambda_h} (D_r)_p$$

or

$$(D_r)_m \cong 11 \text{ mm}$$

In order to obtain an appropriate model riprap size, gravel was sieved such that 100 percent passed through a 12.7 mm sieve, and none passed through a 6.5 mm sieve. An effective resultant size is about 9 mm rather than 11 mm.

This model riprap was used throughout the study wherever riprap was required.

It was later found that the field riprap particles taken from the surface were in fact small because they had been partially broken down by a truck used for end dumping. A more typical riprap size is about 1 foot (300 mm).

Due to the inability to form a bar at the mouth of Le Sueur Creek at above bankfull flow via sediment feed, an approximation of the bar was constructed in place from the riprap material. The bar was cut back slightly from its field dimensions (Fig. 5) so that only piers 7, 8, and 9 were protected by the riprap bar. This riprap served to approximate the stabilizing effect of the bar, allowing it to withstand severe floods without overland erosion. Riprap was also placed from the west bank to between piers 3 and 4 on top of the walnut shell bed, according to the general specification of Fig. 11. Piers 4, 5, and 6 were left completely unprotected, and pier 7 was left protected only on one side.

In addition to several trial runs, four main runs were conducted in this series. Prototype discharges are listed below in cfs.

<u>Run No.</u>	<u>Minnesota River</u>	<u>Le Sueur Creek</u>
5-1	40,000	2,500
5-2	60,000	3,200
5-3	80,000	4,200
5-4	100,000	5,400

The resulting scour at the bridge is shown in Fig. 19. The riprap itself under piers 1 to 4 proved to be quite effective. It was not entrained at any of the flows. It did, however, ravel as crushed walnut shells were eroded from below. The raveling provided a self-launching effect, protecting against scour.

In fact, some deposition of walnut shells was observed on top of the riprap of piers 1 and 2 at the lowest two discharges. This was associated with separation of flow at the tip of the western approach, the prototype version of which is visible in Fig. 4. This separation may have been due to an error in the shape of the spur dike in the model.

The main feature of interest in Fig. 19, however, is the scour between piers 4 and 7. At 60,000 cfs, maximum scour is against pier 6, but has still not reached the seal. At 80,000 cfs, however, the seals of piers 5 and 6 have been left exposed. At 100,000 cfs, the seal of pier 4 is also left exposed, and the point of maximum scour has moved one pier westward. The maximum depth of scour, 692 feet, is similar to the maximum measured prototype depth of scour of 693 ft shown in Fig. 10. (This latter value may still not represent a maximum depth of scour during the flood of 1965 due to the near impossibility of measurement of the flood peak.)

The riprap thus proved effective in protecting the westernmost piers, but only at the expense of the middle piers. The bridge appears barely safe at 60,000 cfs, but is in imminent danger of failure at 80,000 cfs. This behavior proved consistent in all runs of all subsequent series, regardless of the adopted configuration of corrective measures; the bridge is barely safe at 60,000 cfs, but at 80,000 cfs, scour occurs below the seal at at least one of the piers not protected by riprap. The cause of this behavior is the severe constriction at the bridge at flow above 60,000 cfs.

It should be noted that peak scour in this series, and in all series except series 12, was probably exaggerated by the procedure of continuing the run to a verifiable equilibrium. In the field, this equilibrium may not be reached before the hydrograph begins to recede.

Series 6. This series of runs was conducted in order to explore the effectiveness of placing riprap from piers 1 to 6 as a means of providing long-term protection against scour induced by floods. For this reason, the bar composed of riprap at the mouth of the Le Sueur Creek was removed. The entire bed near the bridge was thus left erodible except for the region along piers 1 to 6. The placement of the riprap is shown in Fig. 20.

The riprap was tested at discharges of 22,000, 60,000, and 100,000 cfs in the main stem. No sediment was fed in from Le Sueur Creek. The runs may be categorized as follows:

<u>Run No.</u>	<u>Minnesota River</u>	<u>Le Sueur Creek</u>	<u>Results</u>
6-1a	22,000 cfs	2,200 cfs	riprap to pier 6
6-1b	22,000 cfs	0 cfs	riprap to pier 6
6-2a	60,000 cfs	3,100 cfs	riprap to pier 6
6-2b	60,000 cfs	0 cfs	riprap to pier 6
6-3a	100,000 cfs	5,400 cfs	riprap to pier 6
6-3b	100,000 cfs	0 cfs	riprap to pier 6
6-4	100,000 cfs	5,400 cfs	riprap removed

Patterns of scour are shown in Fig. 20. It is again seen that scour is acceptable at 60,000 cfs, but unacceptable at 100,000 cfs, even though it occurs at a place very different from that observed in series 5. The consistency of scour suggested that it is due to the constriction at the bridge itself, and not the specific placement of the riprap. In order to verify this, all riprap was removed in the last run, and a flow of 100,000 cfs was continued for over 40 hours of model run time. The resulting scour left the seals of every pier exposed. The scour shown in Fig. 20 for this run is probably far in excess of what might be observed in the field, as it represents a continuous flow of 100,000 cfs (about a 74 year flood) for over two weeks of prototype time. It nevertheless serves to illustrate the severity of the constriction at high floods.

The zone of constriction at high flows is indeed a zone of expansion at flows at or below bankfull discharge. This change in nature can be seen by following the photographs represented by Figs. 21 ~ 29.

Figure 21 shows streamline patterns in the Minnesota River with the tributary flow on; Figure 22 shows the corresponding patterns with the tributary flow off. The streaks are produced by a time-lapse exposure of the flow with confetti floating on the surface. In both photographs the streaks in the main stem are seen to shorten as the bridge is approached and the channel flow decelerates and spreads out, and then lengthen as the channel narrows downstream of the bridge. When the reach underneath the bridge constitutes an expansion, the effect of tributary flow is significant, penetrating well into the main flow. This can be seen by comparing Figs. 21 and 22. If the tributary were carrying sediment, a bar would have formed at the mouth of the tributary. (It is shown later than this is indeed the case.)

In Fig. 23, the channel of run 6-1a has been drained in order to illustrate the state of the bed. The channel is deepest near pier 7, or immediately off the tip of the riprap. Part of the eastern end of the riprap has been covered with sediment. It is seen in Fig. 20 that as flow increases, the point of maximum scour moves easterly away from the tip of the riprap.

In Figs. 24 and 25, streamlines are shown for runs 6-2a and 6-2b (60,000 cfs), respectively. The effect of tributary flow on the main stem is greatly subdued due to the slack floodplain water through which the tributary must pass. The artificial dikes along Le Sueur Creek, visible in both photographs, tend to exaggerate the effect of the tributary on the main stem, weak as it is even in their presence. It will be recalled that they were installed earlier in order to force formation of a bar at the mouth of Le Sueur Creek; they failed in this purpose due to the slack water. The flow patterns in Figs. 24 and 25 illustrate why a bar cannot form at the mouth of the tributary at flows well overbank; the sediment would first deposit in the slack water of the floodplain.

Careful observation of the main stem streamlines in Figs. 24 and 25 indicates that the flow as a whole accelerates underneath the bridge due to the constriction of floodplain flows. The potential for general scour thus increases greatly.

The bed at the completion of run 6-2a is shown in Fig. 26. The line of riprap constitutes a sudden obstruction, and considerable general scour is observed in front of it. Below an elevation of about 715 ft, the riprap is one grain thick, the result of raveling from above in response to scour. Maximum scour is, however, seen to be against pier 8. No seals are exposed.

The accelerative effect of the constriction is seen to be accentuated in Fig. 27, denoting streamlines for run 6-3b (100,000 cfs). A comparison of Figs. 25 and 27 indicates that the eastward deflecting action of the

existing spur dike increases markedly as discharge increases from 60,000 to 100,000. Scour is extreme and well below the seals of piers 7 and 8 at 100,000 cfs. This can be seen in Fig. 28.

The result of removing the riprap, and running at 100,000 cfs for over 40 hours, is shown in Fig. 29. All of the piers are exposed below their seals. The rubble at the bottom of the channel represents the remains of the removed riprap. Scour is essentially to the bottom of the river tray just in front of the bridge, where a sheet metal bottom rib is visible. While the scour is unrealistic due to the long duration of the run, the extreme effect of the constriction of high floods is vividly illustrated.

It can be seen in Fig. 21 that a portion of the floodplain has been cut out along the spur dike. This area was later filled with the 0.5 mm sand shown in Fig. 15. This allowed for a quantitative evaluation of scour around the tip of the spur dike during floods. Significant scour of this material at the upstream end of the spur dike, and some deposition of the scoured material at the downstream end, was observed at 60,000 and 100,000 cfs. The acceleration at the tip and downstream deposition are discernible in Fig. 25; the acceleration at the tip is seen to be more intense in Fig. 27.

Series 7. The experiments of the six previous series served to reveal the very different roles played by above-bankfull and below-bankfull flows at the bridge. At above-bankfull stages, it is necessary to bring the flow on the western floodplain into the constriction as smoothly as possible, in such a way as to protect the western approach and western piers. The T-spur dike shown in Fig. 13 provides a means for accomplishing this. It acts to draw the flow away from the western approach and direct it into the channel toward the deeper eastern piers. As such, it has the potential to solve some of the scour problems at flood stages. It does not relieve the constriction, but on the other hand it in itself should not greatly interfere with conveyance under the bridge if designed properly.

The runs of series 7 were devoted to obtaining this design. The T-spur dike was first fabricated from sheet metal so as to allow for easy alteration of the length and angle of the stem and top of the T. A large variety of settings were tested at the single discharge of 60,000 cfs. Flow patterns were ascertained with confetti, and recorded on videotape.

The first design tested called for a stem about twice as long as the one shown in Fig. 30, and T-angled more sharply downstream. The long stem stagnated the water between the stem and the western approach, and forced the floodplain flow into the channel at nearly a right angle to the channel flow. The flow refused to follow the downstream end of the top of the T; it rather separated from it, leading to a very erratic flow skewed too far to the east. By a process of trial and error, the T-spur dike was shortened in stem length and angled so as to avoid separation. The ultimate result of this process was the configuration of Figs. 30 and 31.

The streamlines visible in Fig. 30 indicate a smooth deflection of floodplain flow to the east, with little eddying. Velocities are reduced

on the west side of the bridge, thus preventing excess scour. As seen in Fig. 31, pier 8 was exposed to just below the seal at 60,000 cfs, confirming the previous observation that this discharge represents a threshold value above which the exposure of the seal of at least one pier is probable.

Two features are of interest in Fig. 31. The dikes along Le Sueur Creek have been removed. In addition, quartzite sand has been placed along the outside edge of the spur dike in order to observe scour. The size distribution of the sand is shown in Fig. 15. Scour at the upstream end, and deposition of scoured material at the downstream end of the top of the T-spur, is visible in Fig. 31.

Series 8. The sheet-metal T-spur dike of Figs. 30 and 31 was then formed in concrete and subjected to tests at a variety of flood flows over a period of six weeks. During the entire period, minor adjustments were made to improve performance.

The first tests of the concreted T-spur dike were conducted at 60,000 cfs. A riprapped excavation was provided around the dike in order to improve flow conditions (Fig. 32). Flow patterns were found to be similar to those observed with the sheet-metal T-spur dike (Fig. 33). Swift floodplain flow is pulled away from the western approach well upstream of the bridge, and little separation occurs off the tip of the T-spur dike.

Scour at the piers is somewhat greater than in the case of the sheet-metal dike, as can be seen by comparing Figs. 32 and 31. The concreted T-spur dike apparently protruded sufficiently into the channel to interfere with the conveyance. When tested at 100,000 cfs, the same T-spur dike tended to throw the floodplain flow too far to the east (Fig. 34). The resulting scour at the bridge piers is, however, not much different from the excessive scour associated with the spur dike existing in the field, as can be seen by comparing Figs. 35 and 29. (The slightly smaller degree of scour apparent in Fig. 29 is likely an artifact of the leftover rubble from the previously installed riprap; this rubble was completely removed before the beginning of series 8.)

In order to increase conveyance and to divert the flow less intensely to the east, the tip of the T-spur dike was shortened. A test of 80,000 revealed an improved flow pattern (Fig. 36) but again excessive was observed scour at the piers.

At this point the rationale behind the T-spur dike was reviewed. At discharges above 60,000 cfs, the results of the several series suggest that unacceptable scour at some piers will occur regardless of the type of spur dike, or even the existence of a spur dike. The scour is due to general constriction, and can be alleviated only by riprap, deeper piers, or less constriction. The T-spur dike does, on the other hand, maintain a strong thread of flow against the mouth of Le Sueur Creek and should act to help keep the main channel on the east side. It also helps maintain a bias toward scour on the east side, which can withstand more scour than the west

side due to its deeper piers. As a result, even with intense constriction scour, it can encourage the development of a state under which the bridge would fail only at a discharge considerably higher than that which would cause failure in the existing field configuration up to 1980 (Fig. 5).

Due to the above considerations, attempts to find a T-spur dike configuration that would leave all seals unexposed at discharges higher than 60,000 cfs were abandoned. Instead, a configuration was sought that would lead to a smooth, even, but not excessive deflection of floodplain flows to the east, without loss of conveyance.

To this end, further attempts were made to reduce the eddying and excessive deflection to the east at the highest discharges. It was found that if the area just upstream of the excavation at the downstream tip of the T-spur dike were elevated with riprap, eddying would be avoided. As a result, the spur dike could be angled more nearly downstream without serious separation. These features can be seen by comparing Fig. 37 with Fig. 36.

Figure 37 shows another feature of importance. A first version of the in-channel submerged permeable dike can be seen. The permeable dike is intended to perform best at below-bankfull flows. It was tested in the run of Fig. 37 in order to ascertain beforehand any negative effects on conveyance at very high flow. No such effects were noted.

The geometry of Fig. 37 was tentatively accepted as appropriate. As an added precaution against loss of conveyance, however, the entire downstream end of the top of the dike was amputated at the end of series 9 (Fig. 44). Although detailed records were not taken, a flow of 80,000 cfs was again tested, and the results indicated an adequate but not excessive deflection of floodplain flow to the east, representing a compromise between the patterns of Fig. 37 and Fig. 25. Further testing was performed in series 12.

It should be mentioned that in all flow conditions observed in series 8, the T-spur dike encouraged the formation of a surface cross-jet of floodplain flow, impinging obliquely against the channel flow. This surface cross-jet showed a tendency to meander somewhat. As a result, a generally adequate thread of flow under the bridge would occasionally migrate considerably to the east or west.

Series 9. Attention was now focused on bankfull conditions. At bankfull discharges or below, the T-spur dike is left emerged on the floodplain and serves no useful purpose. The area under the bridge acts as an expansion, and a relatively depositional environment is created.

Two runs were conducted in this series. The first run was a qualitative test of the hypothesis that a bar should form readily at the mouth of the tributary at bankfull flow (22,000 cfs). The effect of a preliminary version of the permeable dike, constructed from a single piece of 1/4" wire mesh, was also observed. Sediment was fed into the tributary at the rate

of 80 grams/minute, or about fifty percent of the feed rate to the main stem. As can be seen in Fig. 38, a bar approximating the dimensions of the one observed in the field in 1968 (Fig. 4) formed. In the figure, the bar is rendered visible by the use of new (light) crushed walnut shells in the tributary, and old (dark) crushed walnut shells in the main stem. In fact the deepest part of the channel was observed to be against pier 6, and a weak bar did develop on the west side of the channel behind the spur dike.

In the next run the same water discharges were used, but the sediment feed to the tributary was cut off. In order to achieve better performance, the permeable dike was made less permeable by adding two more layers of mesh. The angle of the dike was changed, and a prototype distance of 200 ft was maintained between the tip of the dike and the nearest pier. This was done in an attempt to set a design that would minimize debris problems. A smaller second permeable dike was added upstream.

The purpose of the run was to test the ability of the permeable dike to induce deposition behind it and wash away the bar at the mouth of the tributary. Approximately forty-eight hours of run time was required before the new equilibrium was reached. This final state exhibited a gentle eastward deflection of the flow (Fig. 39), and a prominent bar behind the permeable dike (Figs. 40, 41). It was concluded that the concept of the permeable dike is sound.

Series 10. Based on the above experiment, tentative settings for the two permeable dikes were determined. These can be seen in Fig. 42. The downstream permeable dike is tied to the truncated T-spur dike at its upstream end. The top elevation there is at 728 ft, or three feet below bankfull stage. The permeable dike tapers downstream to a final elevation of 722 ft. The shorter permeable dike upstream has a top elevation set at 720 ft. It is thus seen that both permeable dikes are submerged at bankfull flow, and are covered by very deep water (10 ~ 18 ft) at a flow of 60,000 cfs. The intent is to provide flow retardation (inducing sedimentation) and easterly deflection at low flows, but to interfere as little as possible with conveyance at high flows.

Series 10 was devoted to testing the performance of the permeable dikes at flows well below bankfull. A main stem discharge of 7,000 cfs was selected to this end. Increasingly higher sediment loads were fed into Le Sueur Creek; the ability of the permeable dike to limit tributary bar growth, induce deposition on the west side, maintain the correct sense of the bend, and maintain maximum scour against one of the three deep piers was observed. The following runs were performed, all with a main stem discharge of 7,000 cfs and a tributary discharge of 400 cfs.

<u>Run No.</u>	<u>Feed Rate</u> <u>Minnesota River</u>	<u>Feed Rate</u> <u>Le Sueur Creek</u>
	(grams/min)	(grams/min)
10-1	105	0
10-2	105	20
10-3	105	50

The final run constituted a severe test of the permeable dikes; a tributary load of about half that of the main stem is not likely a common occurrence in the field.

The results are summarized in Fig. 43. The bar on the east side at the mouth of the tributary grew to water-surface elevation. Nevertheless, even in run 10-3, a main flow channel was maintained between piers 7 and 8, and maximum scour was at pier 7 (the most westerly of the three deep piers).

The water surface streamlines for run 10-3 are shown in Fig. 44. The deflective action of the permeable dikes can be seen therein. In Fig. 42, the bed topography created by the flow is shown. Deposition behind the downstream permeable dike has maintained a bed elevation of about 720 ft.

Series 11. This series is similar to Series 10, except that the main stem discharge was 22,000 cfs, and the tributary discharge was 1,000 cfs. The following feed rates were used.

<u>Run No.</u>	<u>Feed Rate</u> <u>Minnesota River</u>	<u>Feed Rate</u> <u>Le Sueur Creek</u>
	(grams/min)	(grams/min)
11-1	165	0
11-2	165	33
11-3	165	133
11-4	165	248

As can be seen in Fig. 45, the permeable dikes performed well even under the extremely adverse conditions of run 11-4. Flow streamlines and bed topography for that run are shown in Figs. 46 and 47, respectively.

Series 12. This series was devoted to a complete testing of the truncated T-spur dike, the riprapped excavation around it, and the permeable dikes at above-bankfull flows. In order to allow for a realistic simulation, a step hydrograph was used. Series 12 thus consists of a single run, for which discharge is stepped up gradually from 22,000 cfs up to 100,000 cfs, and then down to 22,000 cfs. The total time of the run was 38 hours

(excluding time when the water was turned off). The timing of each step is shown in Fig. 48.

It is difficult to determine the meaning of the hydrograph if the time duration of each step cannot be scaled up to some field value. In order to determine an approximate scaling, it is necessary to refer to a formula for bed material load. An appropriate formula for sand-bed streams is the Engelund-Hansen formula (Engelund and Hansen, 1967). It has been shown to be among the most accurate formulas at both laboratory and field scales.

Assuming a grain size of 0.7 mm in the model, the Engelund-Hansen formula predicted a bed-material load of 148 grams/minute at bankfull flow in the model, a value close to the observed value of 165 grams/minute. The same formula applied to prototype bankfull conditions yields a bed-material discharge of $2.77 \times 10^{-2} \text{ m}^3/\text{s}$, or $2400 \text{ m}^3/\text{day}$.

Let T_f be some characteristic time scale of the flow. It can be shown (e.g. Parker, 1976) that an appropriate time scale T_s for scour and fill due to sediment transport is given by

$$T_s = \beta T_f$$

where β is equal to the ratio of the volumetric sediment transport rate per unit bed width to the water discharge per unit water surface width. According to the values predicted by the Engelund-Hansen formula, it is found that

$$(\beta)_p = 4.67 \times 10^{-5} \qquad (\beta)_m = 1.6 \times 10^{-4}$$

It thus follows that

$$\frac{(T_s)_m}{(T_s)_p} = \frac{(\beta)_m}{(\beta)_p} \frac{(T_f)_m}{(T_f)_p} = 3.51 \frac{(T_f)_m}{(T_f)_p}$$

Standard distorted Froude modeling of the flow yields the result

$$\frac{(T_f)_m}{(T_f)_p} = \frac{\lambda_h}{\lambda_v^{1/2}} = 3.16 \times 10^{-2}$$

From the above relations, it can be found that

$$(T_s)_p \cong 9(T_s)_m$$

Series 12 is thus seen to simulate a field hydrograph, beginning at 22,000 cfs, peaking at 100,000 cfs 7.5 days later, and returning to 22,000 13 days after initiation of the run. A similar hydrograph from 400 cfs to 4200 cfs was applied to the tributary, but in light of previous results the tributary was not supplied with sediment.

Several important features of the run are summarized in Fig. 48. Water surface elevation and water surface slope follow expected patterns. In the same diagram, the elevation of the point of deepest scour along the bridge is plotted as a function of time. The deepest scour measured for the entire run was at 100,000 cfs, and to an elevation of 688 ft. This value corresponds well with previously mentioned field and model values. It underlines the potential for extreme scour at such flows due to the constriction of the bridge.

In Fig. 48, the point labelled A denotes the time at which the upstream permeable dike failed due to scour. The downstream permeable dike was weighted to the bed and not allowed to fail. Point B denotes the time at which riprap was installed around piers 7 and 8 in order to protect them from scour.

Water surface elevations and bed profiles are shown for the rising limb of the hydrograph in Fig. 49. In going from 22,000 cfs to 60,000 cfs, scour occurs on the east side, and deposition occurs on the west side behind the permeable dike. At 60,000 cfs, the bridge appears barely safe. Between 60,000 cfs and 80,000 cfs, an enormous amount of scour occurs everywhere, ensuring failure of piers 7, 8, and 9. Marginally more scour occurs at 100,000 cfs.

It should be noted that in spite of the strong general scour due to the constriction, the situation described in Fig. 49 would be a considerable improvement over conditions as they existed in the flood of 1965 (Fig. 10). Although a similar amount of scour is realized in both cases, the scour occurs against the deeper eastern piers in Fig. 49 rather than the shallow western piers in Fig. 10. The effect of the T-spur and permeable dikes is to create a more manageable problem.

To this end, piers 7 and 8 were protected with riprap at the time denoted by point B in Fig. 48. The run was then continued for another hour, as shown in Fig. 50. The riprap successfully protected piers 7 and 8, but moved erosion over to piers 5 and 6. It was thus concluded that if the constriction cannot be alleviated by a wider span or culverts under the approach, the existing riprap should be augmented so as to protect the footing of every pier against flows of 80,000 cfs or more.

The declining part of the hydrograph is shown in Fig. 51. The bed eventually filled to near the level at the beginning of the run.

Flow patterns at 40,000, 60,000, 80,000 and 100,000 cfs for the rising limb of the hydrograph are shown in Figs. 52, 53, 54, and 55, respectively. Flow patterns are good at all flows except the highest. They should act to scour the mouth of the tributary. Flow patterns were somewhat more erratic on the declining part of the hydrograph.

Scour patterns at the location of the downstream permeable dike are shown in Figs. 56 and 57. It is seen that very deep piles are required if the dikes are not to fail at flows of 80,000 cfs and larger. On the other hand, local failure of parts of the permeable dikes may be tolerable at high floods.

IMPLICATIONS FOR THE BRIDGE

The model study indicates that the T-spur dike and permeable dikes tested can encourage filling of the western side of the channel, protect the western approach against scour, and deflect the flow against the mouth of the tributary of both above- and below-bankfull stages. They should provide an effective means of encouraging the channel back into its old, more stable configuration.

No amount of flow deflection or redistribution can, however, alleviate the severe scour due to constriction at flows in excess of about 60,000 cfs. If extra conveyance cannot be provided via culverts under the approach or an extended bridge span, then the placement of very large riprap around the footings of all the piers is warranted.

CONCLUSIONS AND RECOMMENDATIONS

The present-day problem at the Trunk Highway No. 169 crossing of the Minnesota River near Le Sueur is likely due to a combination of the following factors.

- 1) Overall severe constriction and scour at the bridge during over-bank floods. The western piers are particularly subject to stress due to the position of the bridge on the east side of the valley.
- 2) An overall expansion and depositive environment at the bridge at below-bankfull stages due to the excavation of the western floodway. Deposition was particularly severe on the east side due to the delta at the mouth of Le Sueur Creek.
- 3) Reversal of the sense of the bend as the bar grew, reinforcing the westward shift of the channel.
- 4) Possible, but as yet unascertained, abnormal sediment delivery from Le Sueur Creek.

The bar was rendered impervious to overland erosion due to dense vegetation. It cannot be attacked from the side by the bend because it lies on the inside of the bend. Corrective measures should be tailored to return the river to its old channel on the east side, so that the tributary enters on the outside of the bend. A low bar should be encouraged to build on the west side in order to hold the low flow to the east. The stress on the western piers during floods should be alleviated by forcing floodplain flows to enter the channel further upstream and deflecting them to the east. These measures should be designed with the intent of increasing flood conveyance over what exists today. To this end the following short-term recommendations are made, based on the results of the model study and other considerations.

1. The two permeable dikes of Figs. 58, 60, and 61 should be built in the winter of 1982. If only one can be built during this period, permeable dike No. 1 (Fig. 58) should be constructed first. The recommended locations are those of Fig. 58. The recommended heights are shown in Figs. 60 and 61. Riprap is recommended along the base of the permeable dikes. Permeable dike No. 1 can be lowered somewhat if more conveyance is desired, but the bar behind it must grow to a height greater than 720 ft (219.5 m), or the bottom of the excavation in Fig. 10, if it is to be effective. Clump-pile construction is recommended; a very general illustration of such a scheme is suggested in Fig. 59.

2. The new channel around the tip of the riprap ending at pier 4 should be closed off to an elevation of at least 722 ft (220 m) using riprap. This should be done immediately after permeable dike No. 1 is finished, or just after the spring, 1983 flood recedes. The purpose of the riprap is to act in concert with the permeable dike to force all the low flow into the pilot channel. It can also protect piers 4 and 5 during floods.

3. The incipient bar at the mouth of Le Sueur Creek extending into the pilot channel (Fig. 6) should be excavated. The pilot channel and the immediately adjacent mouth of Le Sueur Creek should be excavated another 2 ~ 3 ft (0.6 ~ 0.9 m) in order to temporarily remove the existing armor layer. This should not be done earlier than the implementation of recommendation 1 and 2, and if it cannot be implemented by December, 1982, it should be implemented just after the spring 1983 flood recedes. The temporary removal of the armor should accelerate the growth of the pilot channel.

4. The riprapped T-spur dike should be built during the summer of 1983 or 1984, in general accord with the outline of Fig. 58. The riprap on the dike in the excavation and on the apron should be at least as coarse as the limestone quarry material used to protect piers 1 ~ 4 in 1981.

Long-term maintenance is extremely important, as at least several years may be required before a new, stable geometry is realized. The following long-term recommendations are made.

1. The permeable dike and the bridge piers should be kept clear of large debris. This is especially important as regards piers 6 ~ 9.

2. Vegetation should be kept cut down as low as possible on both sides of the pilot channel to improve conveyance and render the banks susceptible to erosion.

3. Vegetation should not be hindered on the new bar behind the permeable dikes. In order to maintain conveyance, however, trees and shrubs higher than 5 ~ 6 ft (1.5 ~ 1.8 m) should be cut down to an appropriate height. Trees should be kept cut down in the excavation and on the apron of the T-spur dike.

4. If and when the main channel is re-established between piers 7, 8, and 9, piers 5 ~ 9 should be protected with riprap placed as deep as possible, i.e. around the footings. The riprap should be as large as possible in order to protect these piers against severe general scour in a flood over 60,000 cfs (1700 cumecs). The permeable dike and the T-spur dike should move the most intense scour to the easterly piers during such an event.

5. If the bar behind the permeable dike begins to grow higher than 725 ft (221 m) over a substantial portion of the area under the bridge, the piles of part of permeable dike No. 1 should be cut down lower to prevent further loss of conveyance.

ACKNOWLEDGEMENTS

Charles C. S. Song provided much helpful advice. Victor Galay originally suggested the use of the T-spur dike. Karl Wikstrom did the photographic work. Bob Bulleigh drafted the diagrams. Harlan van Wye performed most of the later experiments. Pat Swanson typed the report and provided editorial services.

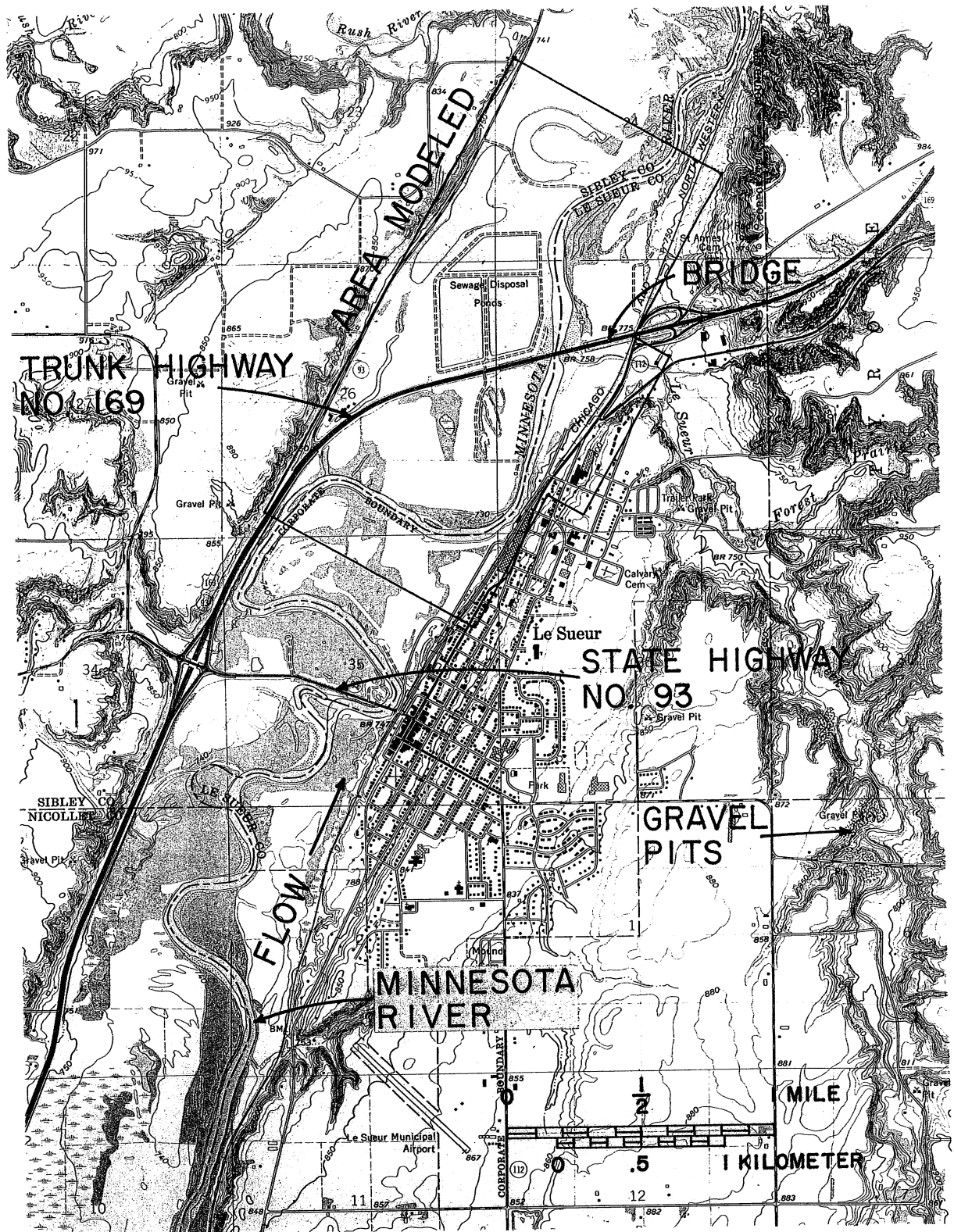


Fig. 1. Topographical map of vicinity of the trunk highway No. 169 bridge; taken from the U. S. Geological Survey topographical map of the Le Sueur quadrangle.

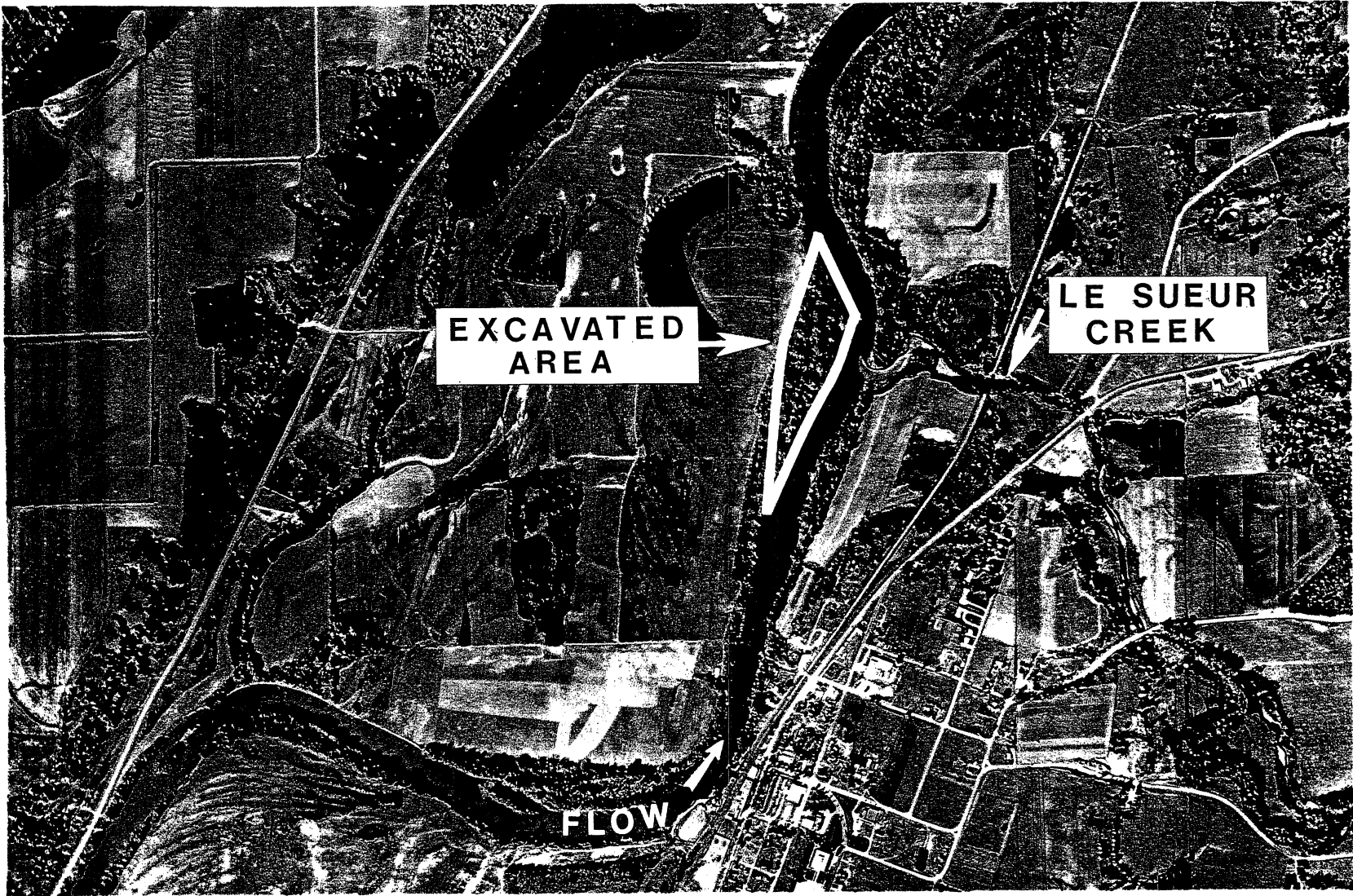


Fig. 2. Preconstruction bridge site on September 28, 1957.

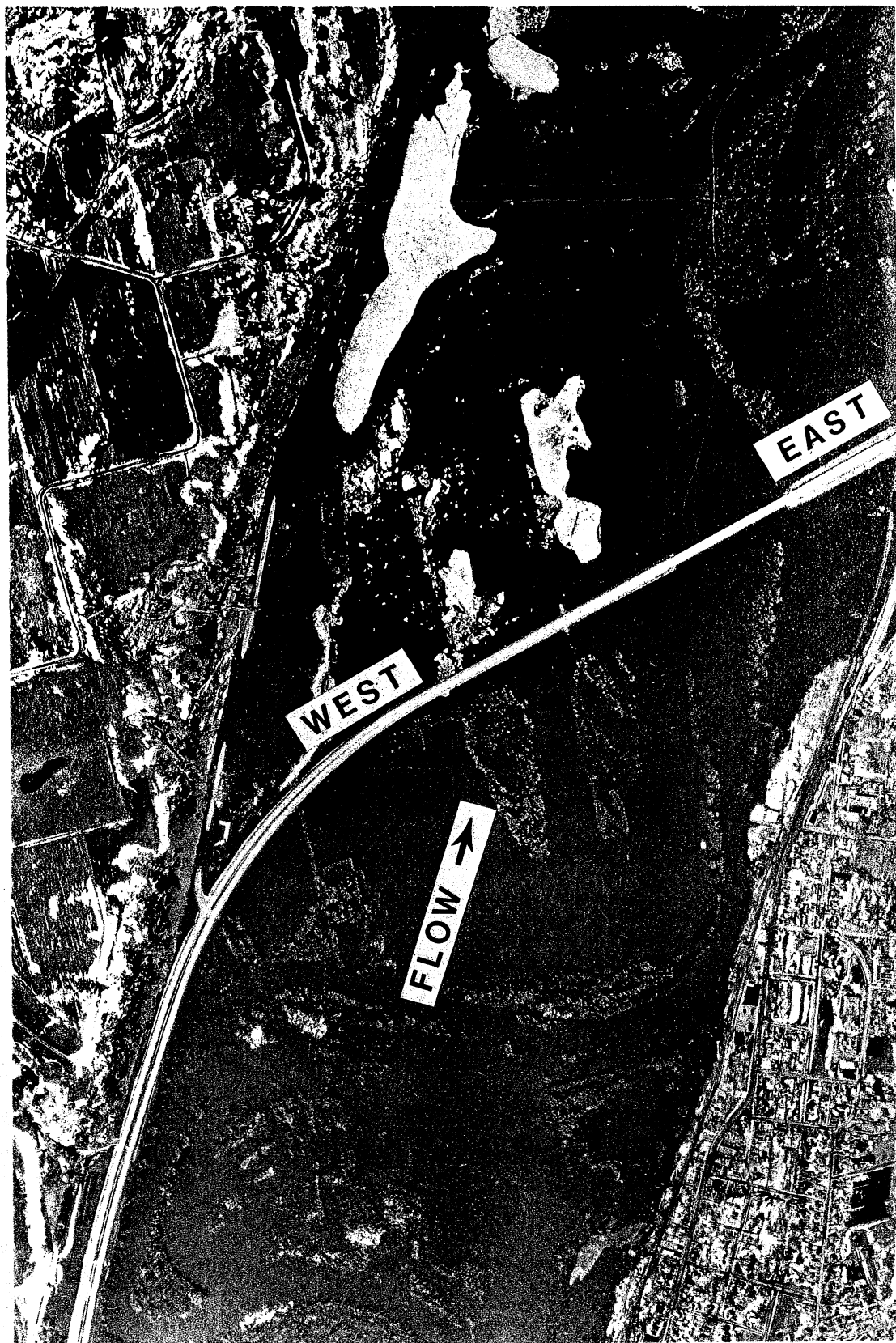


Fig. 3. Bridge site during flood of 1965 (April 9, 1965).



Fig. 4. Bridge site on April 30, 1968.

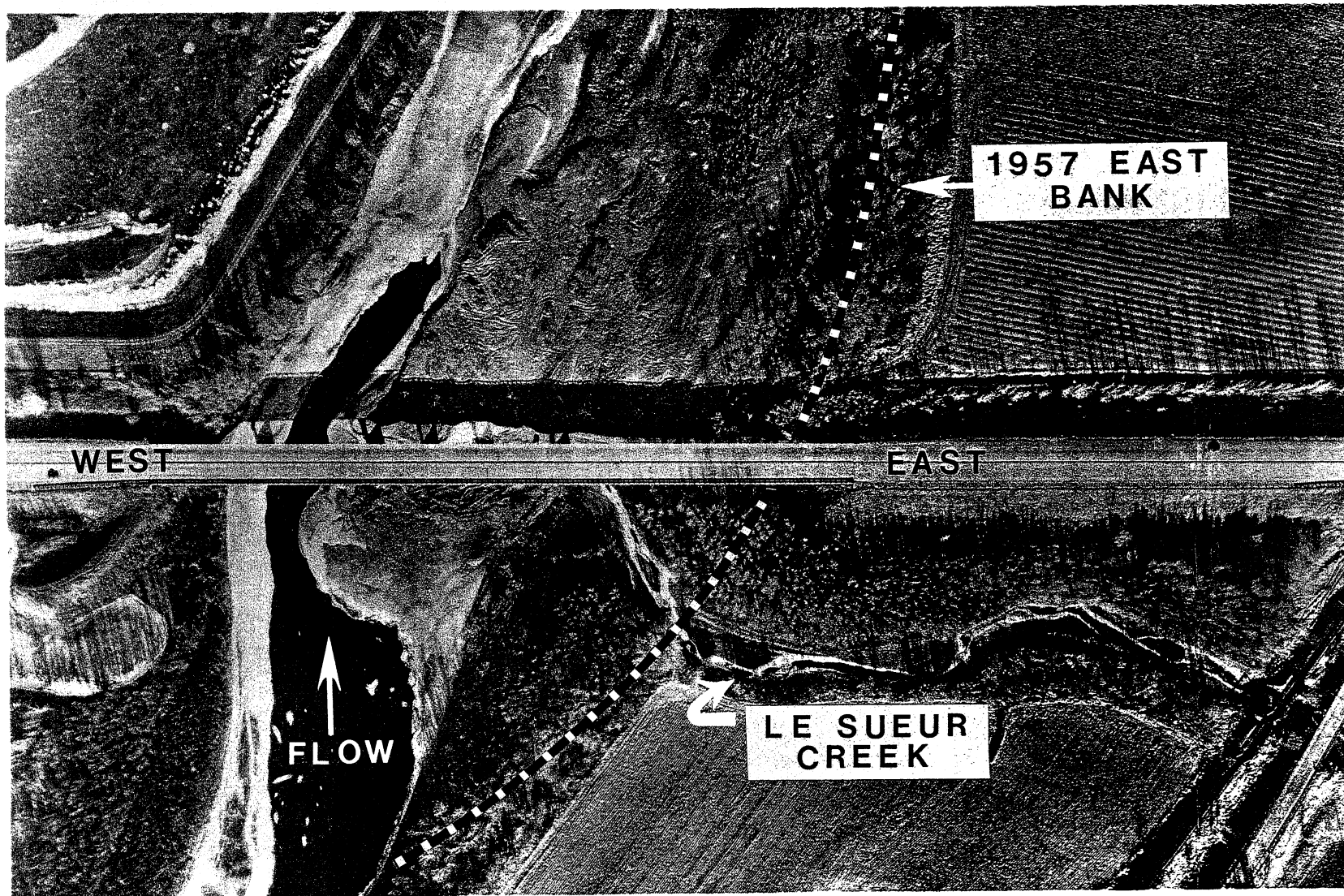


Fig. 5. Bridge site on January 3, 1981.

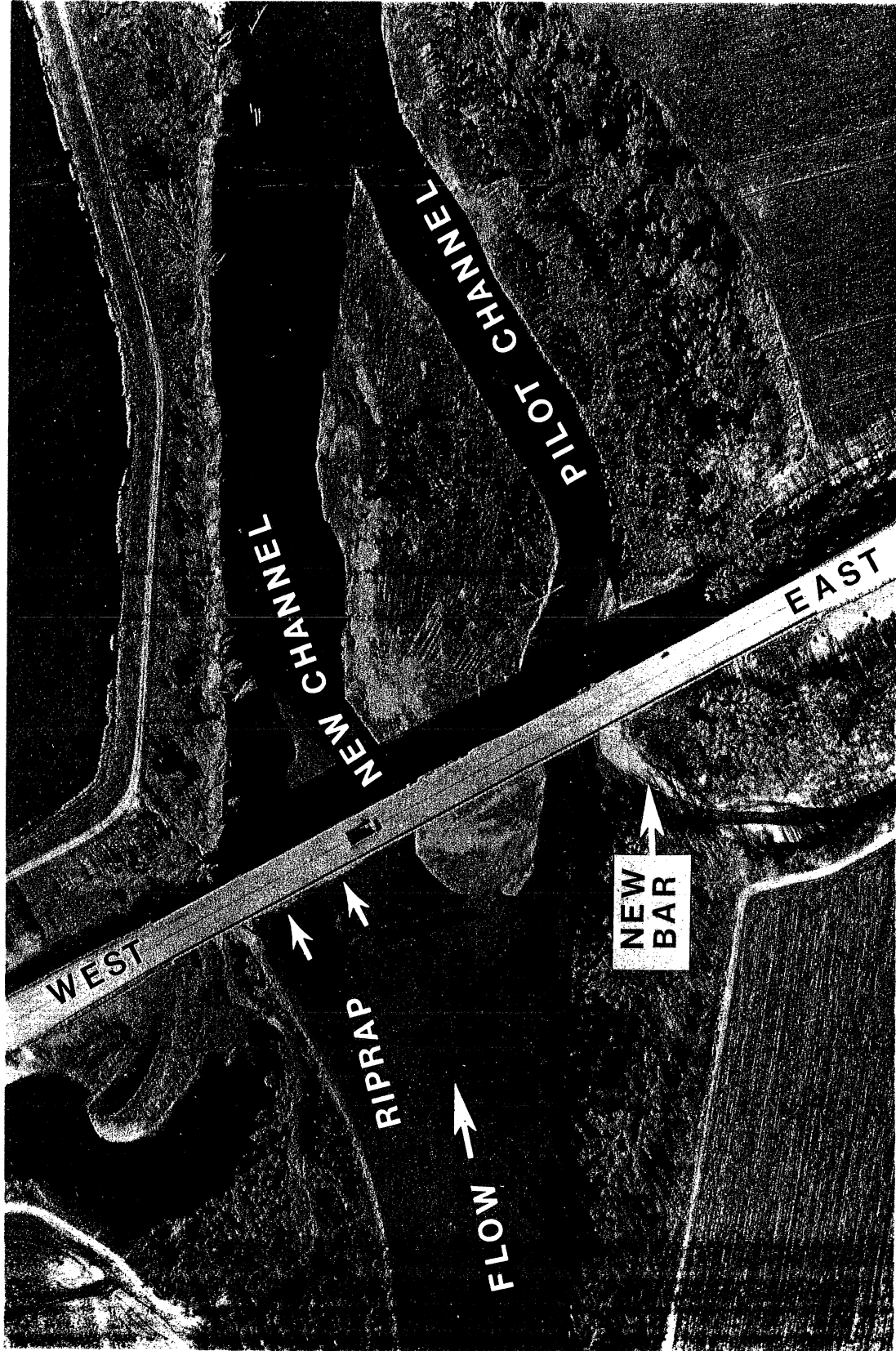


Fig. 6. Bridge site on November 11, 1981.

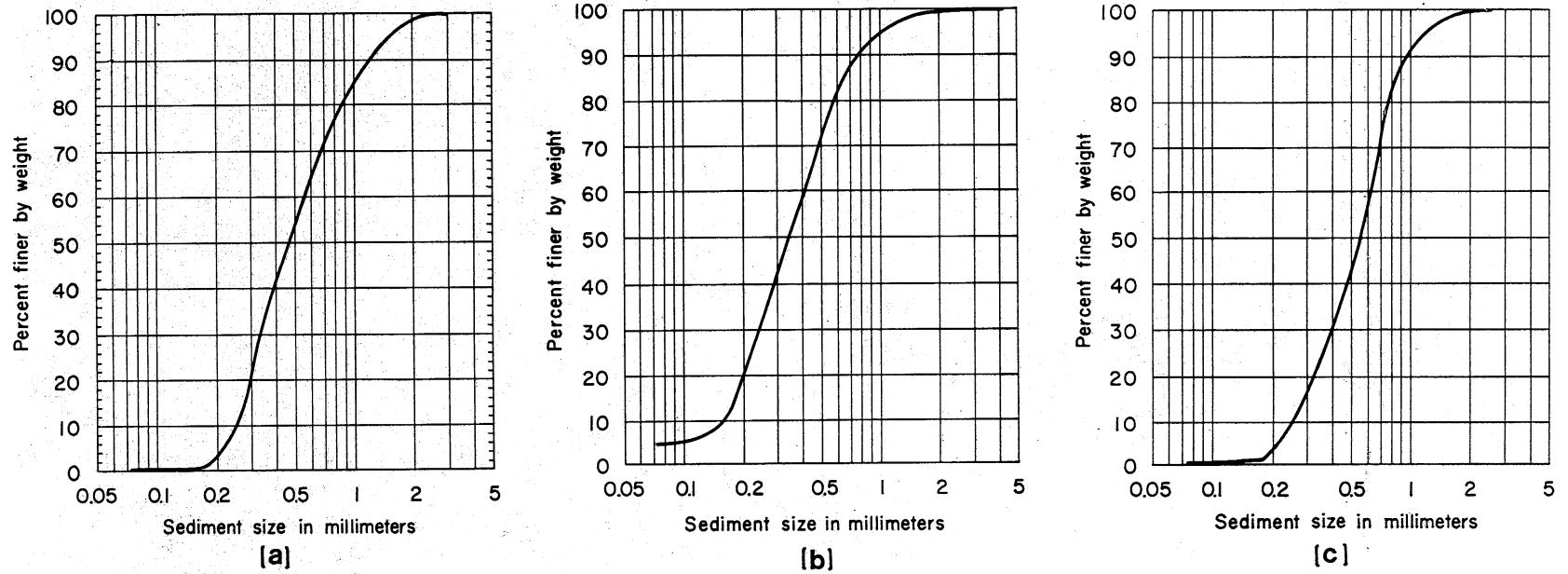


Fig. 7. Three typical size distributions of bed material in the Minnesota River near the Trunk Highway No. 169 bridge.



Fig. 8. View of denuded slope of gravel mining operation from Le Sueur Creek. Aquatic grasses at bottom denote margin of creek. The rubble embankment in the foreground does not appear to be more than a decade old.

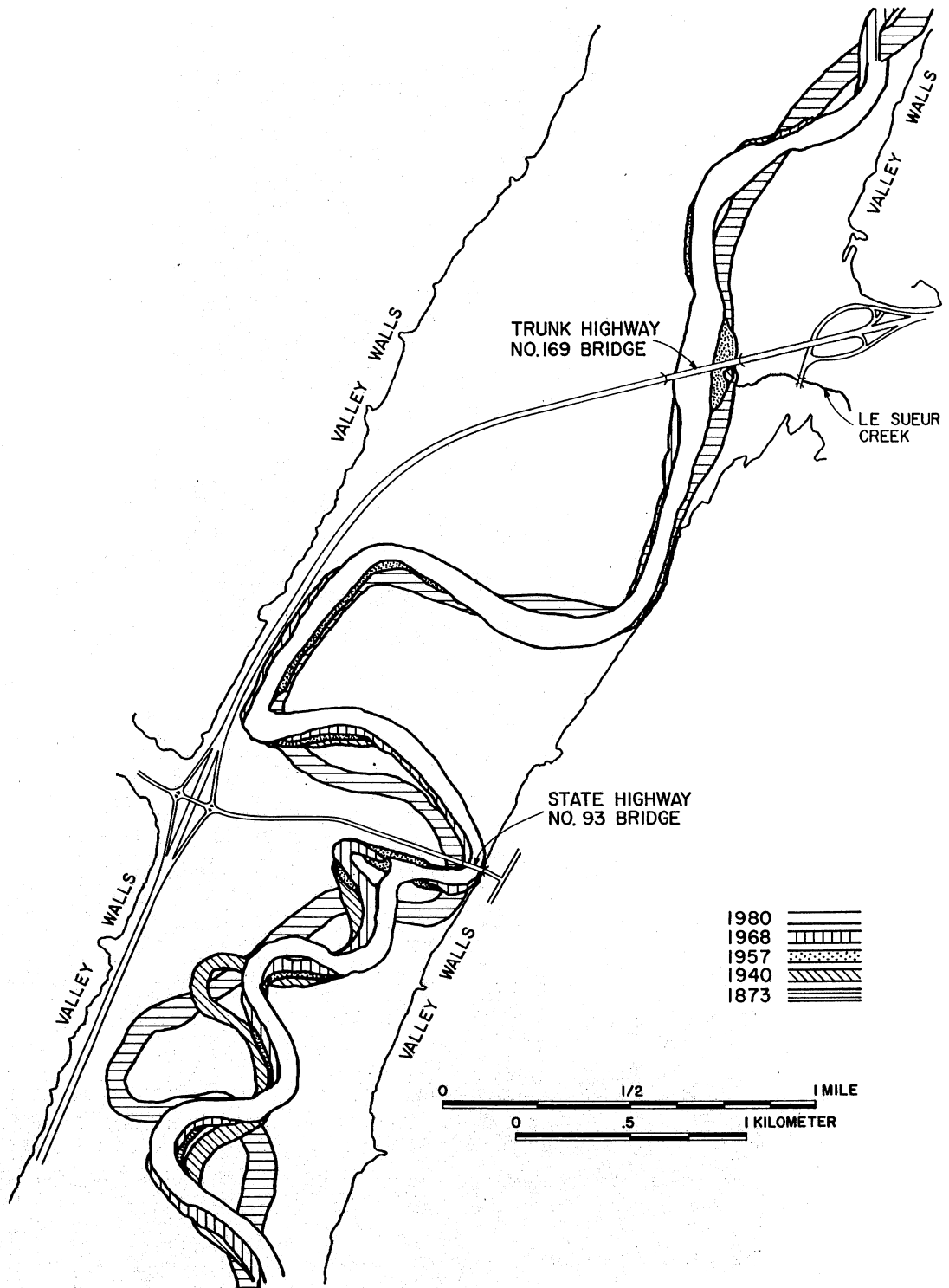


Fig. 9. The 1873, 1940, 1957, 1968, and 1980 channels of the Minnesota River near the State Highway No. 93 bridge.

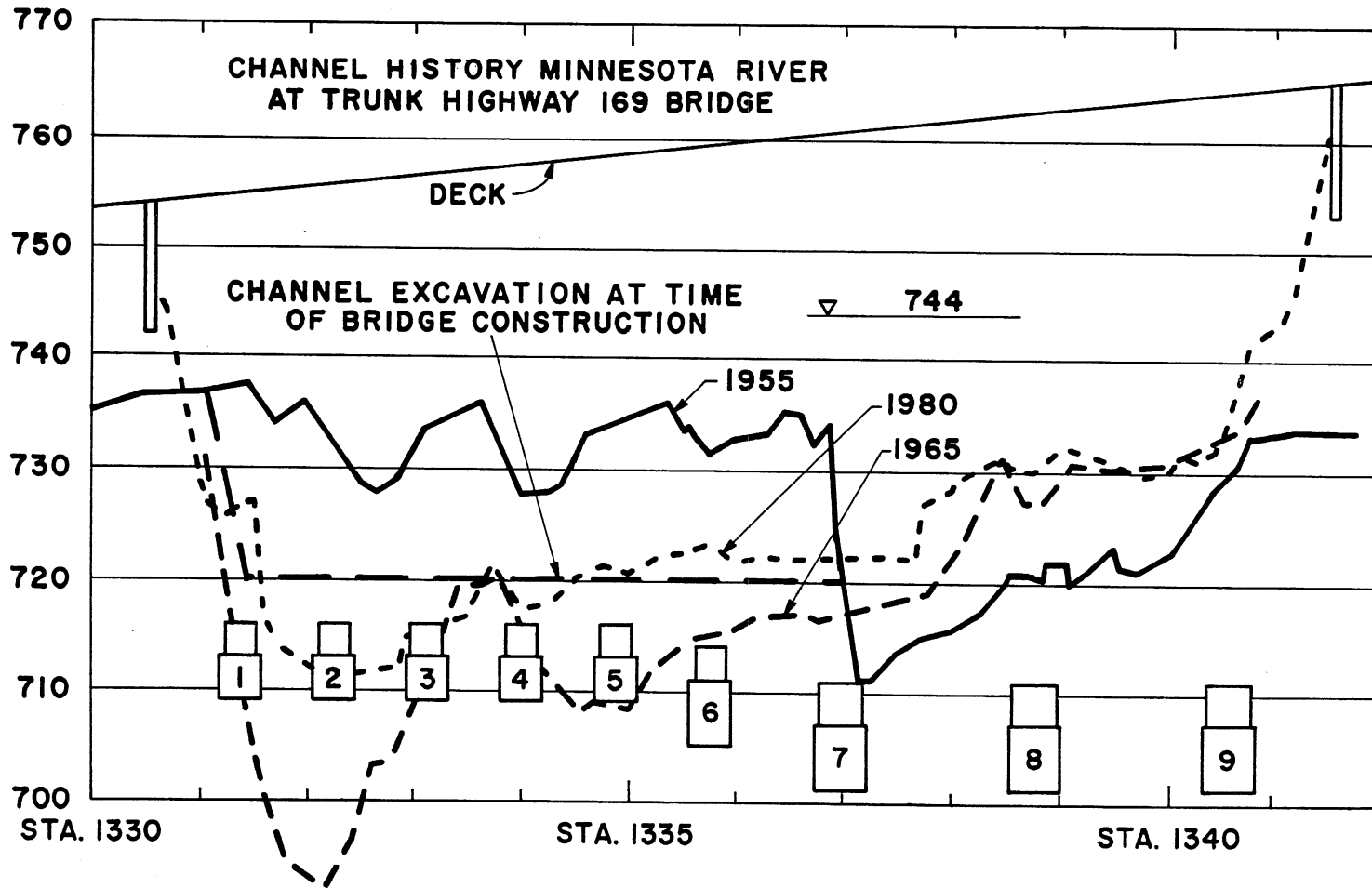


Fig. 10. Sketch of the bridge footings and seals, and several cross sections at the bridge. Elevation is in feet above sea level. The water surface elevation of the peak of the 1965 flood at the bridge was 744 ft above sea level.

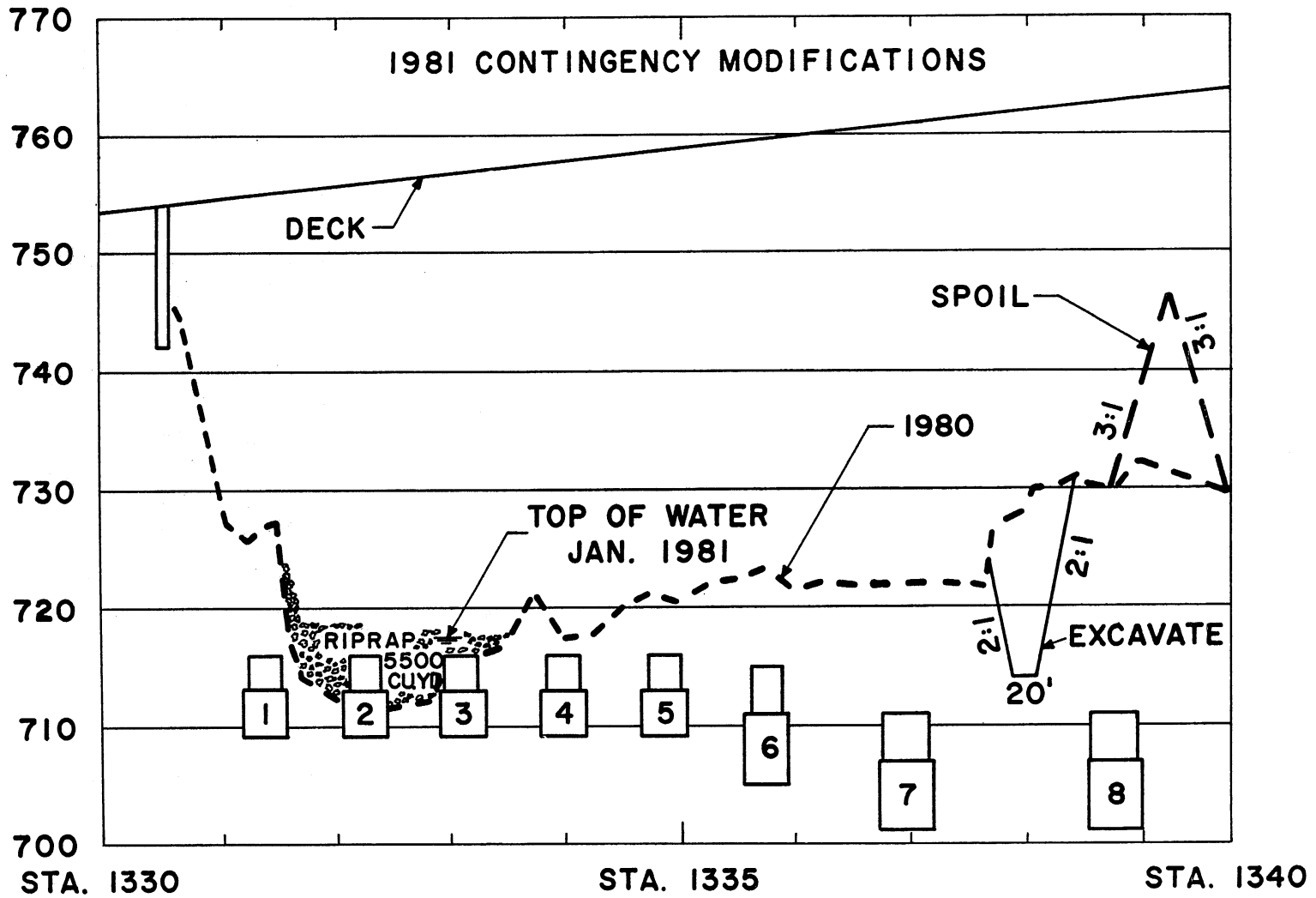


Fig. 11. Sketch of the contingency measures (riprap and excavation of pilot channel) implemented in the summer of 1981. The left side is the west side. Elevation is in feet above sea level.

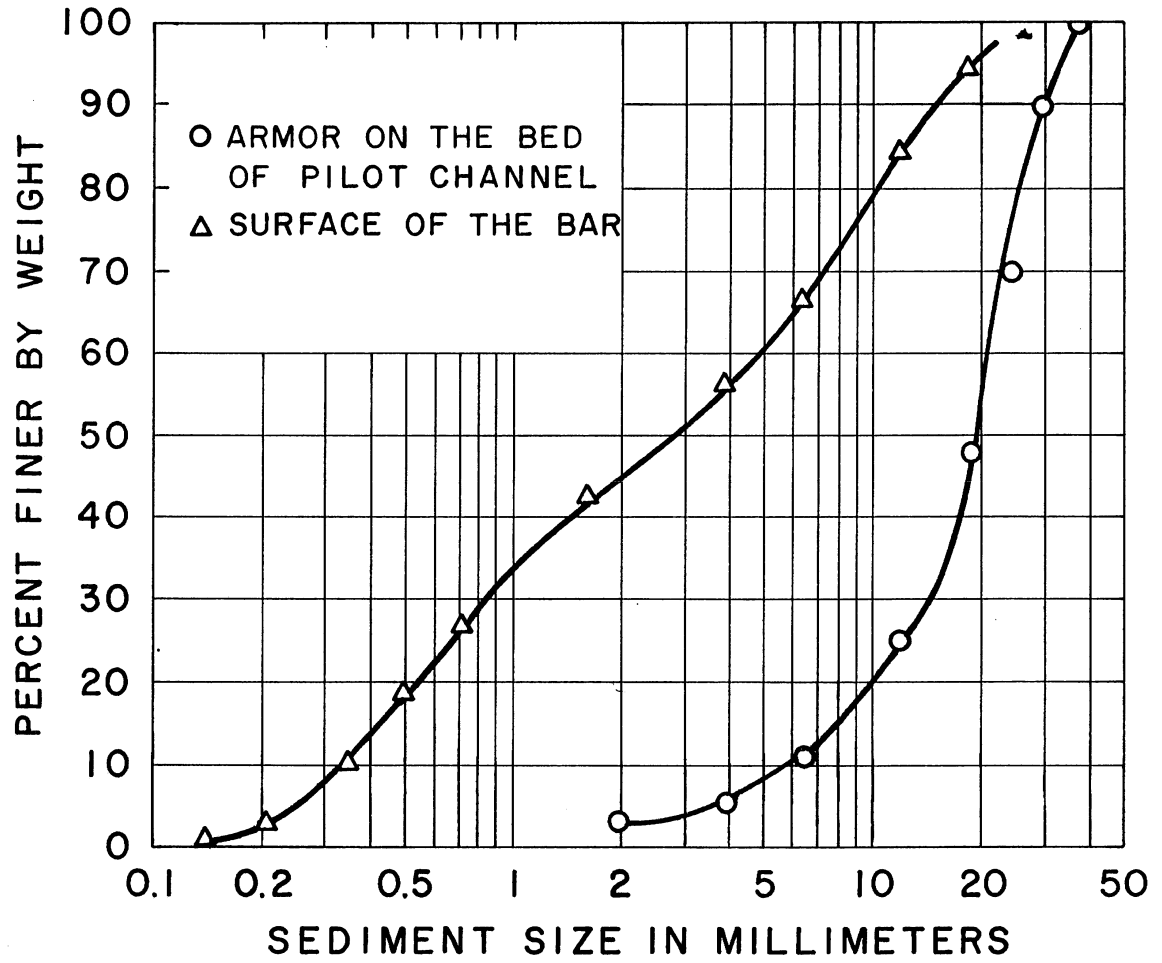


Fig. 12. The head of the bar is covered in many places with pea and coarser gravel. The pilot channel is paved with even coarser material.

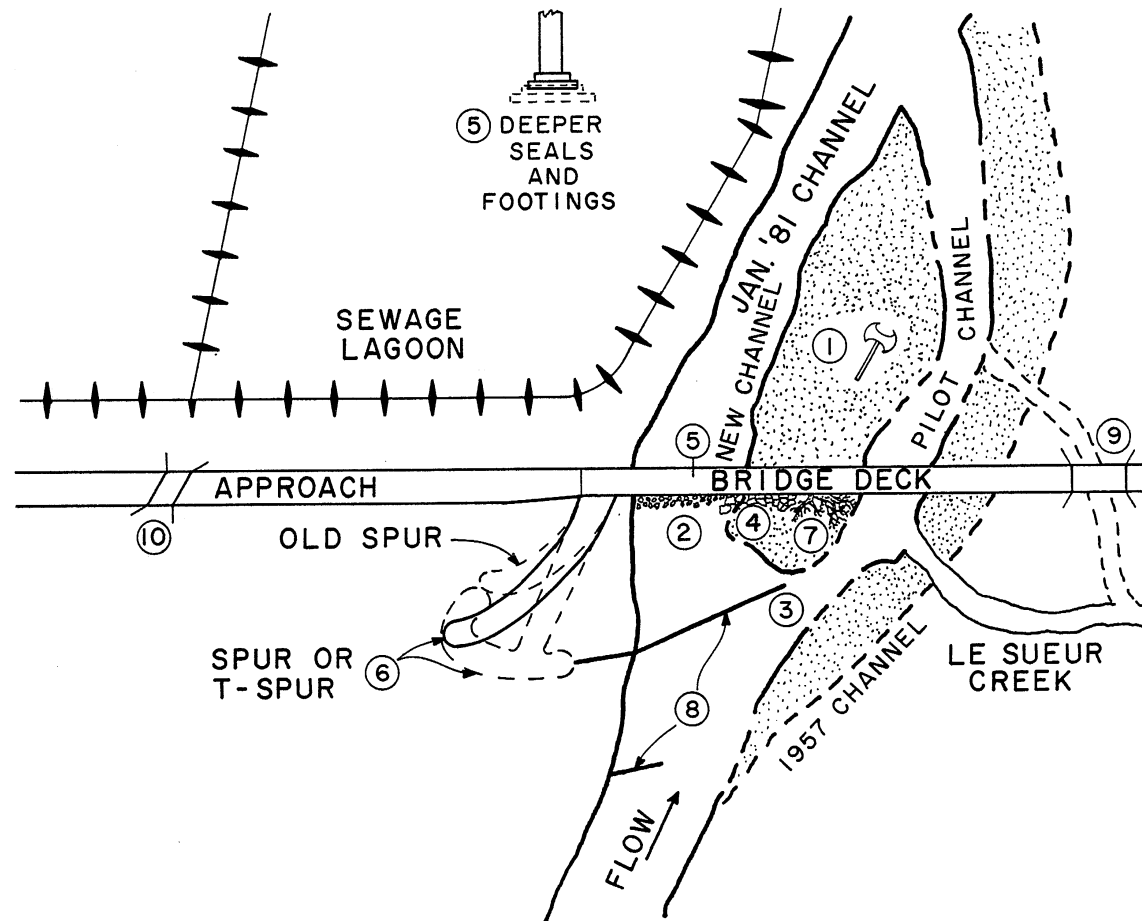


Fig. 13. Various countermeasures: 1) cut down vegetation on bars; 2) riprap to pier 4; 3) pilot channel; 4) riprap to pier 6; 5) deeper footings, piers 1-5; 6) lengthen spur dike; 7) remove channel debris; 8) permeable dike; 9) separate bridge deck, Le Sueur Creek; 10) culvert.

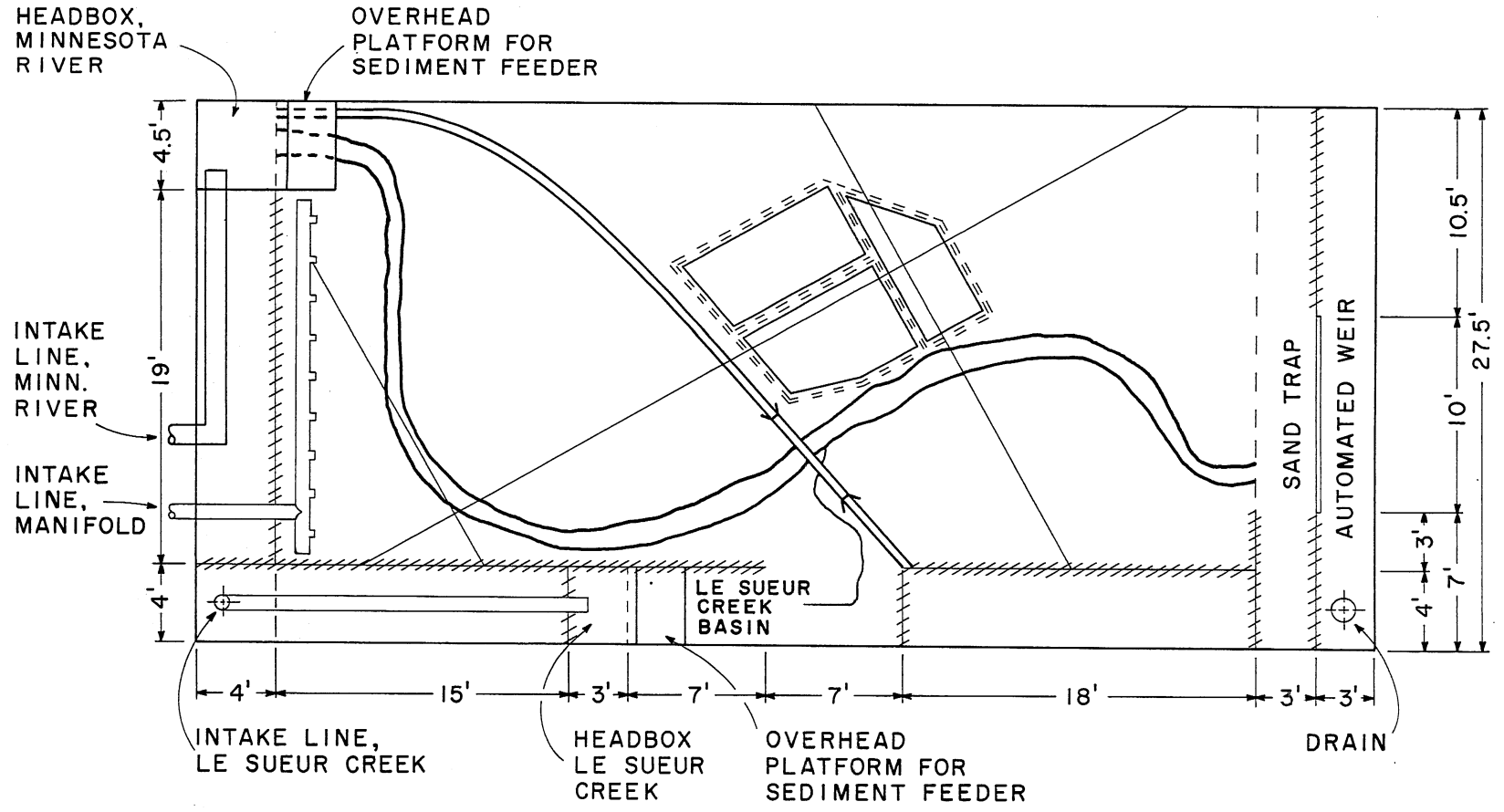


Fig. 14. Schematic of model basin.

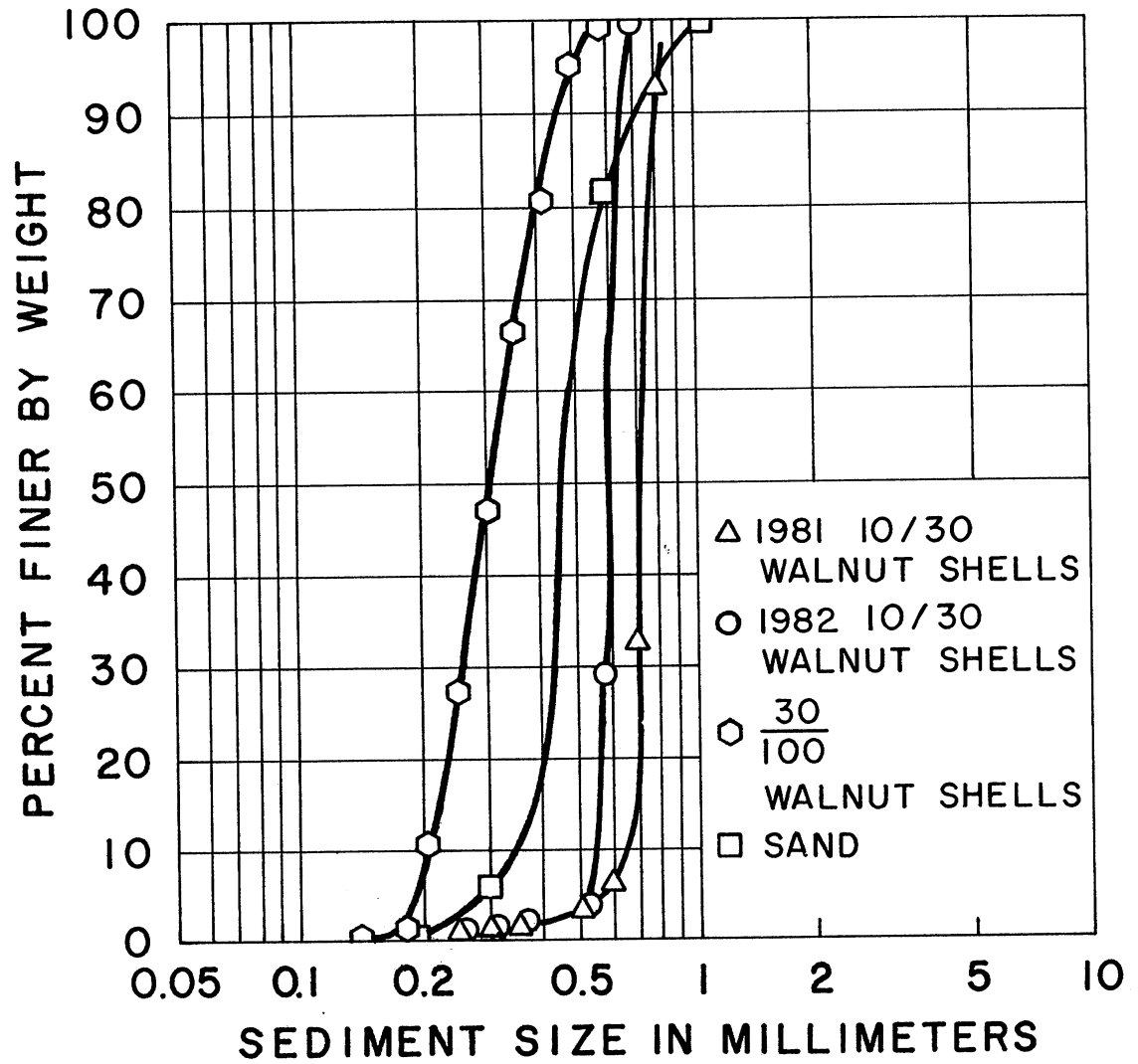


Fig. 15. Size distributions of various model sediments.

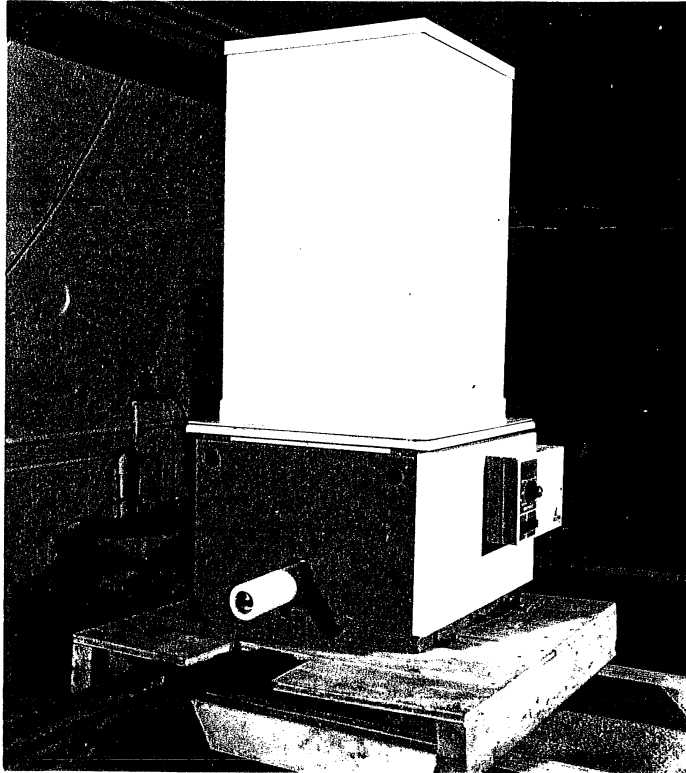


Fig. 16. One of the model sediment feed devices.

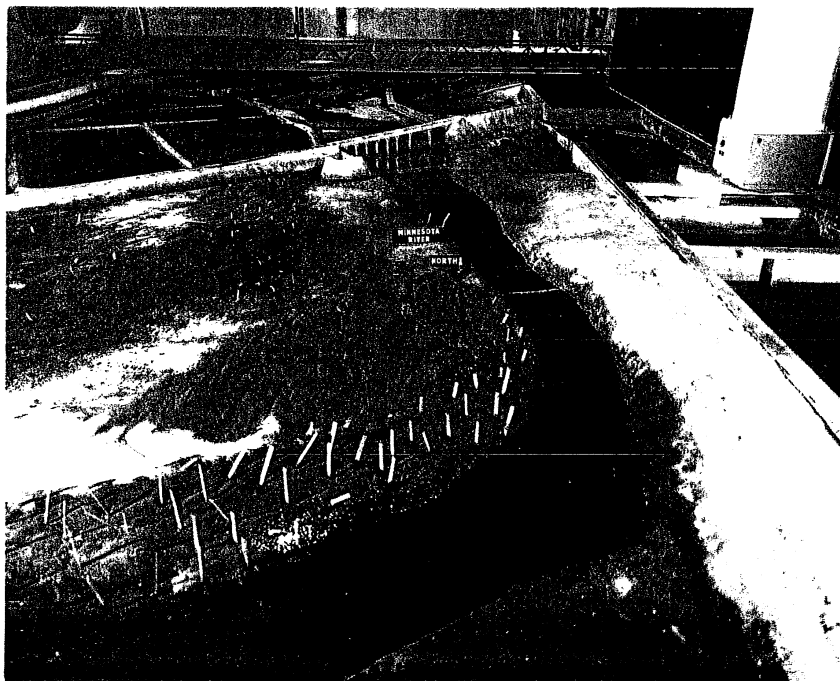


Fig. 17. A view of the model basin looking downstream.

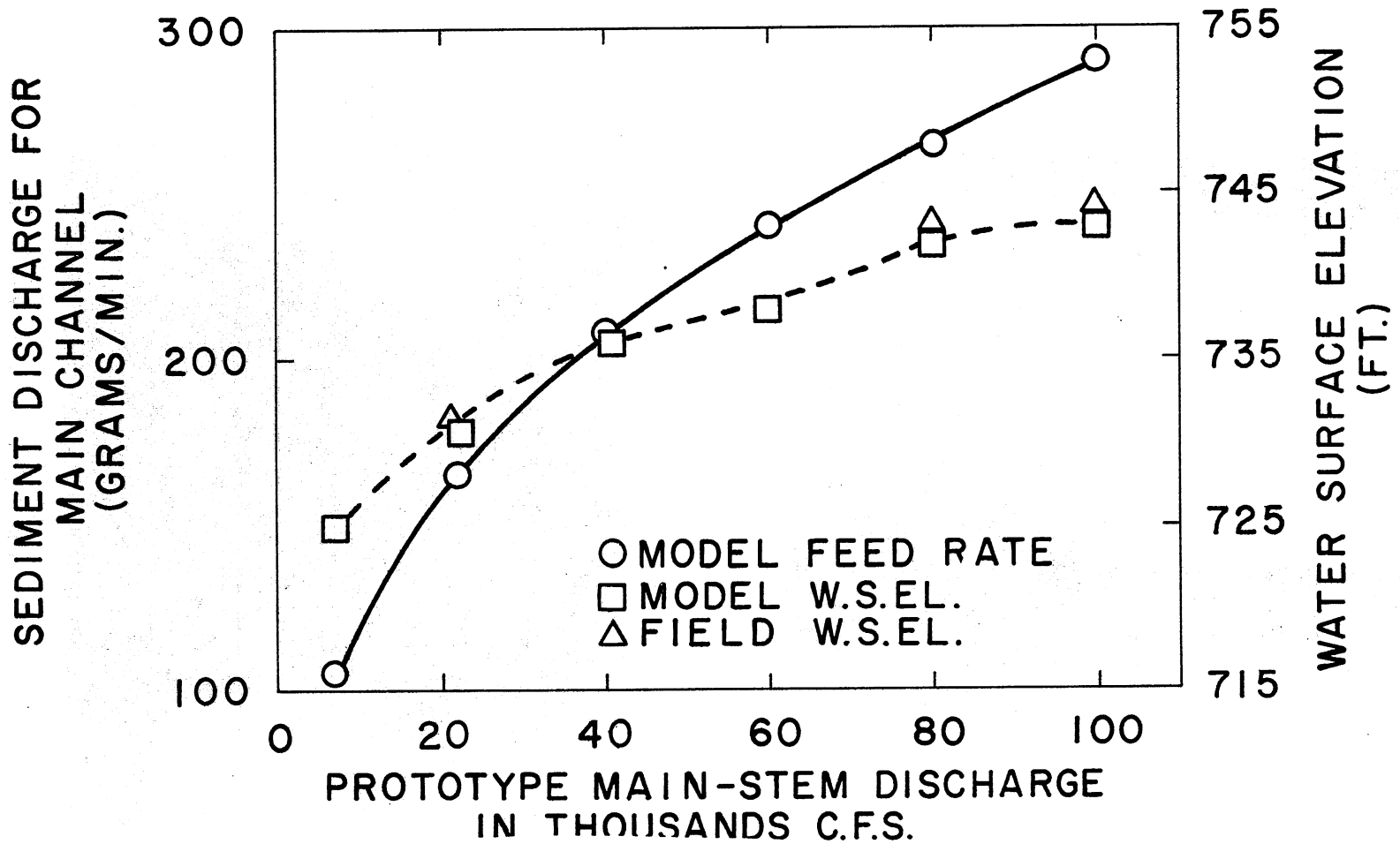


Fig. 18. Results of model calibration. Water surface elevations measured in the model just upstream of the bridge have been scaled up to prototype dimensions; they are compared with water surface elevations from the field. Also shown is the sediment feed rate necessary in the model to obtain equilibrium as a function of prototype water discharge.

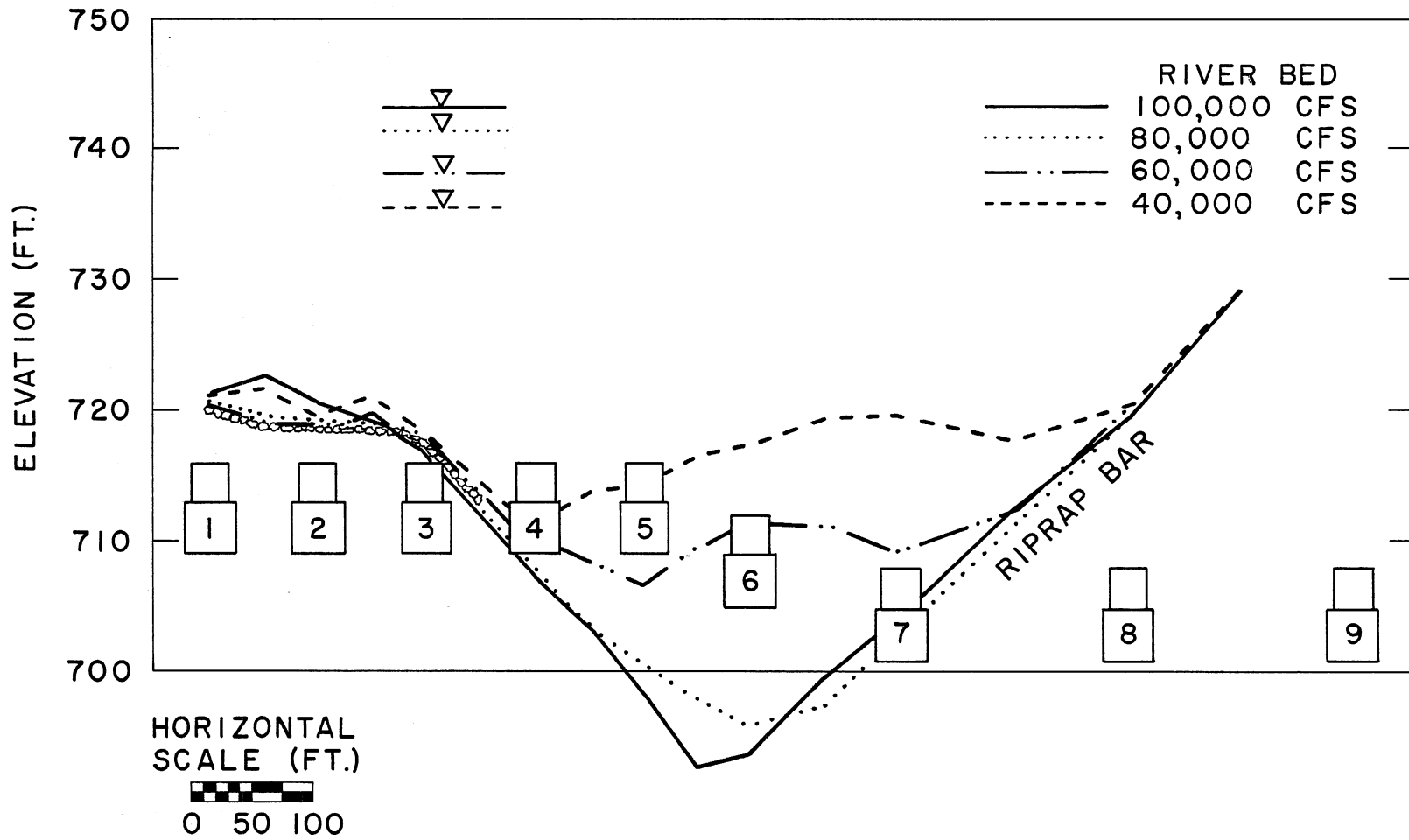


Fig. 19. Bed profiles and water surface elevations at the bridge for the experiments of Series 5.

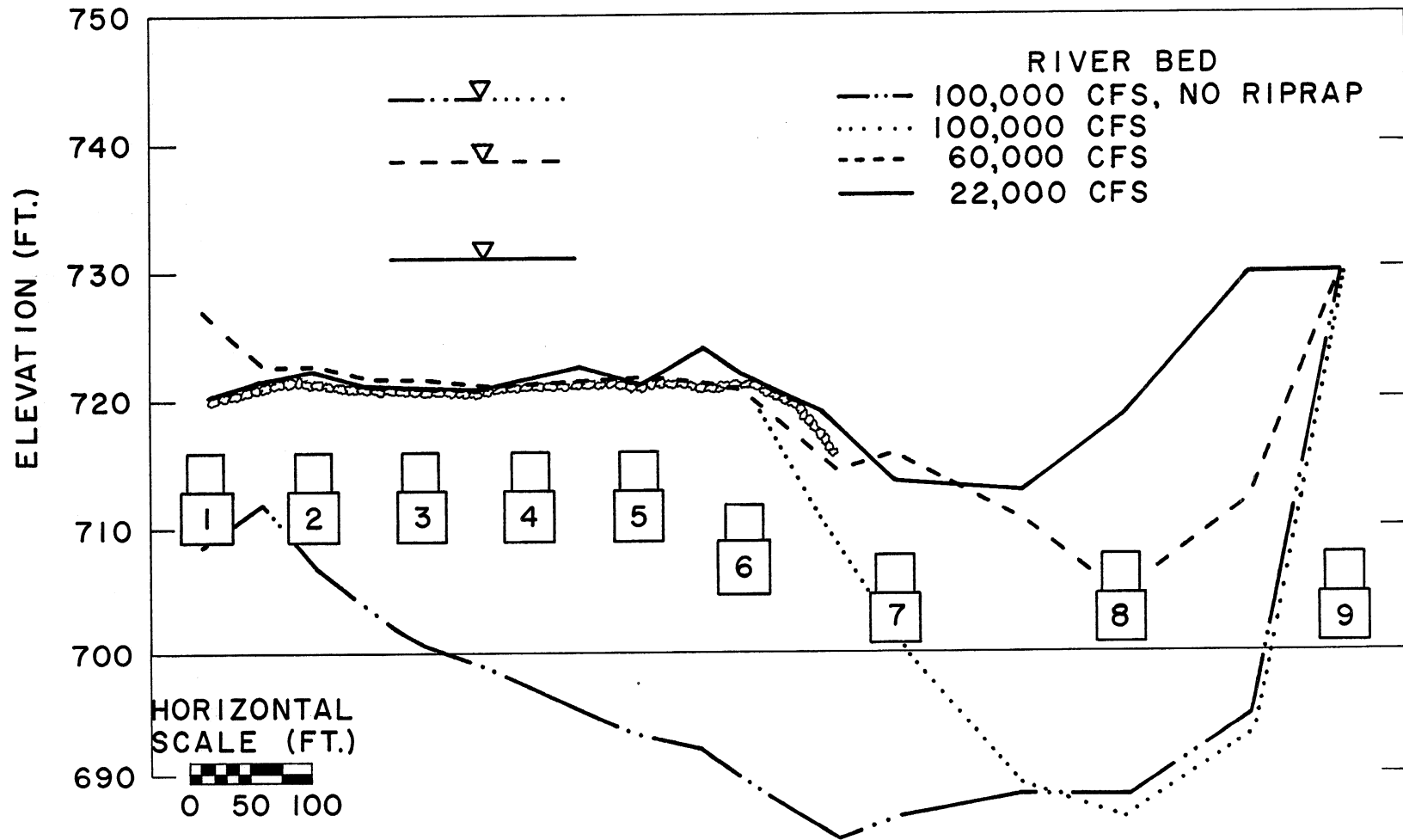


Fig. 20. Bed profiles and water surface elevations at the bridge for the experiments of Series 6.

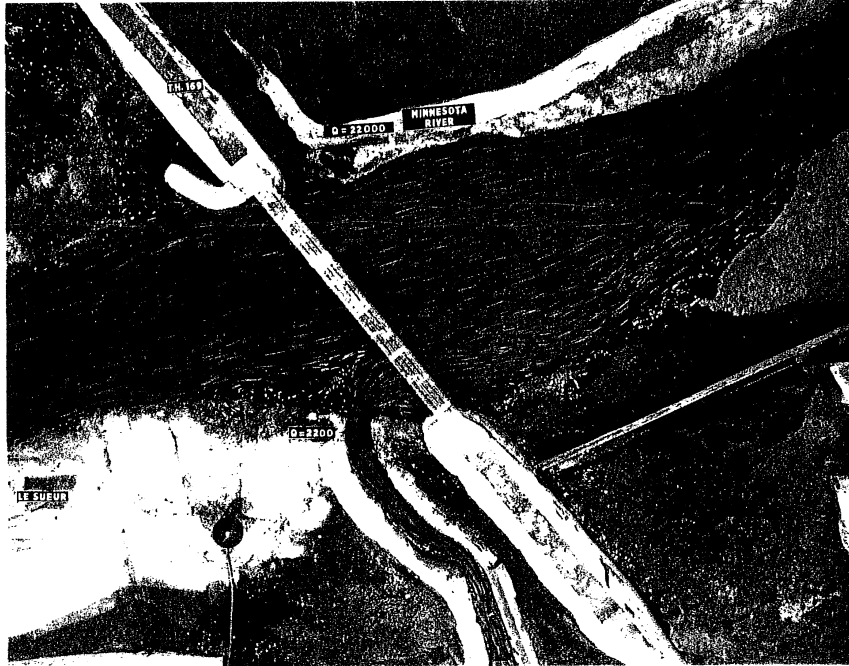


Fig. 21. Streamlines for a mainstem flow of 22,000 cfs and the tributary flow on.

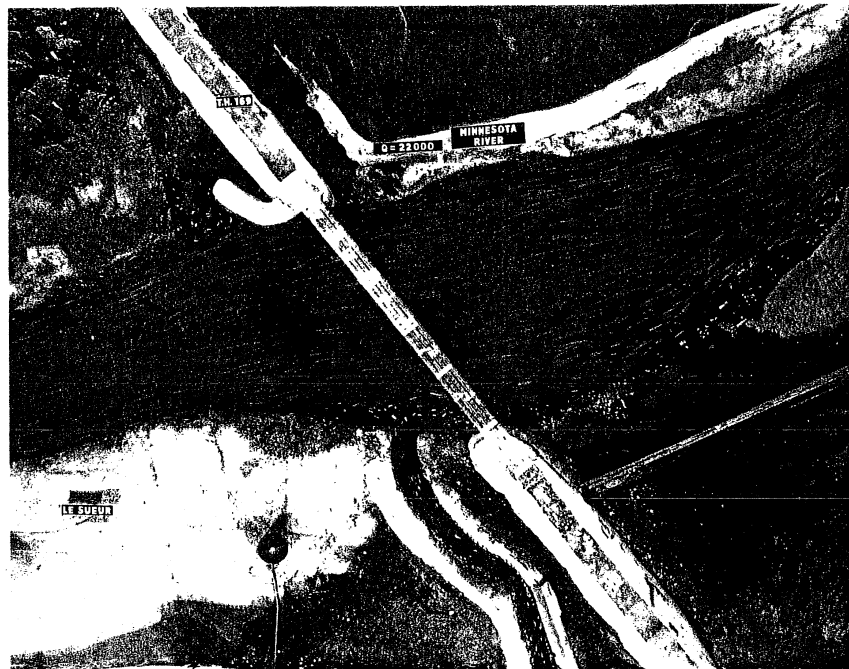


Fig. 22. Streamlines for a mainstem flow of 22,000 cfs and the tributary flow off.

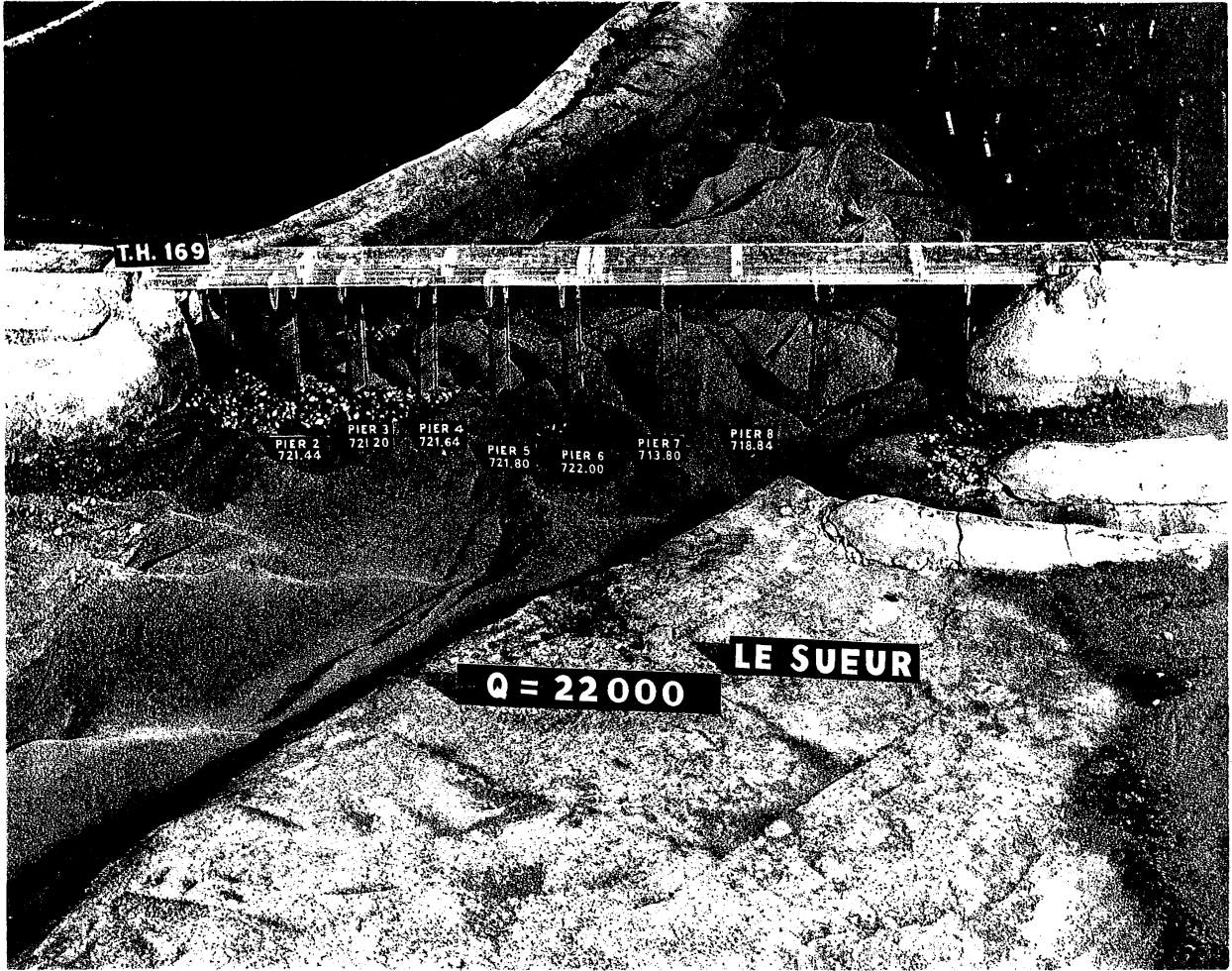


Fig. 23. Bed topography created by a mainstem flow of 22,000 cfs with the tributary flow on. Most of the riprap from piers 1 to 6 is visible.



Fig. 24. Streamlines for a mainstem flow of 60,000 cfs and the tributary flow on.

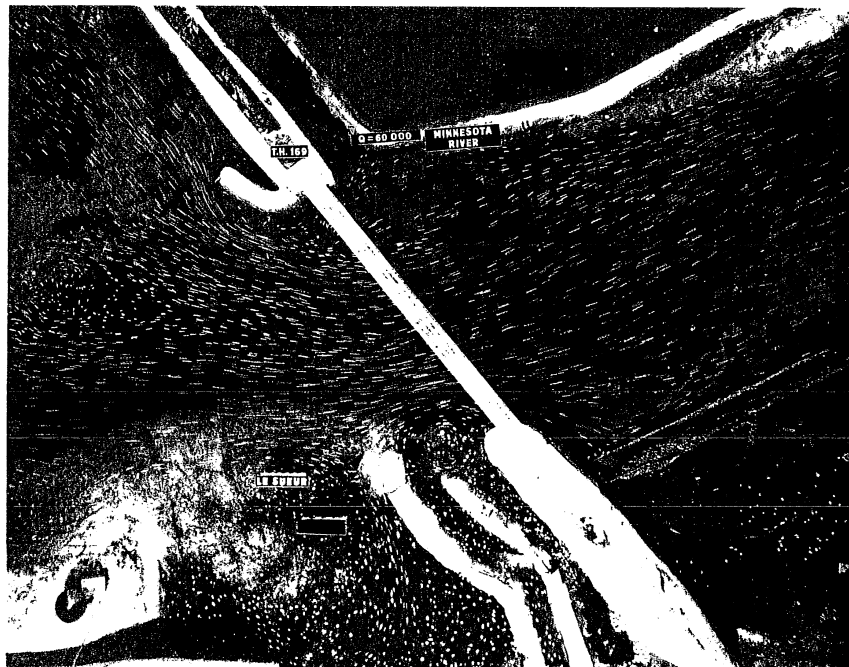


Fig. 25. Streamlines for a mainstem flow of 60,000 cfs and the tributary flow off.

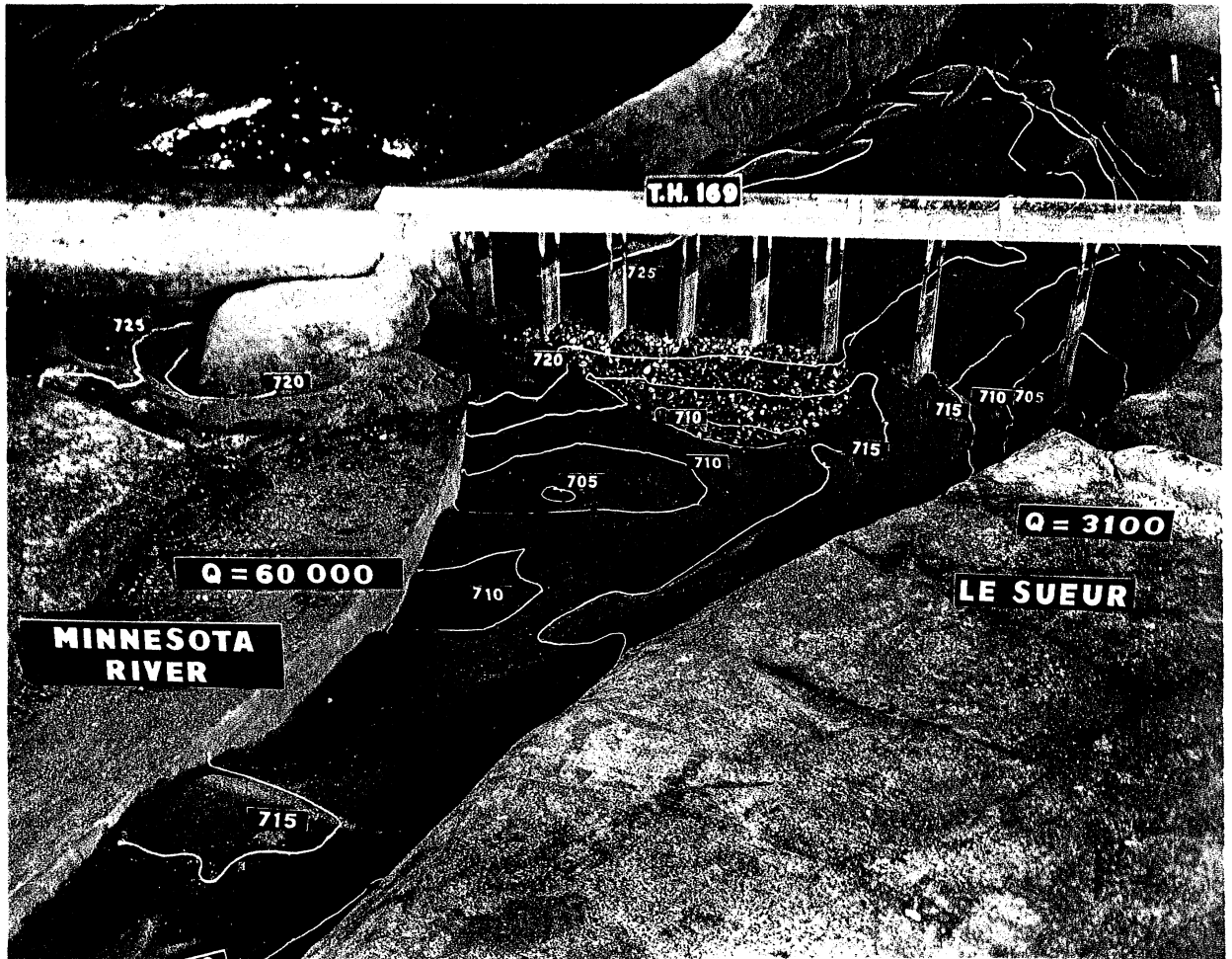


Fig. 26. Bed topography created by a mainstem flow of 60,000 cfs with the tributary flow on.

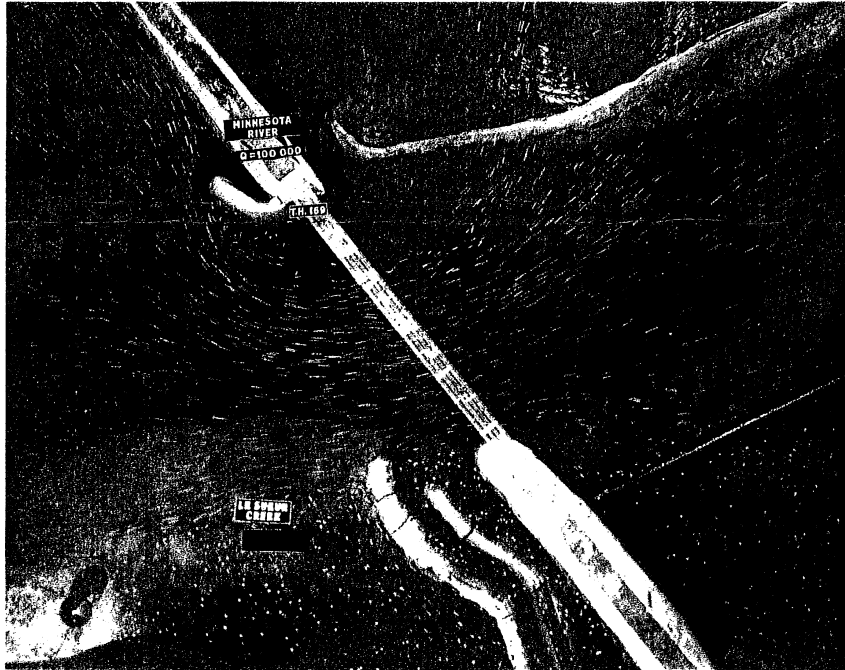


Fig. 27. Streamlines for a mainstem flow of 100,000 cfs and the tributary flow off.



Fig. 28. Bed topography created by a mainstem flow of 100,000 cfs with the tributary flow on.

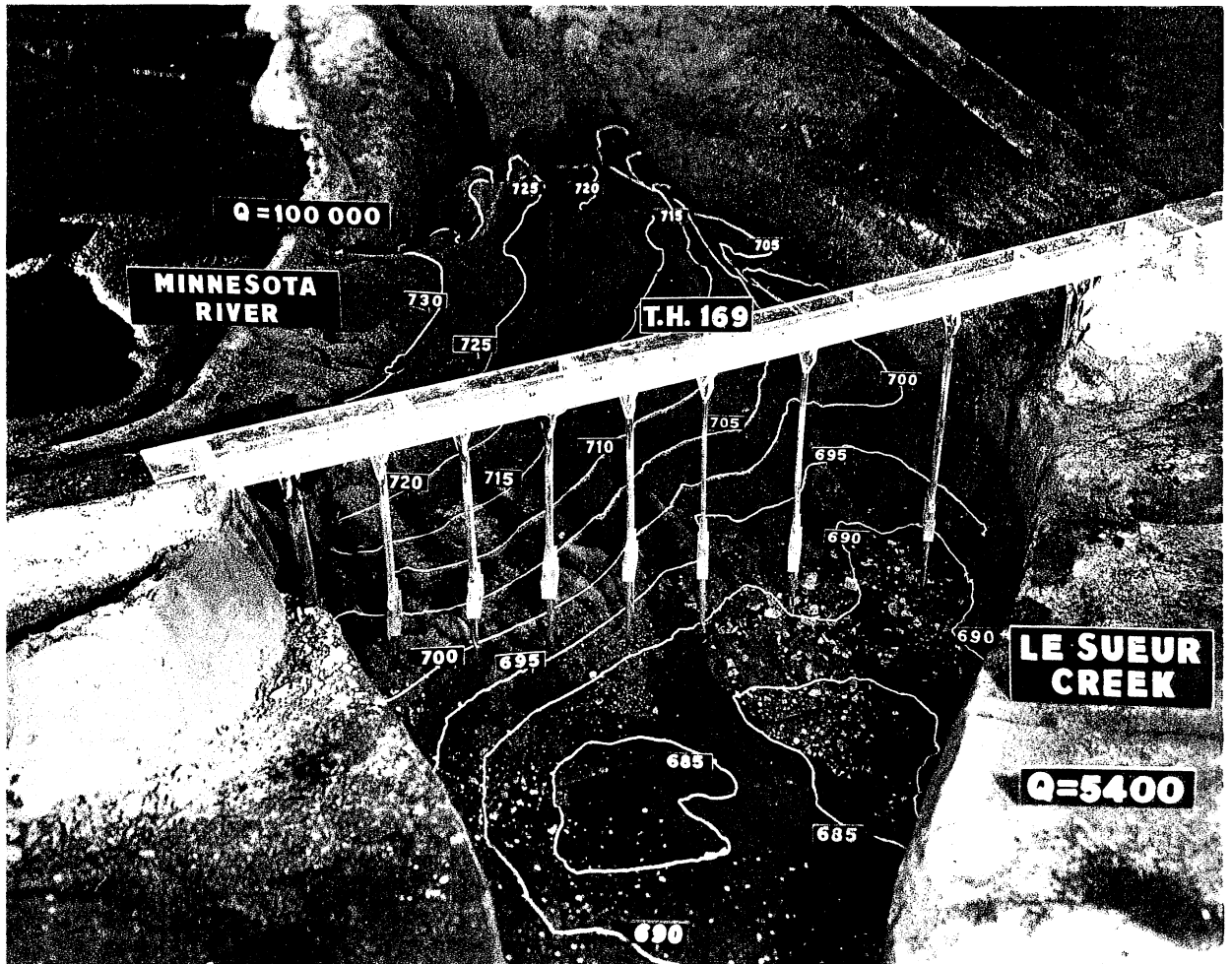


Fig. 29. Bed topography created by a mainstem flow of 100,000 cfs, with all but a remnant of the riprap removed.

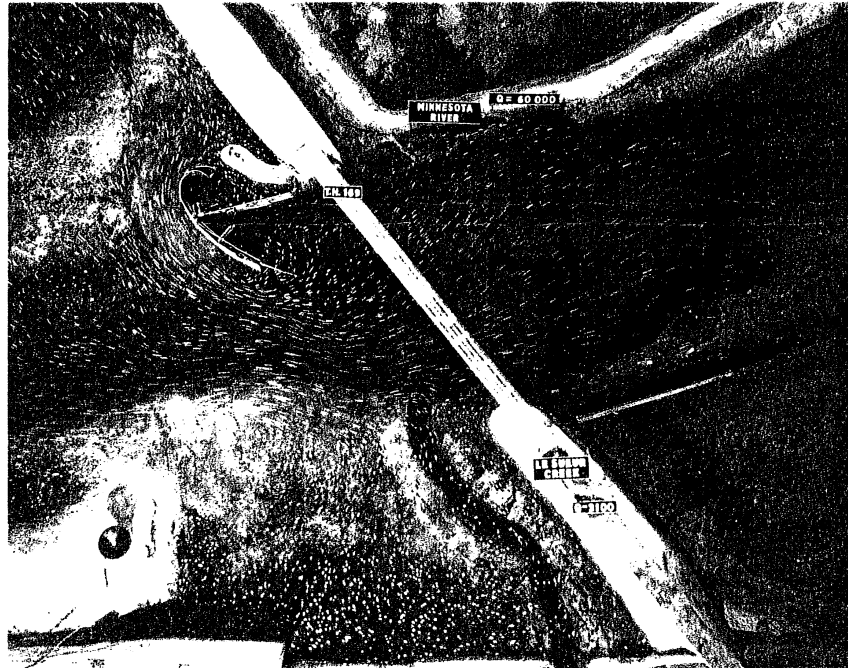


Fig. 30. Flow patterns associated with the best configuration of the sheet-metal T-spur dike at 60,000 cfs.

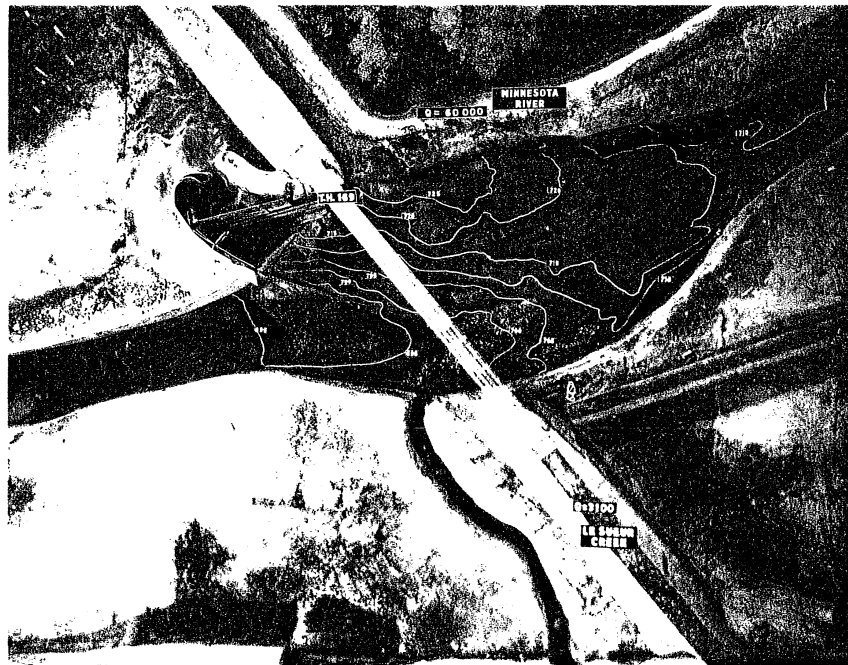


Fig. 31. Bed topography created by a mainstem flow of 60,000 cfs with the sheet metal T-spur dike in place.

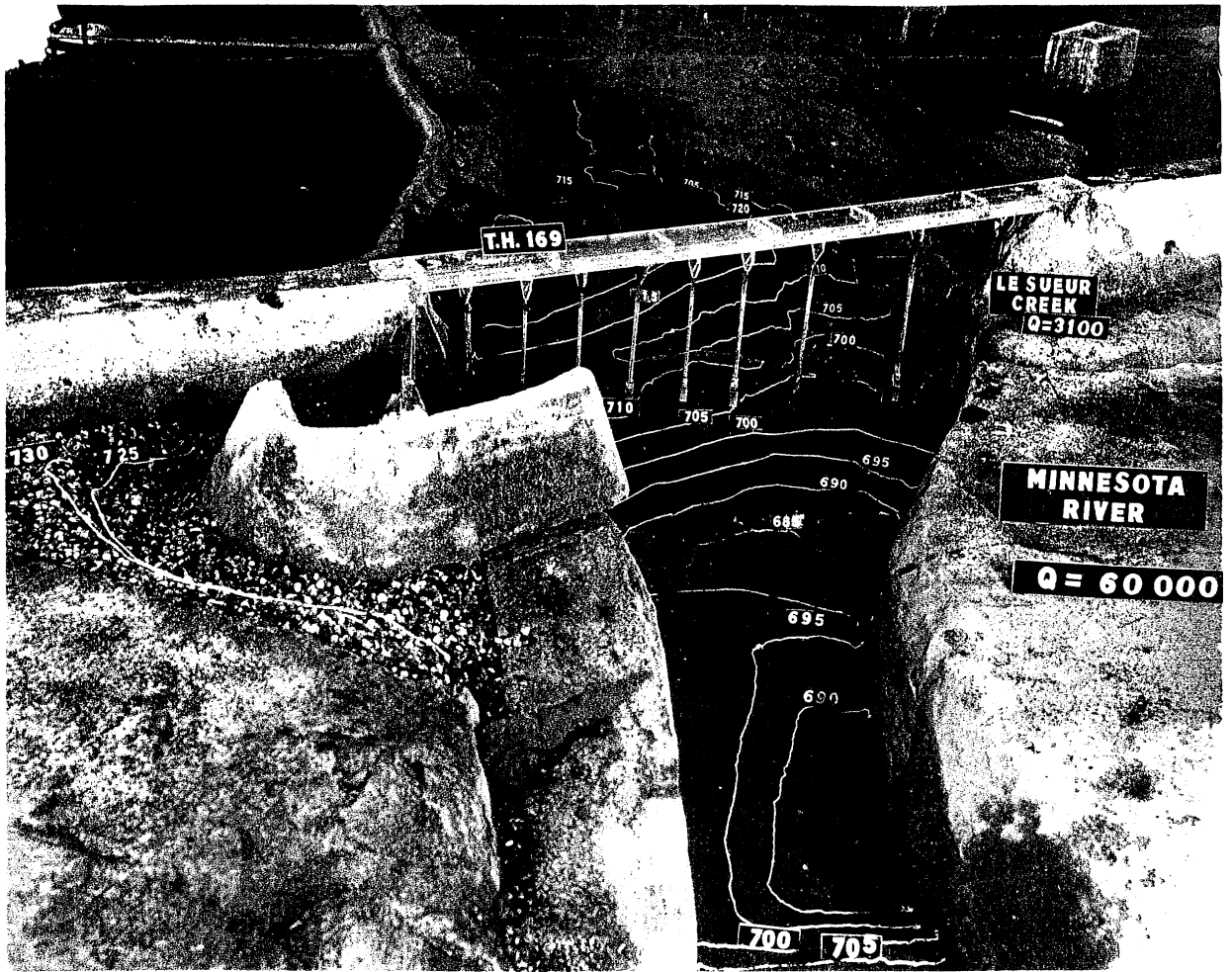


Fig. 32. Bed topography created by a mainstem flow of 60,000 cfs with one version of the concreted T-spur dike in place.



Fig. 33. Flow streamlines at 60,000 cfs associated with the concreted T-spur dike of Fig. 32.



Fig. 34. Flow streamlines at 100,000 cfs with the concreted T-spur dike of Fig. 32 in place.

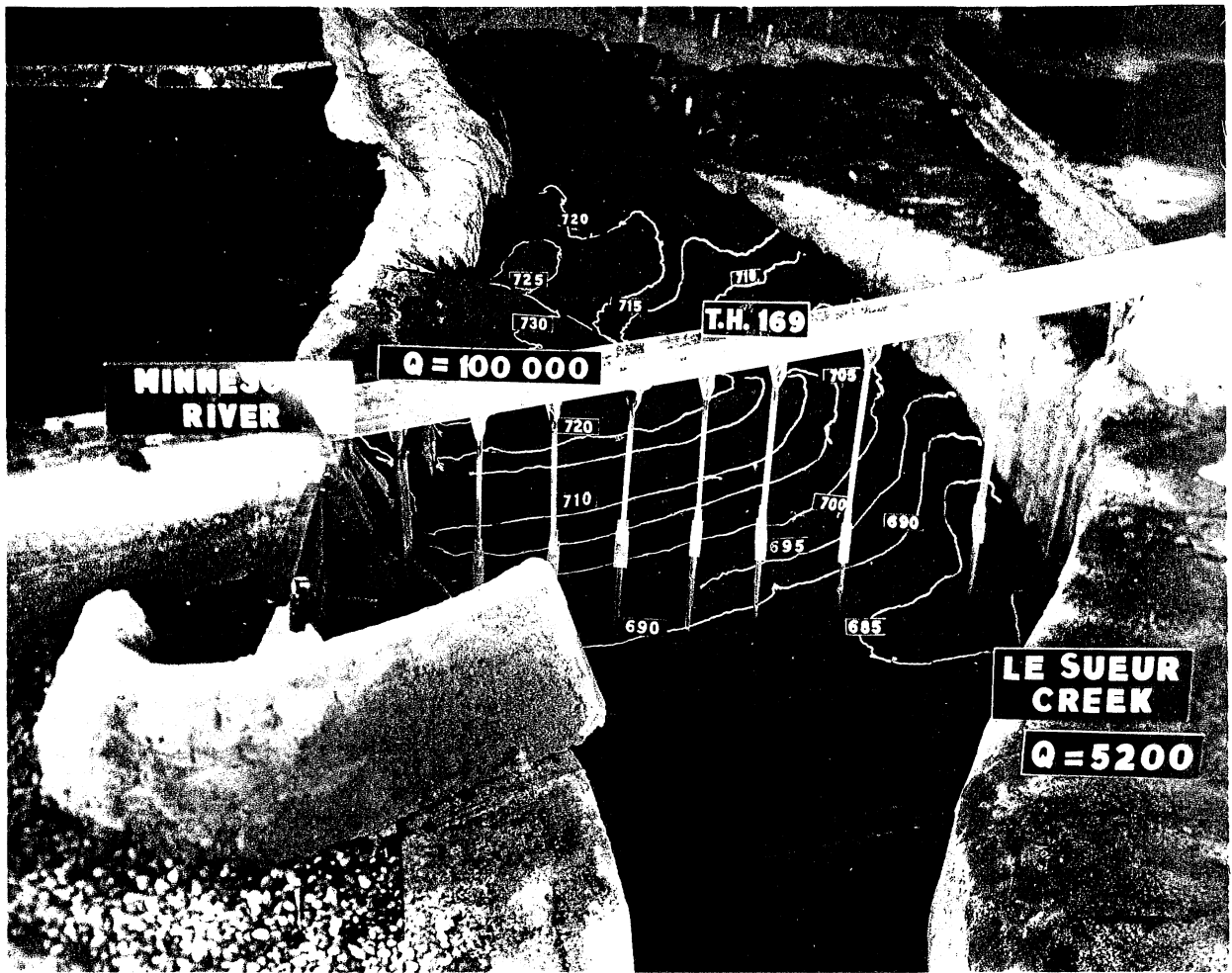


Fig. 35. Bed topography produced by a flow of 100,000 cfs with the concreted T-spur dike of Fig. 32 in place.

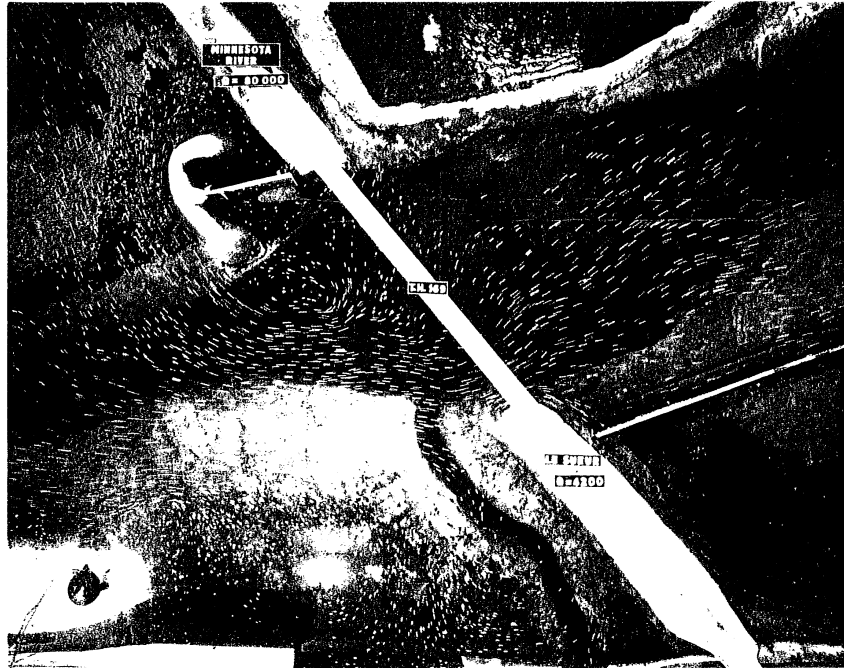


Fig. 36. Flow streamlines at 80,000 cfs, with a shortened version of the T-spur dike. Dike angle has also been modified.

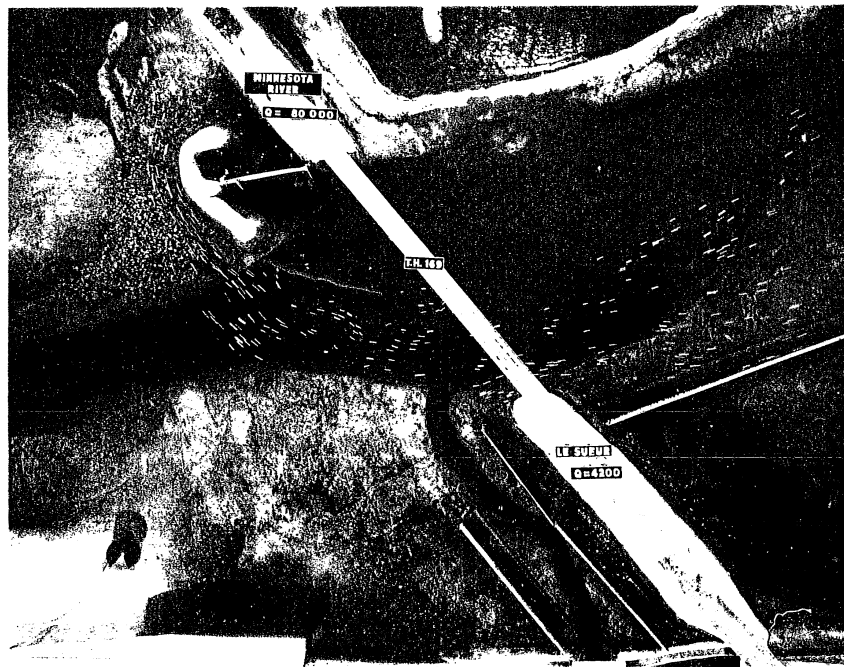


Fig. 37. Flow streamlines at 80,000 cfs, with an excavation, and then an elevated portion, upstream of the T-spur dike. The formed excavation suppresses separation, and allows the tip of the T-spur dike to be angled more strongly downstream.

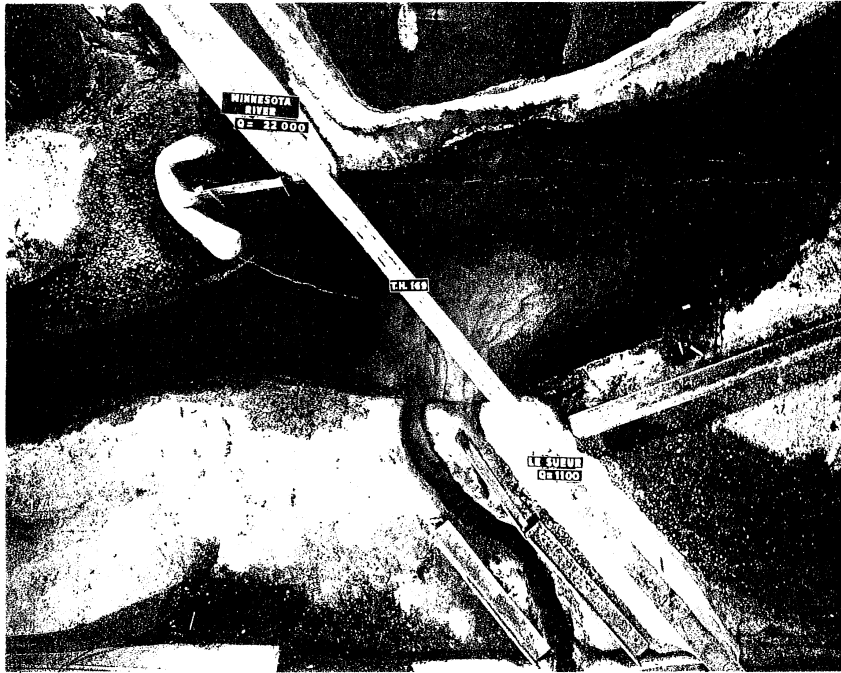


Fig. 38. A view of the bar at the mouth of the tributary created by feeding sediment to the tributary at the rate of 80 grams/minute, or about half the mainstem rate of 165 grams/minutes.

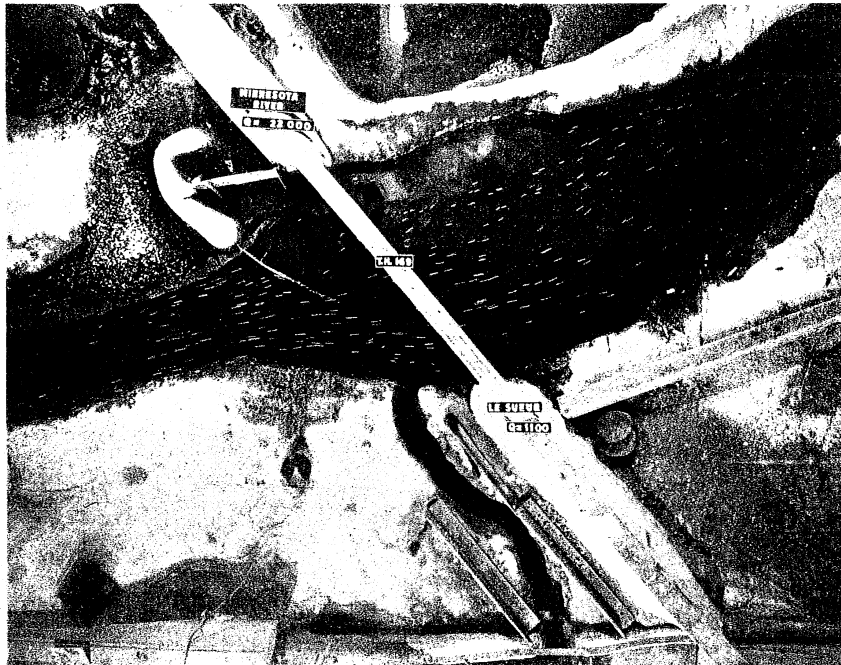


Fig. 39. Flow streamlines at 22,000 cfs with the two permeable dikes in place and sediment feed to the tributary turned off.



Fig. 40. Top view of the bed topography produced by the flow of Fig. 39.

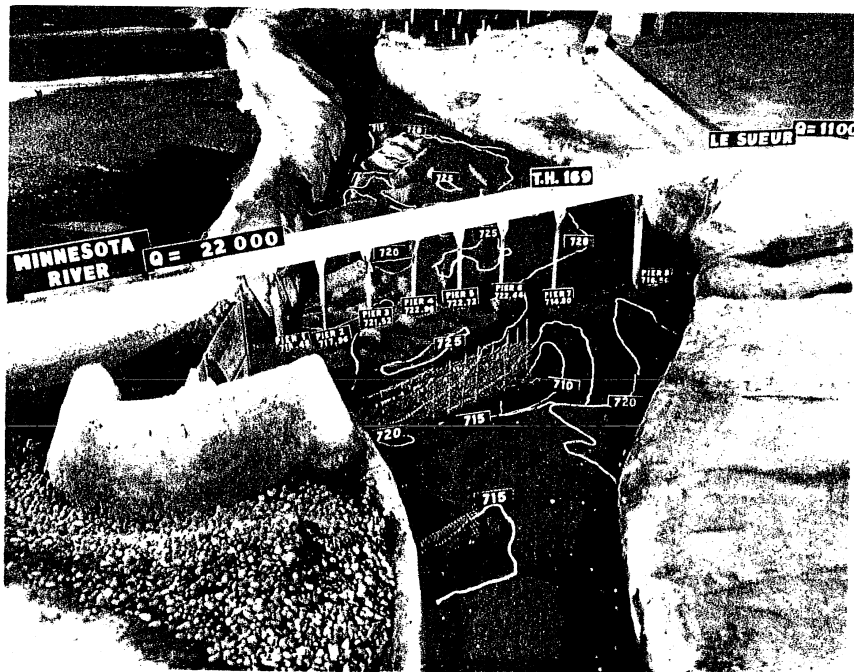


Fig. 41. Side view of the bed topography produced by the flow of Fig. 39.

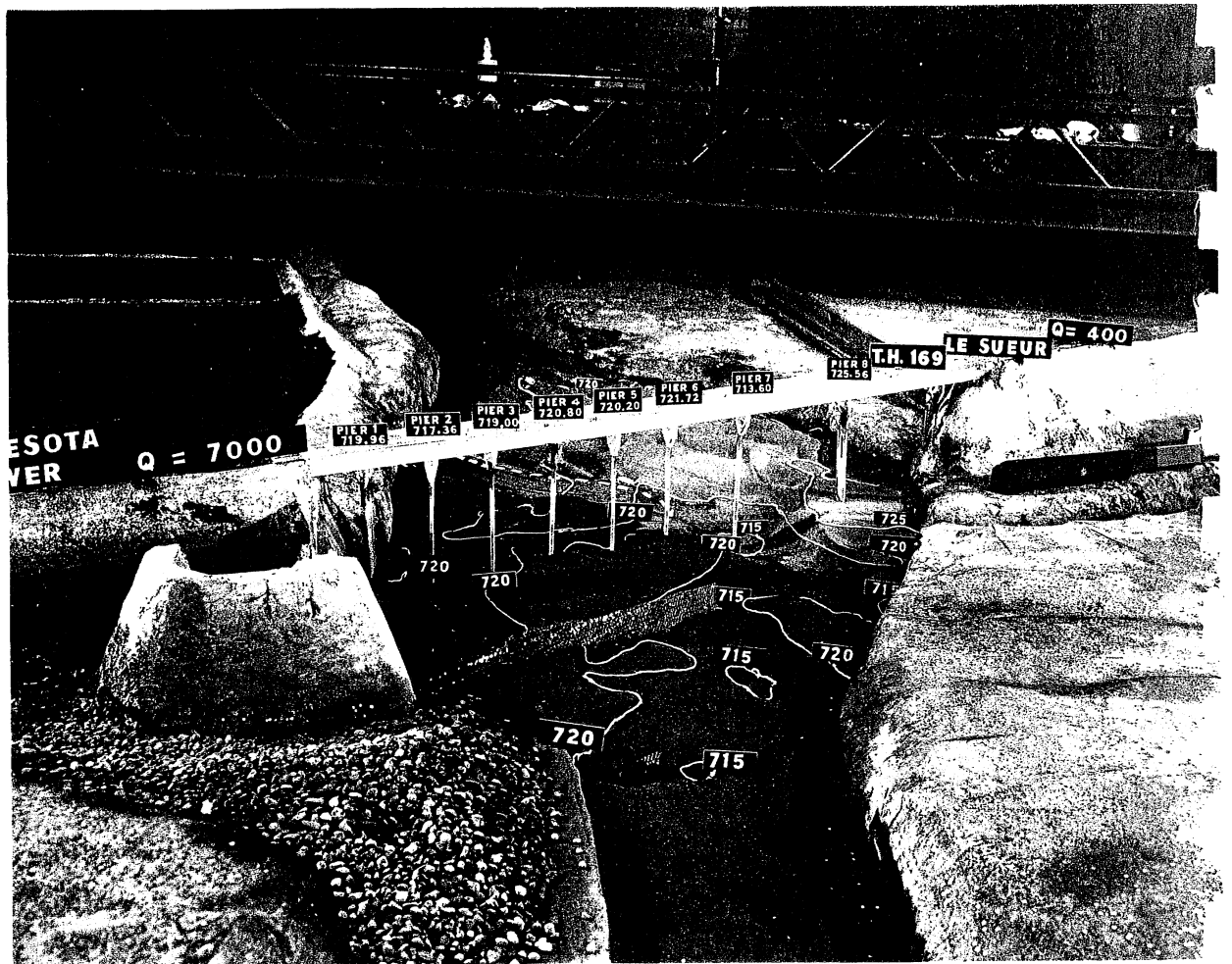


Fig. 42. Bed topography at the end of run 10-3.

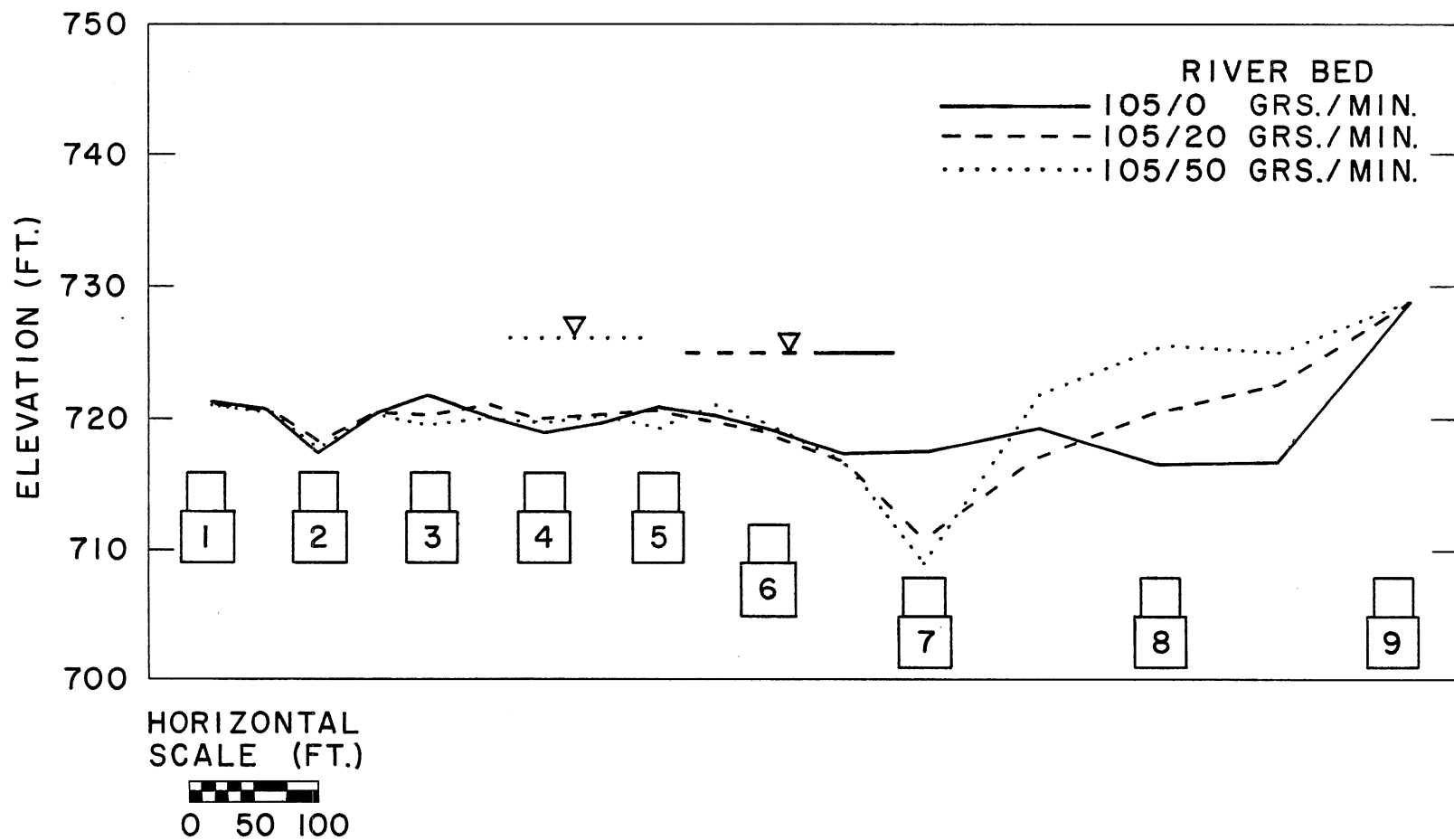


Fig. 43. Water surface elevations and bed profiles for the runs of Series 10. The mainstem and tributary sediment feed rates, in grams/minute, are listed for each run.



Fig. 44. Flow streamlines for run 10-3.

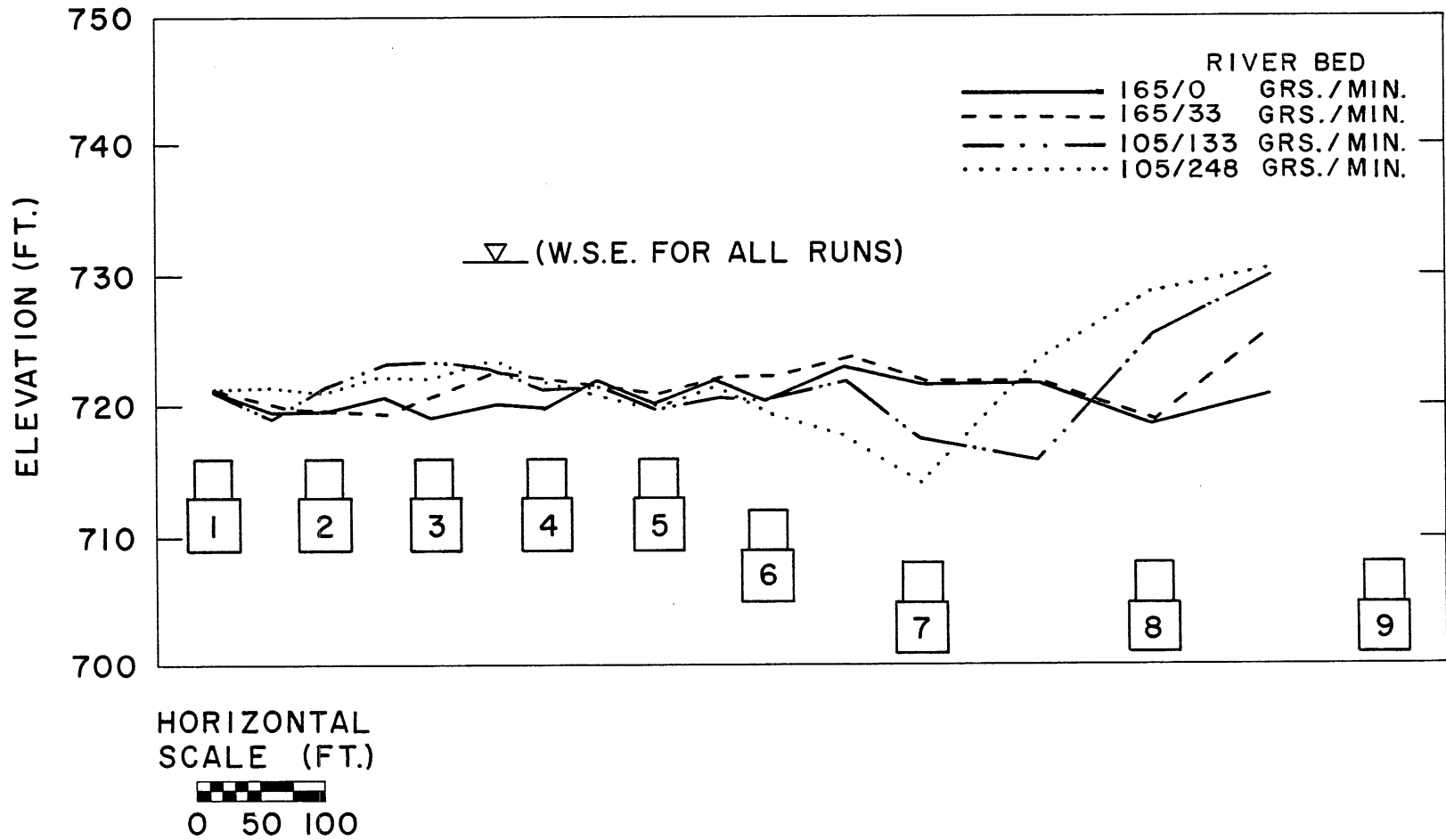


Fig. 45. Water surface elevation and bed profiles for the runs of Series 11. The mainstem and tributary sediment feed rates are listed in grams/minute for each run.

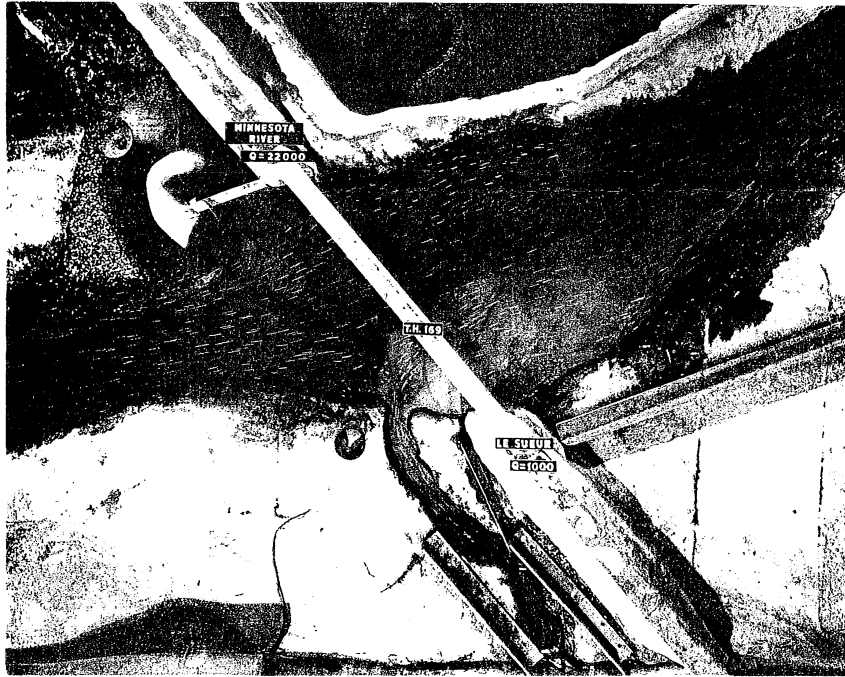


Fig. 46. Flow streamlines for run 11-4.

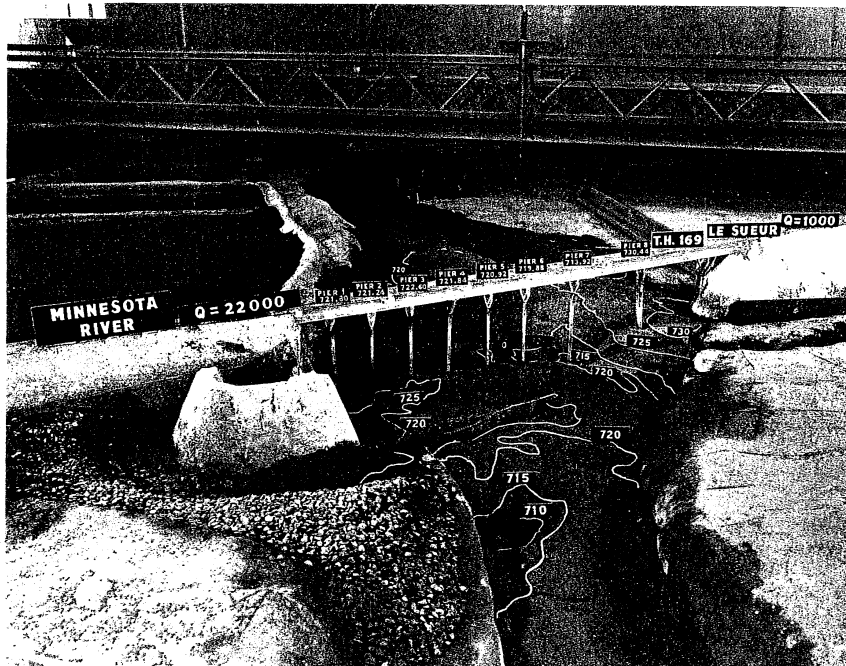


Fig. 47. Bed topography at the end of run 11-4.

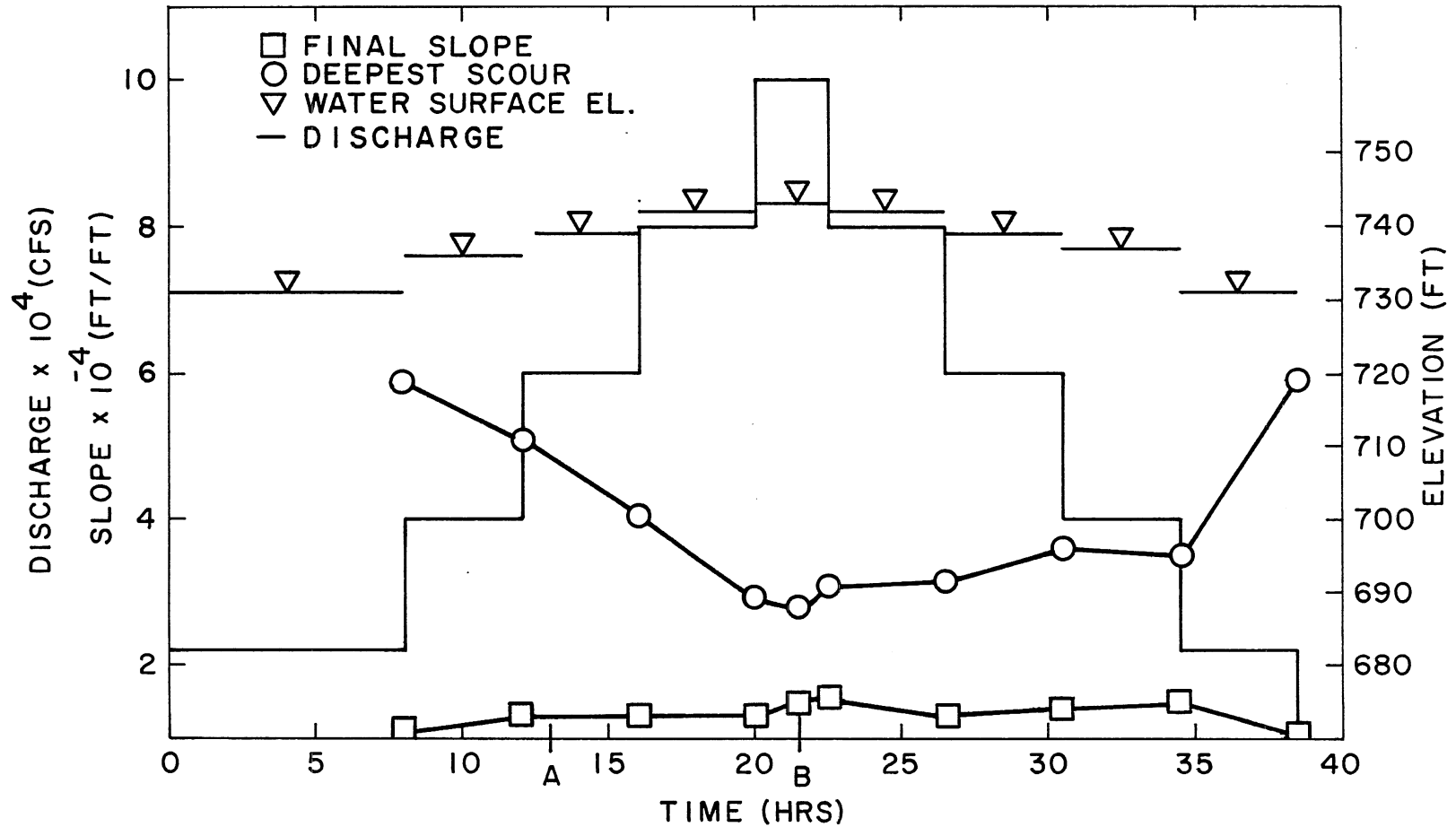


Fig. 48. Water surface elevation, water surface slope, discharge, and minimum bed elevation at the bridge as a function of time for the hydrograph run of Series 12. Time is listed in terms of hours in the model; all other parameters have been scaled up to prototype values.

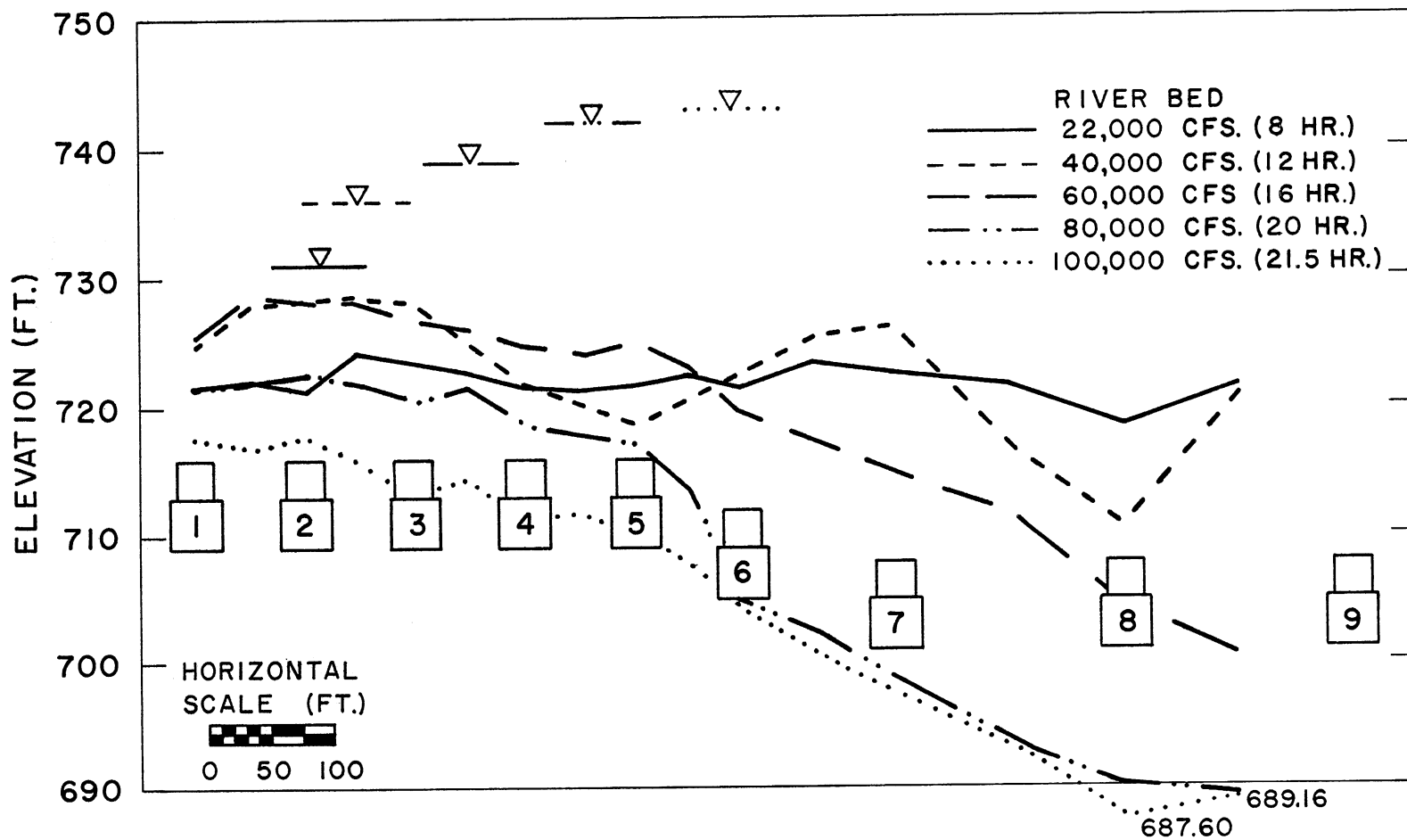


Fig. 49. Water surface elevations and bed profiles for the rising limb of the hydrograph run.

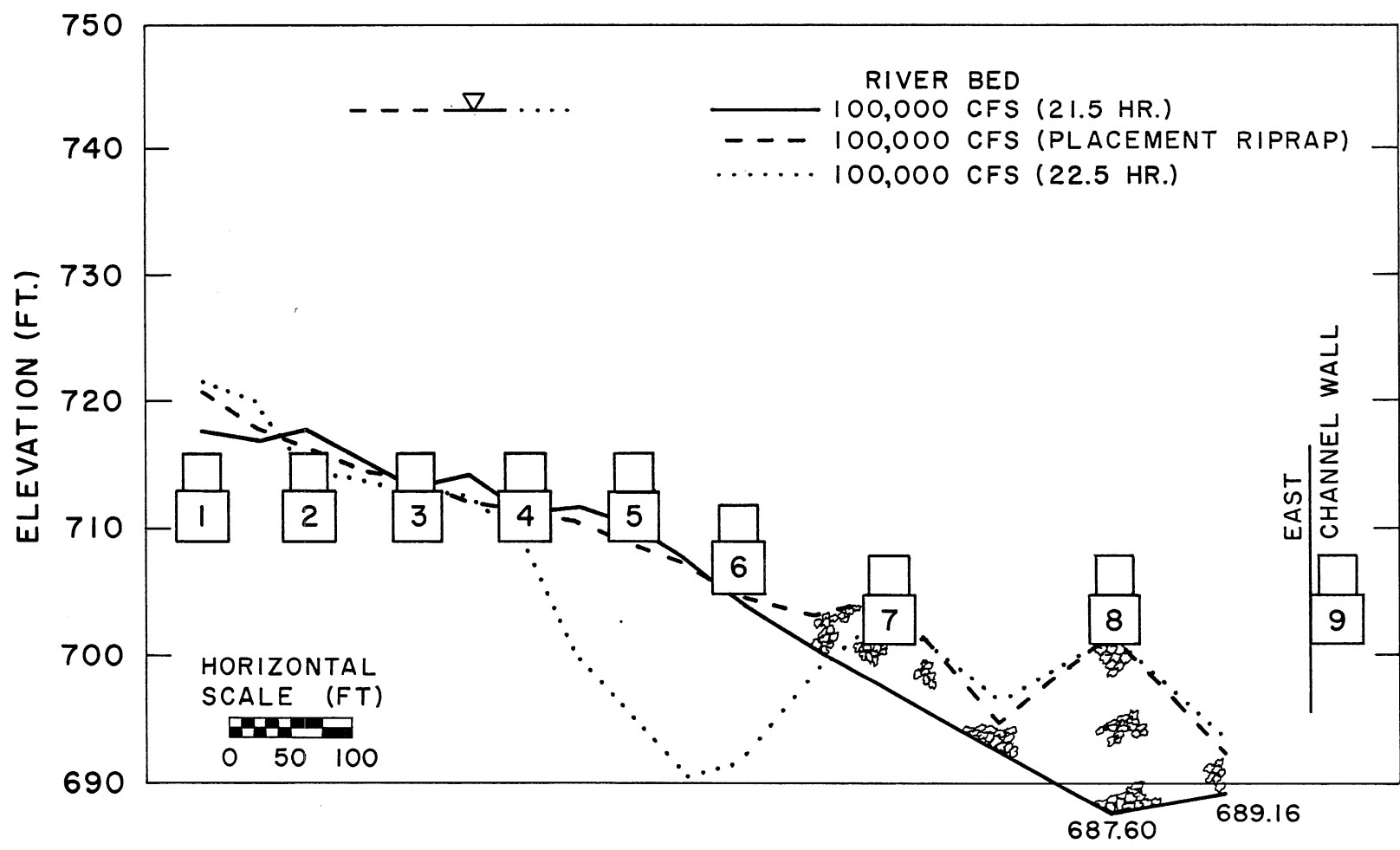


Fig. 50. Water surface elevation and bed profiles at the peak of the hydrograph, before, at the time of, and after placement of riprap.

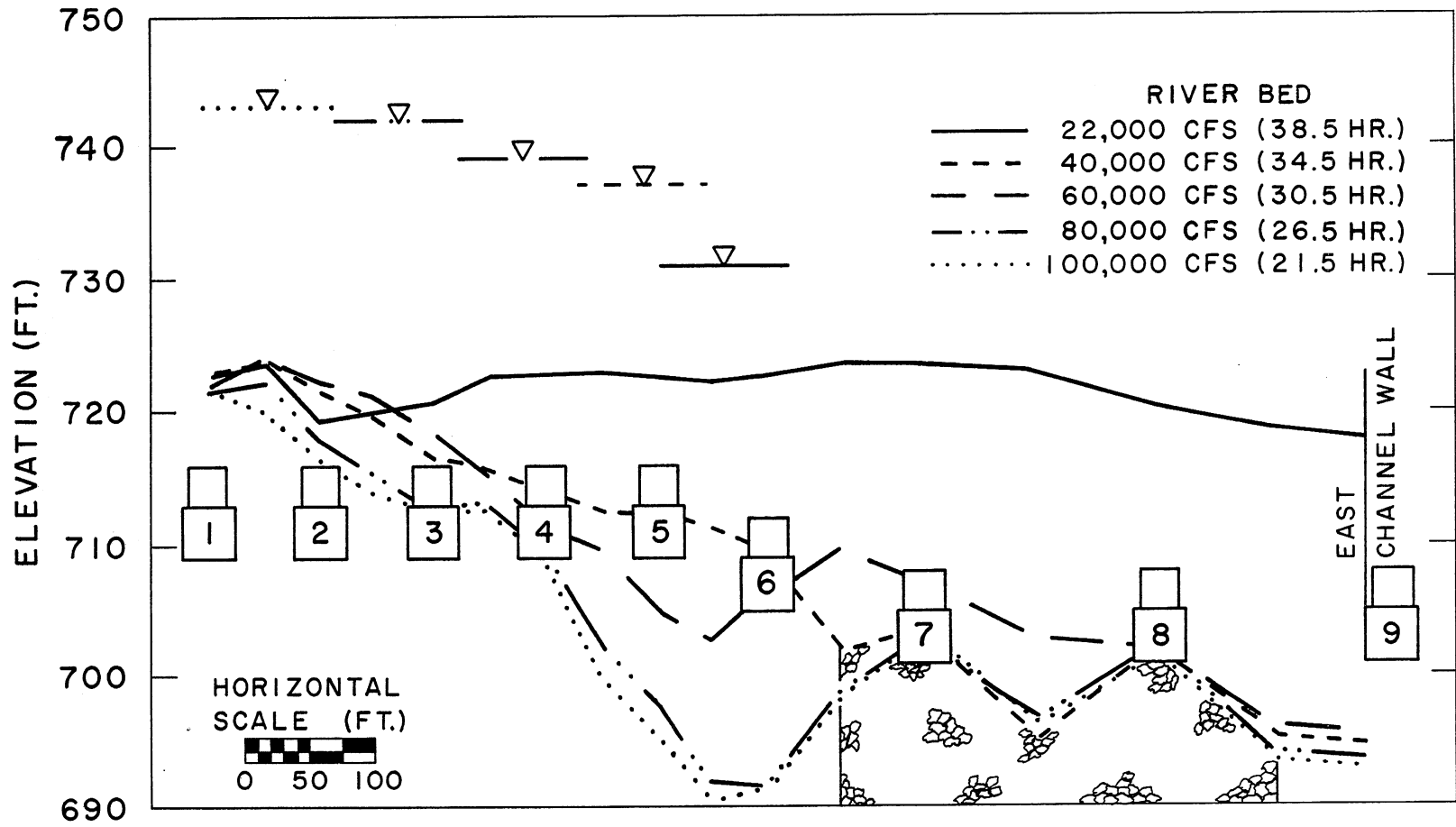


Fig. 51. Water surface elevations and bed profiles for the falling limb of the hydrograph run.

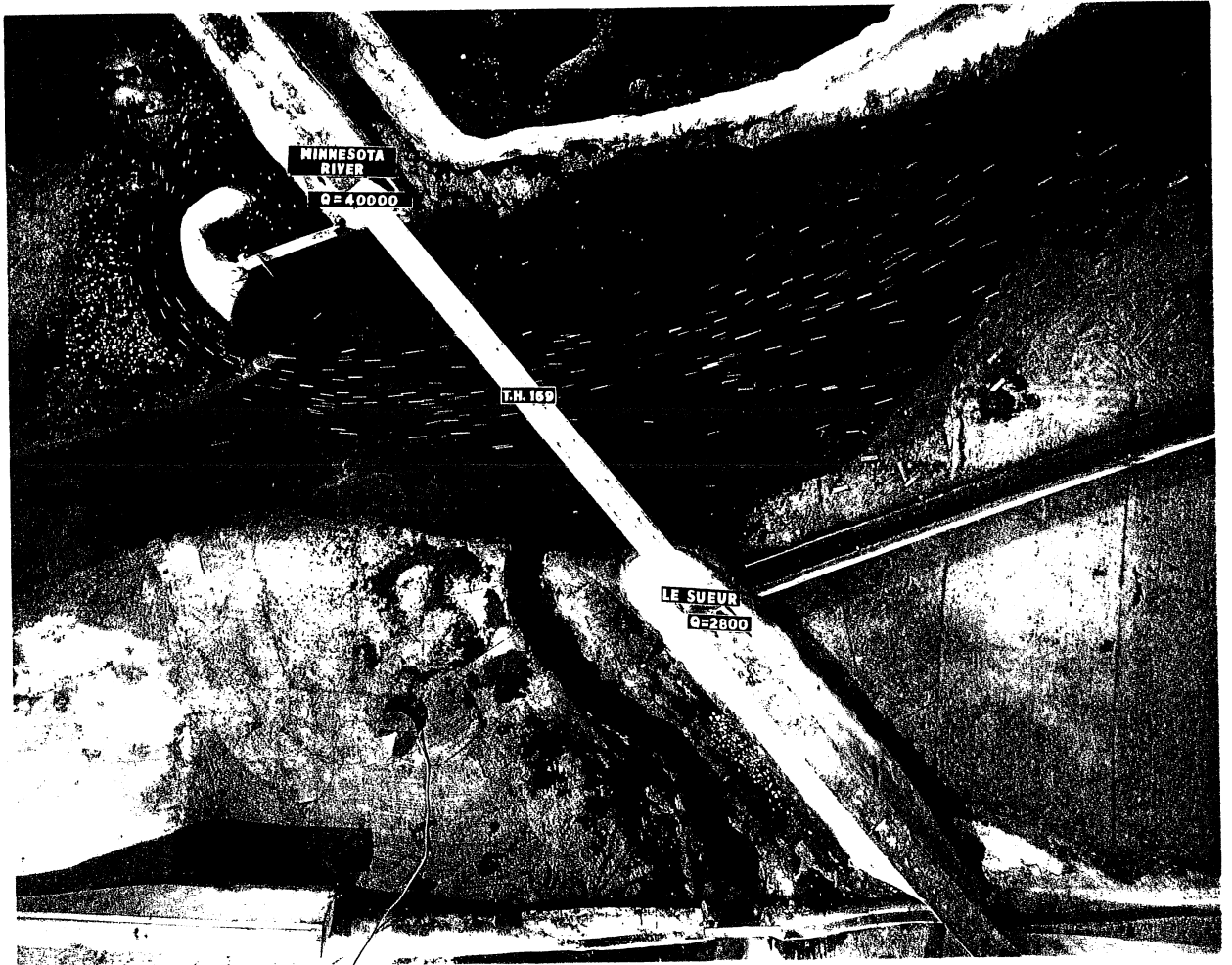


Fig. 52. Flow patterns at 40,000 cfs (rising limb) for the hydrograph run.

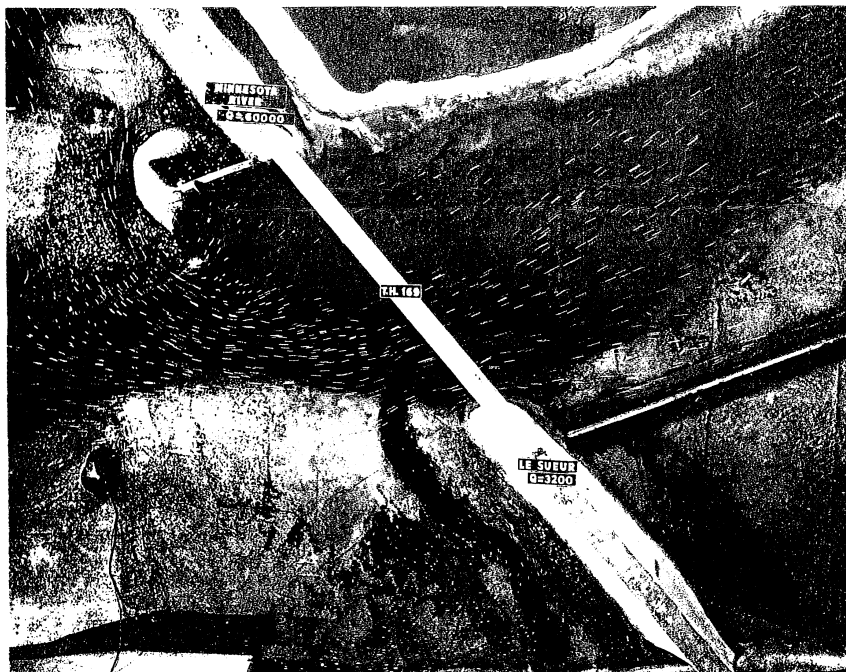


Fig. 53. Flow patterns at 60,000 cfs (rising limb) for the hydrograph run.

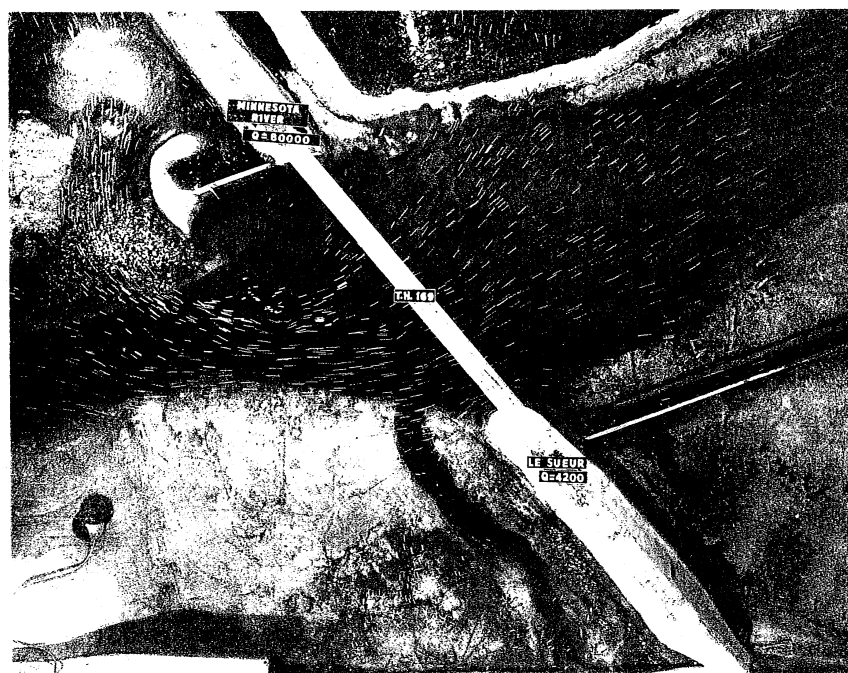


Fig. 54. Flow patterns at 80,000 cfs (rising limb) for the hydrograph run.

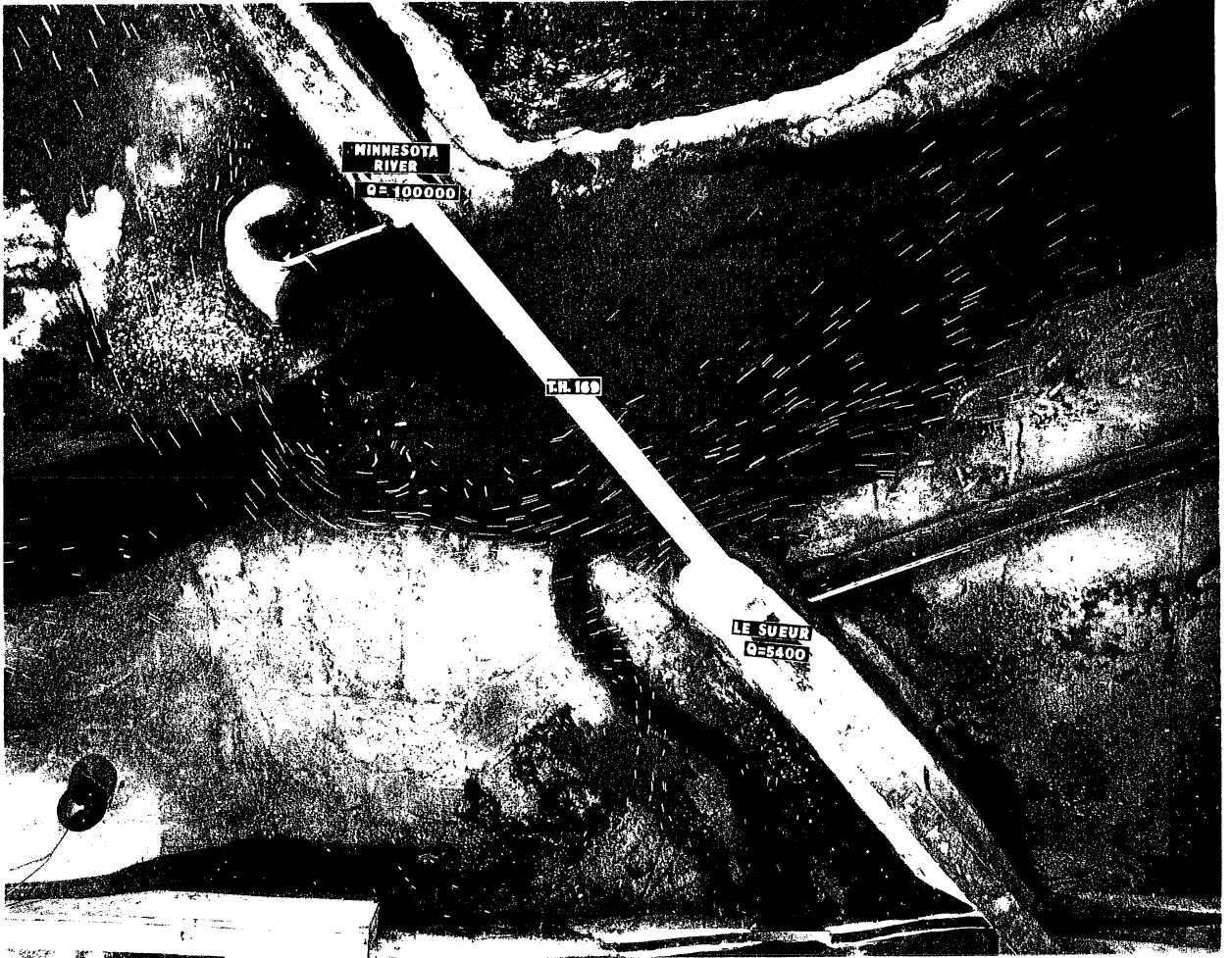


Fig. 55. Flow patterns at 100,000 cfs for the hydrograph run.

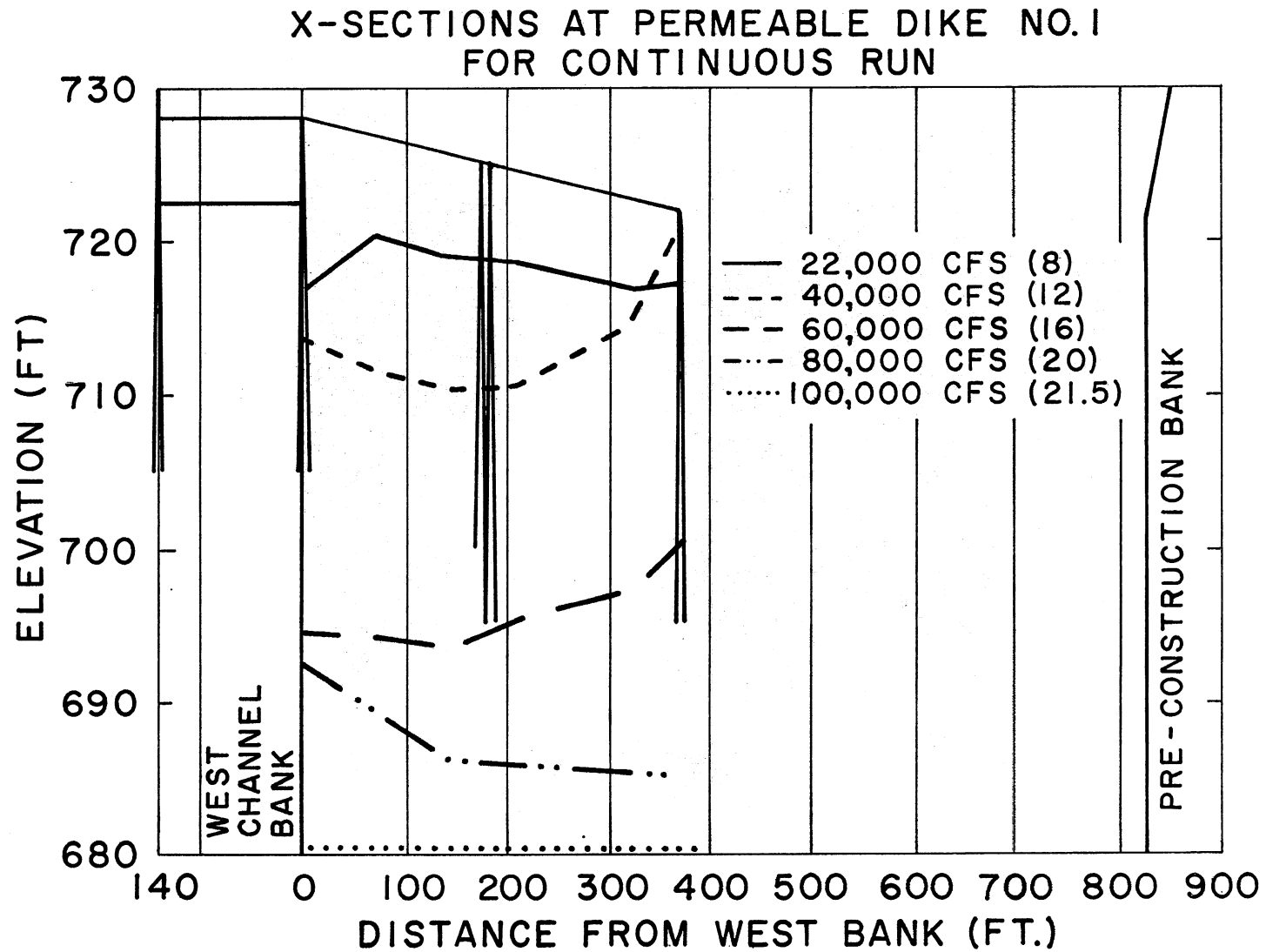


Fig. 56. Bed profiles for the rising limb of hydrograph run near the downstream permeable dike. Next to each discharge (in cfs) in parentheses is the time in hours at which that discharge was terminated.

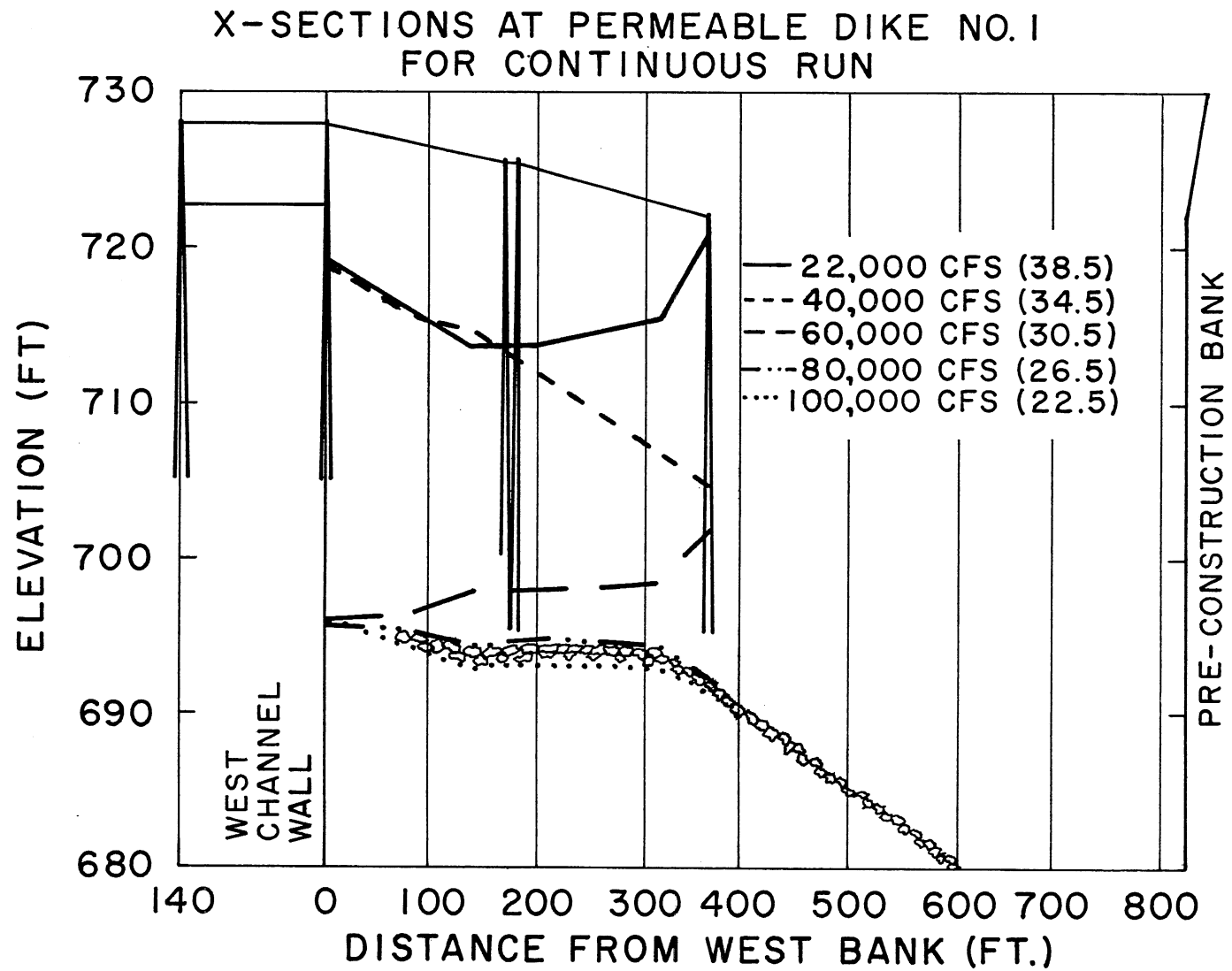


Fig. 57. Bed profiles for the falling limb of the hydrograph run near the downstream permeable dike. Next to each discharge (in cfs) in parentheses is the time in hours at which that discharge was terminated.

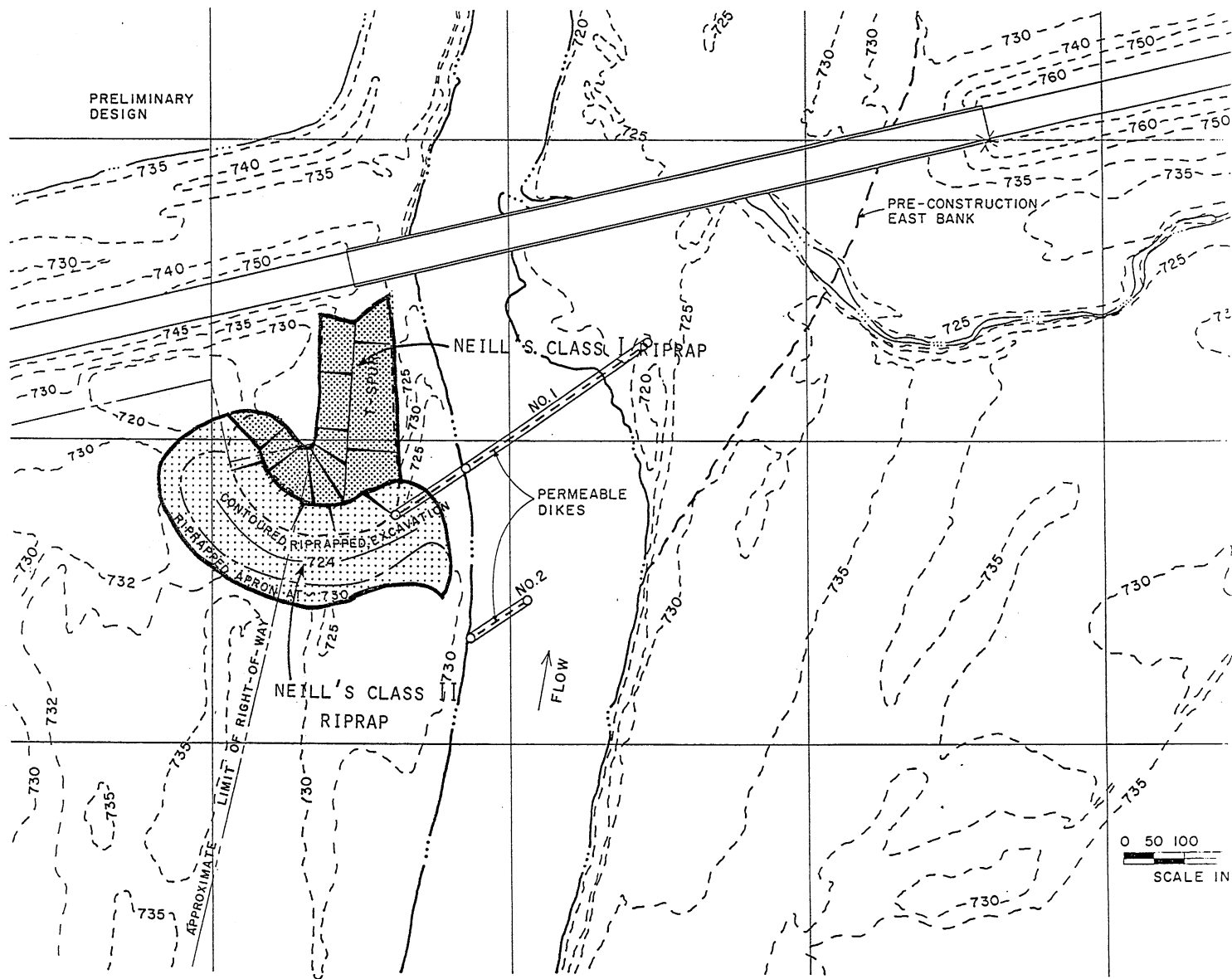


Fig. 58. Plan view of the bridge crossing, with the recommended positions for the T-spur dike and the two permeable dikes.

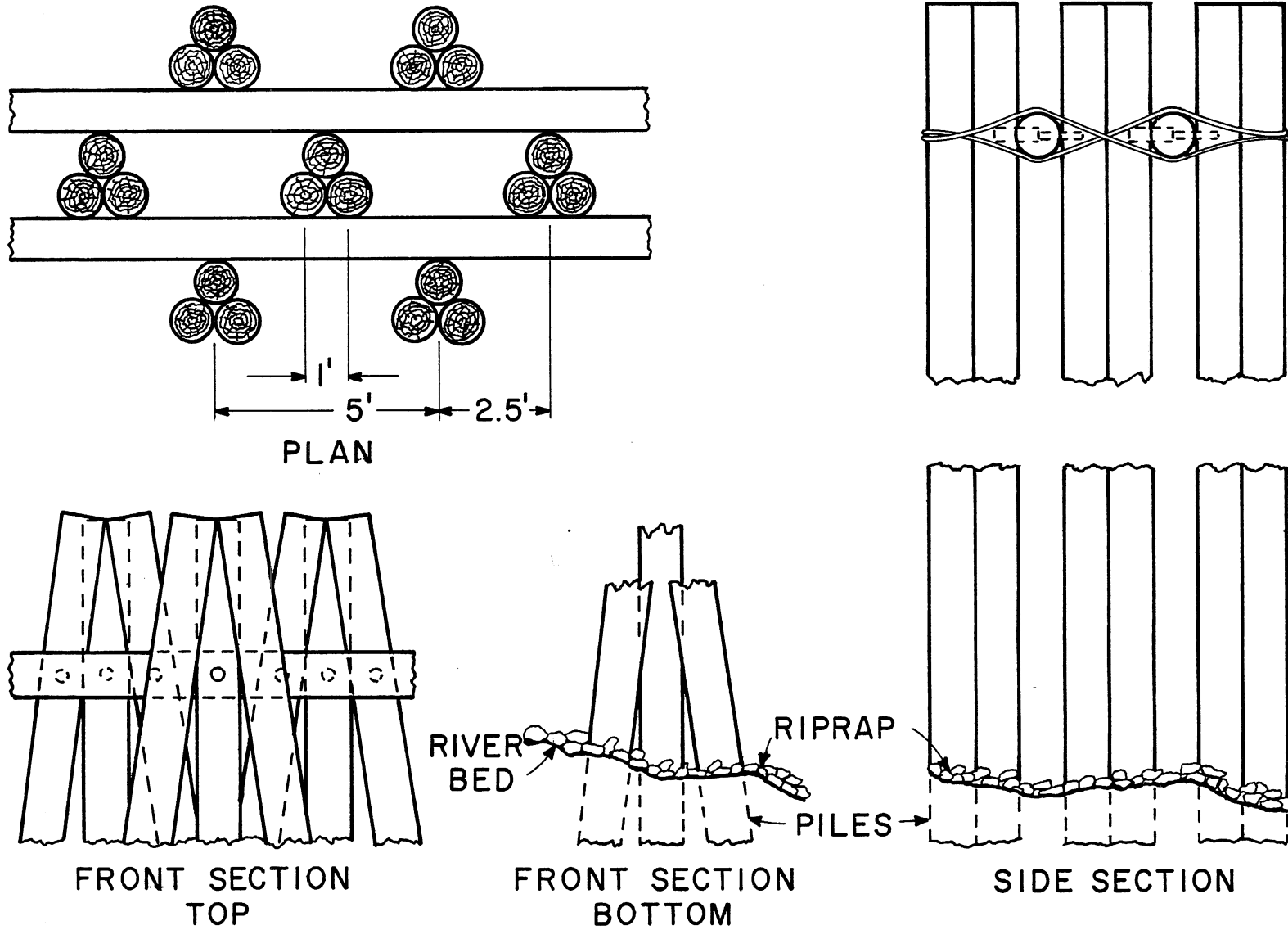


Fig. 59. Possible design for clump-pile permeable dikes.

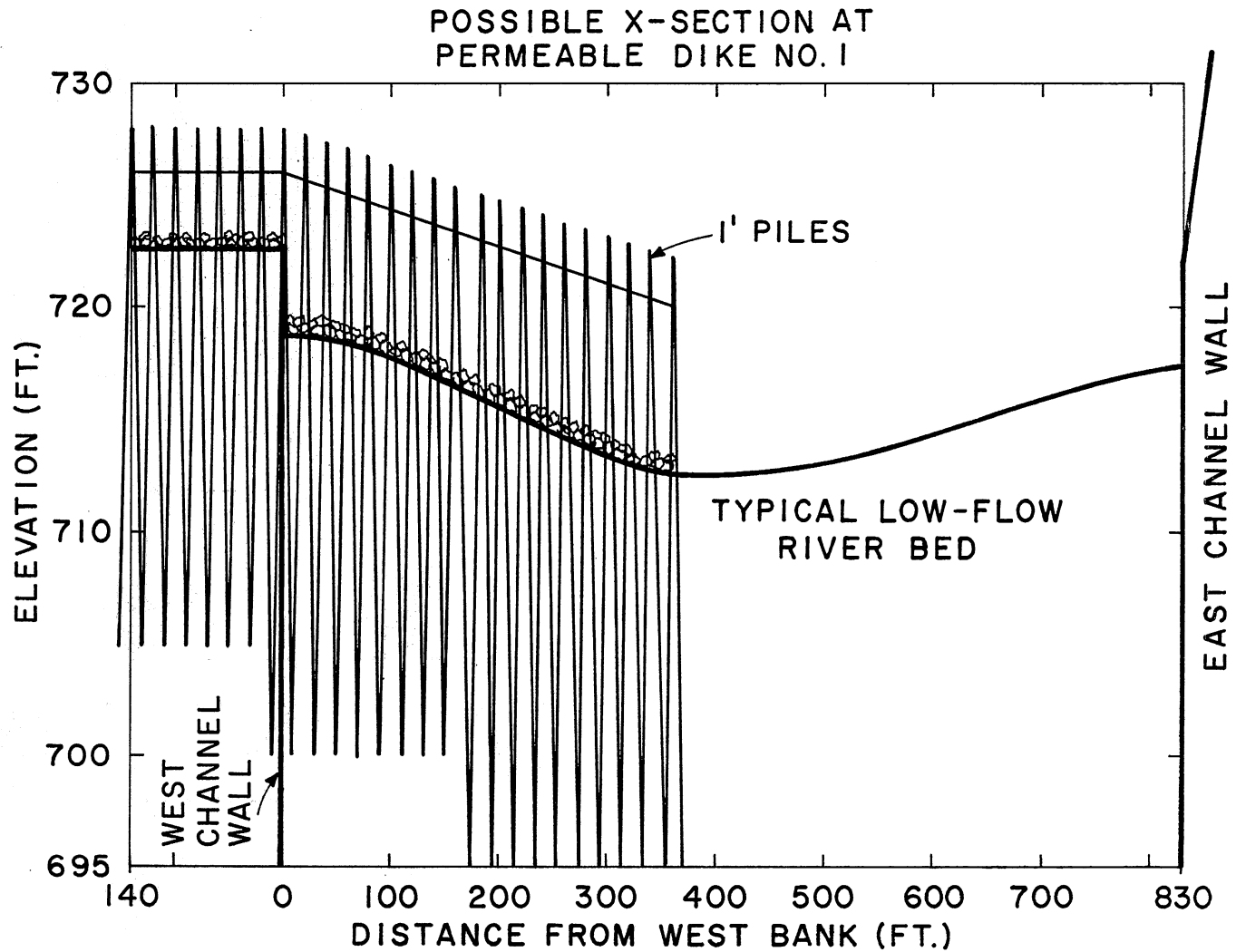


Fig. 60. The diagram illustrates the recommended setting for the top elevation of permeable dike No. 1 (downstream permeable dike), based on the results of the model study. The vertical west and east channel walls are artifacts of the model. The bottom elevation of the piles is shown only as an illustration. Appropriate pile depths must be selected in conjunction with Figs. 56 and 57.

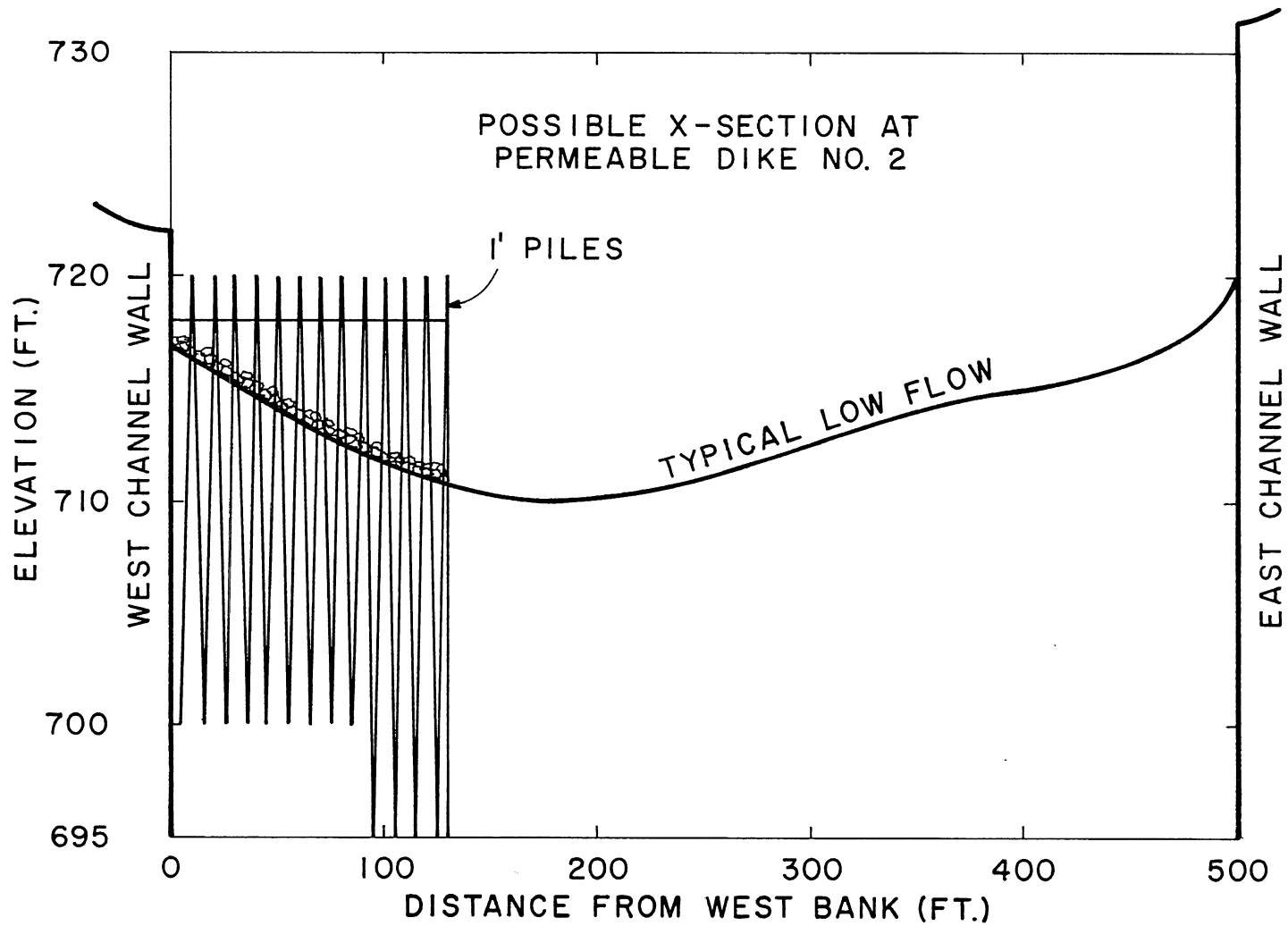


Fig. 61. The diagram illustrates the recommended setting of the top elevation of permeable Dike No. 2 (upstream permeable dike). See Fig. 60 for further explanation.

REFERENCES

1. Anderson, A. G. (1965). Report on Studies of the Stabilization of the Big Sioux River at the Interstate 29 Bridge Crossing. Project Report No. 78, St. Anthony Falls Hydraulic Laboratory, University of Minnesota, 28 pp.
2. Anderson, A. G. and Davenport, J. T. (1968). The Use of Submerged Groins for the Regulation of Alluvial Streams, Symposium on Current Problems in River Training and Sediment Movement, Budapest Acad. of Science, Budapest, Hungary.
3. Brice, J. C., Blodgett, J. C., and others (1978). Countermeasures for Hydraulic Problems at Bridges, Vol. 1, Report No. FHWA-RD-78-162, Federal Highway Administration, Washington, D. C., 169 pp.
4. Brown, S. A., McQuivey, R. S., and Miller, A. C. (1981). Flow Control Structures for Highways in River Environments, Interim Report for Federal Highway Administration, Office of Research and Development, by the Sutron Corp., 154 pp.
5. Dhamotharan, S., Wetzel, J. M., and Dahlin, W. Q. (1977). Maintenance and Regulation of Navigable Channels by the Use of Submerged Constrictions. Paper No. C1, 2nd Intl. Symp. on Dredging Technology, Texas A and M University, Nov. 2-4, 14 pp.
6. Engelund, F. and Hansen, E. (1967). A Monograph on Sediment Transport in Alluvial Streams, Teknisk Vorlag, Copenhagen, Denmark.
7. Guetzkow, L. C. (1977). Techniques for Estimating Magnitude and Frequency of Floods in Minnesota. U. S. Geological Survey, Water-Resources Investigations Report 77-31, St. Paul, Minnesota, 34 pp.
8. Parker, G. (1976). On the Cause and Characteristic Scales of Meandering and Braiding in Rivers. Journal of Fluid Mechanics, Vol. 76, pp. 457-480.
9. Patton, P. C., Baker, V. R., and Kochel, R. C. (1978). Slack-Water Deposits: A Geomorphic Technique for the Interpretation of Fluvial Paleohydrology. In Adjustments to the Fluvial System, Kendall-Hunt Publishing Co., pp. 225-254.

APPENDIX: A GUIDE TO THE VIDEO TAPES

PROJECT 305: VIDEO CASSETTE NO. 1

<u>DATE</u>	<u>COUNTER</u>	
3-30-82	000	<p>Conditions: $Q_{MN}=22,000$ cfs</p> <p>Showing: Flow at established conditions for the original profile.</p>
4-5-82	041	<p>Conditions: $Q_{MN}=60,000$ cfs</p> <p>Showing: Flow profile for entire model.</p>
	062	<p>Showing: Streamlines over the floodplain and in the main channel for the existing spur dike. Streamlines for the main channel are observed to be deflected toward east bank.</p>
4-12-82	089	<p>Conditions: $Q_{MN}=100,000$ cfs</p> <p>Training Structure: (No.1) Existing spur dike, riprap extended through pier No. 6 @ 720 (ft).</p> <p>Showing: Bed profile at piers and scour hole at spur dike.</p>
4-14-82	103	<p>Conditions: $Q_{MN}=100,000$ cfs</p> <p>Training Structure: (No.1) Existing spur dike, riprap to pier No. 6 @ 720 (ft).</p> <p>Showing: Influence of spur dike and tributary wall on streamlines of floodplain and main channel.</p>
4-21-82	120	<p>Conditions: $Q_{MN}=100,000$ cfs</p> <p>Training Structure: (No.2) Existing spur dike, riprap was removed.</p> <p>Showing: Bed profile at bridge with pilings of all piers exposed.</p>

<u>DATE</u>	<u>COUNTER</u>	
5-25-82		Conditions: $Q_{MN}=100,000$ cfs Training Structure: --
	126	Showing: A series of runs used to determine the best geometry of the new T-spur dike. (Changing the angle of intersection with channel wall and the length of the new structure.)
6-17-82		Conditions: $Q_{MN}=60,000$ cfs Training Structure: (No.3) Original T-spur dike extending 2" past the channel wall.
	216	Showing: Its effect on streamlines of the main channel and floodplain.
6-18-82		Conditions: $Q_{MN}=60,000$ cfs Training Structure: (No.3) Original T-spur dike.
	223	Showing: Bed profile at bridge with seals of footings partially exposed, also a scour hole at tip of T-spur dike in the main channel.
6-22-82		Conditions: $Q_{MN}=100,000$ cfs Training Structure: (No.3) Original T-spur dike.
	237	Showing: Streamlines are deflected so that much of flow extends over the east bank.
6-29-82		Conditions: $Q_{MN}=100,000$ cfs Training Structure: (No.3) Original T-spur dike.
	253	Showing: Bed profile at bridge with pilings of all piers extremely exposed.

<u>DATE</u>	<u>COUNTER</u>	
7-2-82		Conditions: $Q_{MN}=80,000$ cfs Training Structure: (No.4) T-spur tail was shortened approximately 2 inches and intersects the channel wall.
	270	Showing: Streamlines of floodplain and main channel.
		Conditions: $Q_{MN}=60,000$ cfs Training Structure: (No.4)
	284	Showing: Streamlines of floodplain and main channel.
7-6-82		Conditions: $Q_{MN}=100,000$ cfs Training Structure: (No.4)
	296	Showing: Streamlines of floodplain and main channel.
7-8-82		Conditions: $Q_{MN}=80,000$ cfs Training Structure: (No.5) T-spur dike intersects channel wall, but the angle between the tail and stem was reduced.
	308	Showing: Streamlines of floodplain and main channel.
7-12-82		Conditions: $Q_{MN}=80,000$ cfs Training Structure: (No.6) Best geometry of T-spur dike with 3" off original T-spur dike and structure retracted 1 inch from channel wall.
	317	Showing: Streamlines of floodplain and main channel, showing some separation yet maintaining flow through piers No. 7, No. 8, & No. 9.

PROJECT 305: VIDEO CASSETTE NO. 2

<u>DATE</u>	<u>COUNTER</u>	
7-12-82		Condition: $Q_{MN}=80,000$ cfs
		Training Structure: (No.6) T-spur 1" from wall.
	000	Showing: Streamlines of floodplain and main channel.
	036	Showing: Bed profile at bridge with all pilings exposed.
	067	Showing: Best geometry and location of T-spur dike acting to keep streamlines within channel walls.
7-13-82		Condition: $Q_{MN}=80,000$ cfs
		Training Structure: (No.6) T-spur 1" from wall.
	113	Showing: Streamlines for floodplain and main channel after an improvement on tributary wall.
	132	Showing: Streamlines shown by walnut shells that dropped out of can at feeder.
7-22-82		Condition: $Q_{MN}=80,000$ cfs
		Training Structure: (No.7) T-spur dike; shortening the stem 1 inch moving it closer to the road; riprap was placed around T-spur to improve scour; first permeable dike set in place; tributary wall removed.
	146	Showing: Streamlines of floodplain and main channel.

<u>DATE</u>	<u>COUNTER</u>	
8-2-82		Conditions: $Q_{MN}=22,000$ cfs $Q_{SED}=165$ grms/min $Q_{L.S.}=1,100$ cfs $Q_{SED}=80$ grms/min Training Structure: (No.7) T-spur dike; permeable dike No. 1; positioned towards pier No. 7 and trimmed down.
	212	Showing: Streamlines of main channel, (permeable dike causes little disturbance) and bar formation at creek mouth. Conditions: $Q_{MN}=22,000$ cfs $Q_{SED}=165$ grms/min $Q_{L.S.}=1,100$ cfs $Q_{SED}=0$ grms/min Training Structure: (No.8) T-spur dike; permeable dike No. 1; and permeable dike No. 2 placed upstream.
	247	Showing: Effects of permeable dikes on streamlines of main channel. The deflection is more gradual.
8-3-82		Conditions: $Q_{MN}=22,000$ cfs $Q_{SED}=165$ grms/min $Q_{L.S.}=1,100$ cfs $Q_{SED}=0$ grms/min Training Structure: (No.9) (Tail section of T-spur dike was shortened) Permeable dike No. 1 set at 728(ft) west, 722(ft) east and positioned towards pier No. 8; permeable dike No. 2 set at 720 (ft).
	261	Showing: Bed contour and pier elevations at bridge.

<u>DATE</u>	<u>COUNTER</u>	
8-11-82		Conditions: $Q_{MN}=7,000$ cfs $Q_{SED}=105$ grms/min $Q_{L.S.}=400$ cfs $Q_{SED}=0$ grms/min Training Structure: (No.9)
	285	Showing: Streamlines for average flow.
8-12-82	301	Showing: Bed contours and elevations at piers.
8-16-82		Conditions: $Q_{MN}=7,000$ cfs $Q_{SED}=105$ grms/min $Q_{L.S.}=400$ cfs $Q_{SED}=20$ grms/min Training Structure: (No.9)
	322	Showing: Most flow is directed towards pier No. 7; although confetti gets caught on permeable dike (distorting flow), the velocity behind permeable dike is less on the west than on east side.
8-17-82	339	Showing: Bed contours and elevations at piers.
8-17-82		Conditions: $Q_{MN}=7,000$ cfs $Q_{SED}=105$ grms/min $Q_{L.S.}=400$ cfs $Q_{SED}=50$ grms/min Training Structure: (No.9)
	368	Showing: Streamlines and bar formation.
8-19-82	389	Showing: Bed contours and elevations at piers (dashed line shows area reworked during draining).

<u>DATE</u>	<u>CONTOUR</u>	
9-1-82		Conditions: $Q_{MN}=22,000$ cfs $Q_{SED}=165$ grms/min $Q_{MN}=1,000$ cfs $Q_{SED}=0$ grms/min Training Structure: (No.9)
	409	Showing: Contours of river bed and elevations at piers.
9-3-82		Conditions: $Q_{MN}=22,000$ cfs $Q_{SED}=165$ grms/min $Q_{L.S.}=1,000$ cfs $Q_{SED}=33$ grms/min Training Structure: (No.9)
	419	Showing: Effects of permeable dikes and a 20% feed rate from tributary on main channel streamlines.
9-7-82	430	Showing: Bed contours and elevations at piers; the deepest portion being at pier No. 8.
9-13-82		Conditions: $Q_{MN}=22,000$ cfs $Q_{SED}=165$ grms/min $Q_{L.S.}=1,000$ cfs $Q_{SED}=133$ grms/min Training Structure: (No.9)
	446	Showing: Effects of permeable dikes and an 80% feed rate from tributary on main channel streamlines. Shows growth of bar at creek mouth.
	459	Showing: Bed contours and elevations at piers. Deepest portion shifts to pier No. 7.

<u>DATE</u>	<u>COUNTER</u>	
9-15-82		Conditions: $Q_{MN}=22,000$ cfs $Q_{SED}=165$ grms/min $Q_{L.S.}=1,000$ cfs $Q_{SED}=248$ gms/min Training Structure: (No.9)
	473	Showing: Effects of permeable dikes and a 150% feed rate from tributary on streamlines and bar growth.
	480	Showing: Bed contours and elevations at piers with deepest portion between piers No. 6 & No. 7.
<p>The following is documentation for the continuous run, with training structures and no sediment feed from the tributary.</p>		
9-16-82		Conditions: $Q_{MN}=22,000$ cfs $Q_{L.S.}=1,000$ cfs
	493	Showing: Streamlines.
9-17-82		Conditions: $Q_{MN}=40,000$ cfs $Q_{L.S.}=2,800$ cfs
	503	Showing: Streamlines (excellent performance).
		Conditions: $Q_{MN}=60,000$ cfs $Q_{L.S.}=3,200$ cfs
	526	Showing: Streamlines (acceptable performance).
9-20-82		Conditions: $Q_{MN}=80,000$ cfs
	542	Showing: Streamlines (effects of flood plain noticeable).
		Conditions: $Q_{MN}=100,000$ cfs
	561	Showing: Streamlines (riprap placed at piers No. 7 & No. 8 & permeable dike No. 1).
9-21-82		Conditions: $Q_{MN}=80,000$ cfs
	574	Showing: Streamlines (scour hole & riprap have some effect).
9-22-82		Conditions: $Q_{MN}=60,000$ cfs.
	602	Showing: Streamlines (performance not as good as at start).

305: CASSETTE NO. 2
PAGE 6

<u>DATE</u>	<u>COUNTER</u>	
9-22-82		Conditions: $Q_{MN}=40,000$ cfs
	616	Showing: Streamlines (scour hole fills and performance improves).
9-23-82		Conditions: $Q_{MN}=22,000$ cfs
	631	Showing: Streamlines
	656	END

Addendum to Project Report No. 213

MODEL STUDY OF THE MINNESOTA RIVER

NEAR TRUNK HIGHWAY NO. 169 BRIDGE, MINNESOTA

by Gary Parker, Ismael Martinez, and Randy Hills

1. ERRATUM

Page 1, line 28. The sentence should read, "The Trunk Highway No. 169 bridge..." instead of "The Trunk Highway No. 93 bridge..."

On page 28 of the report, the following sentence appears in the fourth paragraph from the top. "Between 60,000 cfs and 80,000 cfs, an enormous amount of scour occurs, ensuring failure of piers 7, 8, and 9." The statement refers to the experimental results of series 12. Strictly speaking, it is incorrect. What was observed in the experiments between the quoted discharges was scour below the seals of the affected piers, resulting in exposure of the piles. Exposure of the piles is highly undesirable, but it does not necessarily ensure failure. Exposure of several piles actually occurred during the flood of 1965 without failure of the bridge.

Page 67, Figure 45. In the upper right-hand corner "105/133 GRS./MIN." should read "165/13 GRS.MIN.," and "105/248 GRS./MIN." should read "165/133" GRS/MIN."

2. HORIZONTAL FLUID LOADING ON PERMEABLE DIKES

Approximate design calculations, which will be forwarded to the Minnesota Department of Transportation, indicate that at flows from 60,000 cfs to 100,000 cfs, an appropriate conservative estimate of horizontal fluid loading on the two permeable dikes of Fig. 58 is about 50 to 60 pounds per square foot. The added effect of ice or debris has not been estimated.

3. RIPRAP SIZE SCALING

On page 18 of the report, a method of calculating the relation between model and field riprap size is presented. This method is based on Shields stress similarity. An alternative, much more conservative method based on velocity is delineated below. Neill (1973) presents a diagram for riprap sizing at bridges, the form of which can be accurately approximated by the relation

$$\frac{V}{\sqrt{gD_s}} = 1.76$$

In the above, V denotes mean flow velocity near the riprap, D_s denotes riprap grain size, and g denotes the acceleration of gravity. If similarity in the parameter $V/(gD_s)$ is assumed, then model riprap grain size $(D_s)_m$ and prototype riprap grain size $(D_s)_p$ are related as follows:

$$\frac{(D_s)_m}{(D_s)_p} = \lambda_v$$

In the above λ_v denotes the vertical scale ratio, which was equal to 1/40 for the model study in question. On page 18 of the report, it is noted that the median size of the riprap actually used in the study was 9 mm. This scales up to a prototype median size of 36 cm, or 14 inches, using the above velocity similarity criterion. For comparison, Neill's class I and class II riprap gradations are scaled down to model dimensions using the velocity similarity below.

Neill's Class I Riprap (V up to 9 ft/s)

	Prototype	Model
100% smaller than	18"	11.4 mm
80% smaller than	14"	8.9 mm
50% smaller than	12"	7.6 mm
20% smaller than	8"	5.1 mm

Neill's Class II Riprap (V up to 13 ft/s)

	Prototype	Model
100% smaller than	30"	19.0 mm
80% smaller than	24"	15.2 mm
50% smaller than	20"	12.7 mm
20% smaller than	12"	7.6 mm

The riprap used in the model study is seen to be close to Neill's class I riprap. For a given riprap size found to work successfully in the model, velocity scaling indicates that a much larger riprap size must be used in the field than Shield's scaling. This inherent conservatism dictates that velocity scaling is preferable.

4. ADDITIONAL TEST

On page 31 of the report, it is recommended that additional riprap from piers 5 to 9 should be added, so as to protect the footings of these piers during periods of severe scour associated with floods in excess of 60,000 cfs. Riprap has already been placed between piers 1 and 4 in the prototype, so the implication of this recommendation is riprap protection across the entire channel. It was not actually shown that appropriately sized riprap would in fact prevent scour below the seals during a model flood of 100,000 cfs. In order to verify this, the model tray was reactivated during the week of February 7 to 11, 1983. Riprap was placed continuously across the channel, from pier 1 to pier 9, with a downstream width roughly equal to that of the bridge. The bottom of the riprap was at the level of the bottom of the seal of each pier, and the top of the riprap

was at the level of the top of the footings. The riprap gradation, summarized below, was chosen to simulate a class I riprap.

Model Riprap Used in Special Study

		Prototype
100% smaller than	10.0 mm	15.7"
80% smaller than	8.2 mm	12.9"
50% smaller than	7.0 mm	11.0"
20% smaller than	5.5 mm	8.6"

This riprap successfully withstood a flood of 100,000 cfs in the model. The riprap ravelled forward into a deep scour hole just upstream of the bridge, providing good protection with only minor settling. Complete documentation of the special run is available on videotape.

5. FIELD RIPRAP SIZING FOR ROOTING PROTECTION

With a water surface elevation of 744 ft, it is easily shown that the prototype average velocity under the bridgeway at a flood of 100,000 cfs is about 9 ft/s, with the riprap placing specified above. It is thus conceivable that Neill's class I riprap might be only barely stable under the condition tested. For added safety, it is recommended that a riprap similar to Neill's class II riprap be actually installed in the field. It will be impossible to install this riprap immediately, as the footings of the most easterly piers are buried in sediment today. Installation should commence after the installation of the most downstream permeable dike. This permeable dike should deflect the river eastward. As this deflection occurs, the riprap can be filled in from the west, starting from pier 5. The addition of the riprap should aid the desired easterly deflection of the channel.

6. FIELD RIPRAP SIZING FOR THE T-SPUR DIKE

A xerox copy of Fig. 58*of the report is attached to this addendum. Recommended riprap sizings are indicated directly on the xerox copy. A riprap similar to Neill's class II is recommended at locations where stress is expected to be highest; otherwise riprap similar to Neill's class I is indicated.

7. REFERENCE

Neill, C. R., 1973. "A Guide to Bridge Hydraulics," University of Toronto Press.

Fig. 58 is updated as page 78 in text of book.

